2010

Mapping Riparian Vegetation in the Lower Colorado River Using Low Resolution Satellite Imagery

Kelly J. Amundsen
Cleveland State University

MAPPING RIPARIAN VEGETATION IN THE LOWER COLORADO RIVER USING LOW RESOLUTION SATELLITE IMAGERY

KELLY J. AMUNDSEN

Bachelor of Science in Geography

The Ohio State University

June, 2003

Submitted in partial fulfillment of requirements for the degree

MASTER OF SCIENCE IN ENVIRONMENTAL SCIENCE

at the

CLEVELAND STATE UNIVERSITY

December 20, 2010

This thesis has been approved for the

Department of Biological, Geological,

and Environmental Sciences and for the

College of Graduate Studies of

Cleveland State University

by

_____ Date:
Wentworth B. Clapham, Jr., BGES/CSU
Major Advisor

_____ Date:
Mark A. Tumeo, BGES/CSU
Advisory Committee Member

_____ Date:
John P. Holcomb, Jr., Mathematics/CSU
Advisory Committee Member

DEDICATION

To Atabey, for his presence in my life and guidance
through the trials of graduate school.

To Mom, Dad, Andy, Kevin, Kim, and Sarah,
for their support, willingness to listen, and
excellent ideas about self-preservation.

To Michelle, Ann, Ynes, Jaime, Joe, Jen,
Alison, D.C., Max, and Beth for being in the hole
with me and helping me see the way out.

To Dr. Reynolds for mentoring, support, advice,
expertise, employment, and laughs.

To Anya, Toni, Terri, and (I suppose) Tina,
for furs and purrs.

ACKNOWLEDGEMENTS

I would like to thank several people for their contributions to this project. First, I thank my major advisor, Dr. Clapham, for bringing me onto the project, for providing the opportunity for me to experience “real” scientific collaboration, and finally, for sharing his expertise and enthusiasm. Next, I thank my advisory committee members, Dr. Tumeo and Dr. Holcomb, for keeping my sights on both the task at hand and on the end goal with their invaluable ideas, guidance, and advice. I thank Mary Wells for her efforts both in the field and in the lab on this work. I would like to issue a special thank you to Dr. Pam Nagler of the U. S. Geological Survey for being an advocate of the importance of women in the sciences. Finally, I would like to thank the Ohio Alliance and the U. S. Bureau of Reclamation for providing the funding for this research.

MAPPING RIPARIAN VEGETATION IN THE LOWER COLORADO RIVER USING LOW RESOLUTION SATELLITE IMAGERY

KELLY J. AMUNDSEN

ABSTRACT

In the Western United States, monitoring water usage is a complex task carried out by the U.S. Bureau of Reclamation (USBR). It may be argued that USBR's greatest challenge is equitably distributing the waters of the Colorado River, particularly the Lower Colorado River, where water rights have been established and contested several times. To help meet the demands of water management in the Lower Colorado River Basin, USBR estimates the amount of water lost from the basin each year via evapo-transpiration by riparian vegetation in the Lower Colorado River riparian zone. Key components of those estimates include maps of the vegetation itself, which provide a measure of the acreage covered by each dominant species.

Previous mapping efforts have relied extensively on costly in-situ field measurements using the Anderson-Ohmart Classification scheme (which was developed for habitat evaluation, not species identification) and data-dense high resolution aerial photographs. This study employs low resolution Landsat imagery and simple classification and clustering algorithms to identify heterogeneous species assemblages in the Lower Colorado River as possible alternatives to Anderson-Ohmart and/or high resolution aerial photographs.

Our results show that the method developed here is able to identify heterogeneous riparian species assemblages, but certain vegetative species can be mapped with greater accuracy than others. Pending an error assessment to be carried out in a future field season, we believe our method to be an inexpensive, relatively simple update to USBR's existing mapping procedures.

TABLE OF CONTENTS

LIST OF TABLES

LIST OF FIGURES

CHAPTER I

BACKGROUND

1.1 Introduction

The U.S. Bureau of Reclamation (USBR), of the Department of the Interior is tasked with overseeing the equitable distribution of water resources, located either on the surface or below the ground, in the Western United States. This task includes monitoring and accounting for the use of all water taken from the Colorado River (*Arizona v. California*, 547 U.S. 150, 2006).

The Lower Colorado River riparian zone is a particular area of interest to USBR, because water from the Lower Colorado River supports industry, agriculture, and urban use in Nevada, Arizona, California, and Mexico. However, Arizona and California have repeatedly disagreed over interpretation of the *Colorado River Compact of 1922* (Norviel et al. 1922), the original document delineating water allotments to the interested parties. Because the water allotments are so highly contested, USBR must carefully monitor the distribution and usage of ALL water in the Lower Colorado River Basin.

1.2 Legal History of the Lower Colorado River Basin

Legislation of the Lower Colorado River Basin, beginning in the 1920's and still being deliberated today, regulates how much water each state in the region is permitted to draw from the river. The original water allotments have been challenged, upheld, and re-challenged several times in the past century, mostly by the State of Arizona and several Native American tribes in the area (*Arizona v. California*, 376 U.S. 340, 1964; 383 U.S. 268, 1966; 439 U.S. 419, 1979; 466 U.S. 144, 1984; 531 U.S. 1, 2000; 547 U.S. 150, 2006). These challenges to the laws led to court-mandated monitoring of water usage in the basin by the Department of the Interior (Bureau of Reclamation, 2009).

Major legal landmarks involving the distribution of water in the Lower Colorado River Basin include:

1. *The Colorado River Compact of 1922*
2. *The Boulder Canyon Project Act of 1928*
3. *The U.S. Supreme Court Decree in Arizona v. California, 376 U.S. 340, 1964*
4. *USBR Record of Decision, 2007*

1.2.1 The Colorado River Compact of 1922

In 1922 seven western states created an interstate agreement called the Colorado River Compact (Norviel, et al., 1922). The Compact promised each of the seven signatory states (Colorado, Utah, Wyoming, New Mexico, Arizona, Nevada, and California) a guaranteed amount of water each year from the river. Furthermore, the Compact split the states into an Upper Basin (Colorado, Utah, Wyoming, New Mexico, and northern Arizona) and a Lower Basin (Central and Southern Arizona, Nevada, and

California), with the boundary of the two placed at Lee Ferry (see map in Figure 1.1). With this compact, the Lower Colorado River Basin was officially born.

The Colorado River Compact allocated 7.5 million acre-feet per year of water to the Upper Basin and another 7.5 million acre-feet per year to the Lower Basin. (One acre-foot is defined as the amount of water needed to cover one acre of land with water one foot deep and is equivalent to 325,851 gallons.) The Compact further stated that the Upper Basin states could not withdraw water from the river to the extent that 7.5 million acre-feet per year could not be delivered to the Lower Basin. Additionally, 1.5 million acre-feet per year had to flow to Northern Mexico, where the Colorado River drains into the Gulf of Mexico. Representatives from each state signed the Colorado River Compact, and President Herbert Hoover approved it.

1.2.2 The Boulder Canyon Project Act of 1928

In 1928 Congress passed the Boulder Canyon Project Act, which officially ratified the Colorado River Compact of 1922 and gave permission to the U.S. Bureau of Reclamation (USBR) to construct Hoover Dam. Moreover, the Act divided up the water allotment promised to the Lower Basin states. Of the 7.5 million acre-feet per year of water promised to the Lower Basin, 4.4 million acre-feet per year was awarded to California, 2.8 million acre-feet per year was given to Arizona, and 0.3 million acre-feet per year was given to Nevada. Arizona, unhappy with the water allotments in both the Colorado River Compact and the Boulder Canyon Project Act, refused to ratify the Compact until 1944, but this was not the end of Arizona's complaints.

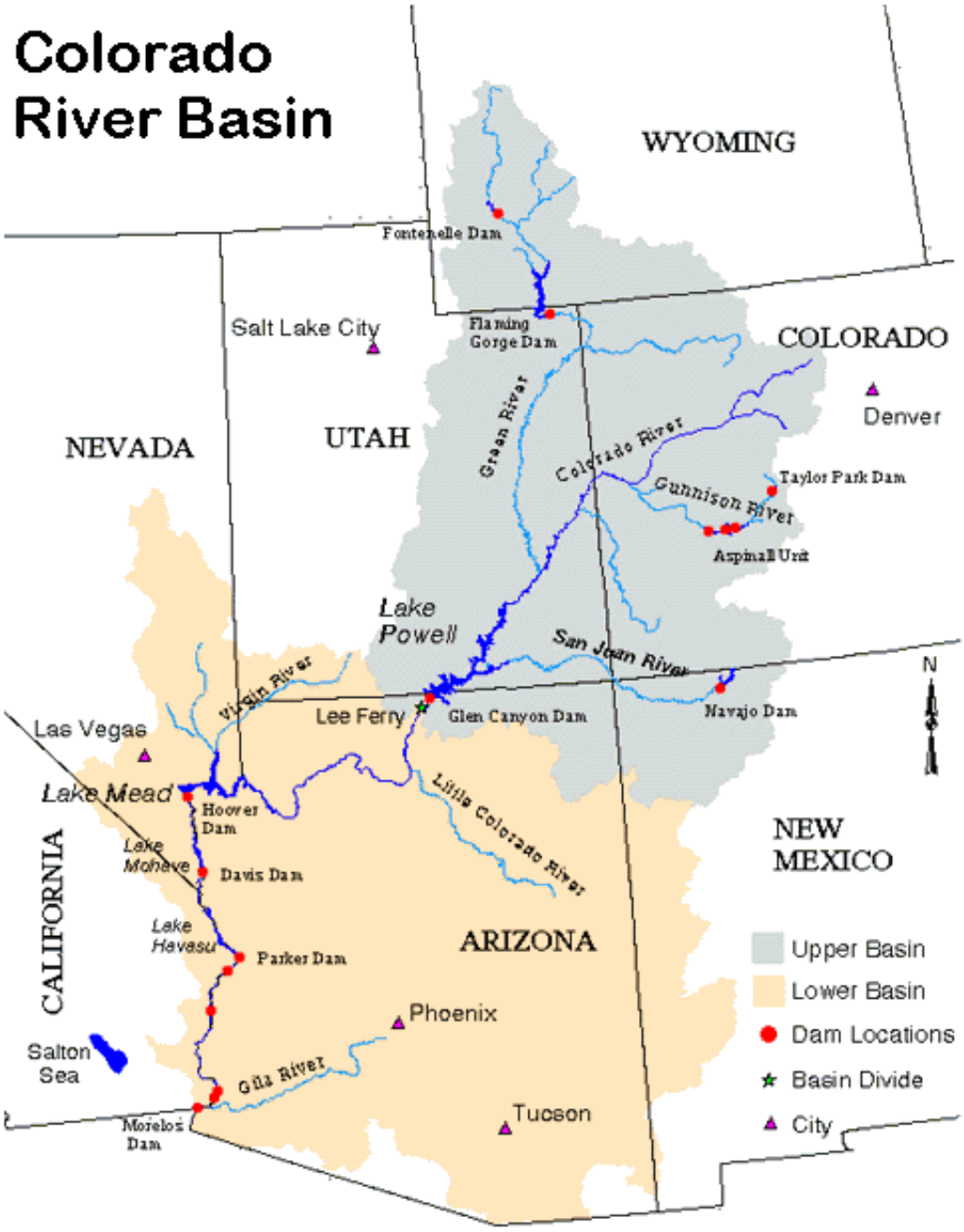

Map courtesy of the Colorado River Commission of Nevada

Figure 1-1. Map of the Colorado River Basin. Important features shown include the Upper/Lower basin divide at Lee Ferry and the Lower Basin south of Parker Dam. The bulk of this thesis refers the portion of the Lower Colorado River riparian zone (immediate flood plain) south of Parker Dam.

1.2.3 The U.S. Supreme Court Decree in Arizona v. California, 376 U.S. 340, 1964

In 1953 the Court granted the State of Arizona leave to file a bill of complaint against California (*Arizona v. California, 344 U.S. 919, 1953*), which claimed that California was drawing more than its fair share of water from the Lower Colorado River In 1964 the U.S. Supreme Court entered a decree (*Arizona v. California, 376 U.S. 340, 1964)* that upheld the water allotments from the Boulder Canyon Project Act. The decree also ordered the Secretary of the Interior to more closely monitor how much water was being drawn from the Colorado River at several points of diversion and to provide its findings in an annual report. The Secretary tasked USBR to carry out this function (Dwyer, 2010). The resulting reports, called the "Compilation of Records in Accordance with Article V of the Decree of the Supreme Court of the United States in Arizona v. California Dated March 9, 1964", also known as Decree Accounting reports, have been published annually since 1964. They are reviewed by the Department of the Interior to ensure that the states in the Lower Colorado River Basin do not exceed their legal water allotment.

1.2.4 USBR Record of Decision, 2007

By 2007 the Colorado River was providing drinking water for 27 million people and irrigation water for 3.5 million acres of farmland in the United States (Bureau of Reclamation, 2007). But, in the late 1990's, the Western U.S., including the entire Colorado River Basin, entered a period of drought that persists in some areas to the present day. Water levels in Lakes Mead and Powell declined over this period, with Lake Mead reaching its lowest levels in 54 years in late August, 2010. In 2007 USBR issued a Record of Decision which detailed how water allotments would be lowered in the Lower

Colorado River Basin, based on levels in Lake Mead, during drought conditions.[1] However, climate studies of the region suggest that the current drought conditions are normal, and the water levels in the 1920's (when the original water allotments were determined) were abnormally high (U.S. Geological Survey, 2004). Given the new data, water allotments may require renegotiation and new legislation.

1.3 Key Features of the Lower Colorado River Basin

1.3.1 Location and Climate

The study region in this thesis consists of an approximately 190 mile[2] stretch of the Lower Colorado River riparian zone from Parker Dam to Imperial Dam, comprising most of the border shared by California and Arizona. The riparian zone in this stretch of the river varies in width from approximately 10 miles to nothing. Surrounding areas of note include Salton Sea and Imperial Valley 50 miles to the west, Las Vegas 200 miles to the north, and the U.S. Department of Defense's Yuma Proving Ground to the immediate east (one of the largest military proving grounds in the world).

The area is part of the Sonoran Desert, one of North America's most extreme deserts, but irrigation water from the river supports extensive agriculture in the narrow riparian corridor. All irrigation is done by the flood technique, via an extensive network of diversion dams and canals. The primary crops grown in the area are cotton and alfalfa, though a variety of fruits, vegetables, and a few grains are also cultivated there.

[1] The USBR Record of Decision, 2007 states that shortage conditions may be declared when Lake Mead levels drop to or below an elevation of 1,075 feet above sea level. In late August, 2010 Lake Mead's water elevation was 1,087 feet above sea level. Visit http://www.usbr.gov/lc/region/g4000/hourly/hourly.html to obtain Lake Mead's water elevation, measured within the past hour.

[2] In this case, 'mile' refers to river miles, or the distance traveled by the Colorado River as measured along the center of the channel.

The climate of the region is arid desert. The average rainfall for much of the area is 2 inches per year, and temperatures routinely exceed 110-120 degrees in the summer. Despite these extreme conditions, the Lower Colorado River supports a seasonal tourism industry, which peaks in the winter when residents of Colorado, Wyoming, and other cold regions of the west drive people to warmer climates.

1.3.2 Colorado River Indian Tribes Reservation

The Lower Colorado River is also a politically charged region, even beyond the battle between California and Arizona for water. A large portion of the area consists of the Colorado River Indian Tribes Reservation, or CRIT, established in 1865. CRIT houses members of the Mojave, Navajo, Chemehuevi, and Hopi Tribes, though only the Mojave and Chemehuevi Tribes consider CRIT their ancestral homeland. The Navajo and Hopi people were relocated to the area after the establishment of the reservation. CRIT and other Native Tribes have successfully sued and earned the right to negotiate their own water allotments separately from the States of California and Arizona (*Arizona v. California*, 460 U.S. 605, 609, 615, 1983).

The main economy of CRIT has long been based on producing cotton, alfalfa, and sorghum. Recently, CRIT has been trying to develop its tourism industry with a casino, Native Tribal museums, and river-related activities (jet skiing, for example). One of the biggest tourist draws in CRIT is the town of Poston, known for having been the location of a Japanese-American internment camp from 1942-1945.

1.3.3 Cibola National Wildlife Refuge

The Lower Colorado River also houses the 18,000 acre Cibola National Wildlife Refuge. Cibola serves as a sanctuary for many species of birds and other wildlife,

including the endangered Willow Flycatcher. Unfortunately, invasive salt cedar trees have outcompeted much of the native cottonwood, willow, and mesquite trees in Cibola. Programs are being put in place to remove the salt cedar and replant with native trees, but not all experts agree that removing the salt cedar is a good idea. Since the arrival of the exotic tree, many birds have started preferentially nesting in the salt cedar instead of the native trees. One of these bird species is the Willow Flycatcher, whose endangered status extends legal protection to its habitat. Some suggest that this is an environmentally sound reason to leave the salt cedar alone. Others argue that the salt cedar contributes to surface soil salinity, which greatly affects the surrounding agricultural productivity and the quality of runoff into the Colorado River mainstem (McGinley, 2007).

1.4 Remote Sensing and its Role in Monitoring Water Usage

Remote sensing is the practice of gathering information about something through indirect measurements. Remote sensing of the Earth's surface has numerous applications, including surveying, mapping, environmental studies, and more. Since the dawn of the modern satellite era in the early 1970s, space-borne sensors have improved in global coverage and/or spatial and spectral resolution. The invention of the charge-coupled device (the birth of digital photography) made satellite and airplane mounted sensors more efficient at capturing and transmitting data (Xie et al., 2008). Such improvements have allowed researchers to study the Earth in greater detail and more quickly than could be done by field surveys.

USBR routinely uses remote sensing methods to assist them in monitoring water loss from the Lower Colorado River riparian zone, via methods incorporated into USBR's Lower Colorado River Accounting System (LCRAS) (Bureau of Reclamation,

2008). LCRAS is a series of methods used to estimate water loss from the Lower Colorado River Basin via the evapo-transpiration (ET) of water by plants to the atmosphere and evaporation of water from open water sources. ET is carried out by both agricultural crops and natural vegetation. By combining maps of agricultural crops, natural riparian vegetation groups, and open water sources with meteorological data, USBR is able to estimate the amount of water lost to the atmosphere via ET and direct evaporation each calendar year in the Lower Colorado River Basin.

LCRAS uses remote sensing data (both satellite imagery and aerial photographs) to map agricultural crops, riparian vegetation, and open water in the Lower Colorado River region (Bureau of Reclamation, 2009). The accuracy of the resulting maps is critical to achieving accurate estimates of ET and evaporation for LCRAS. Thus, USBR has a direct need for accurate, easily updateable ground cover maps of the Lower Colorado River riparian zone. Inaccurate maps may produce inaccurate measurements of ET and water loss from the region.

The crop fields in the riparian zone have been well-delineated and are fairly simple for USBR to update using satellite imagery (Bureau of Reclamation, 2008). Likewise, open water sources are not greatly taxing for USBR to map. However, the natural vegetation is much more heterogeneous in nature and therefore more challenging to map, by species. Existing maps of the natural riparian vegetation species are estimates of the dominant plant species only, by sub-region, which often exclude stands of less dominant species altogether (Anderson and Ohmart, 1976). Therefore, estimates of ET by the natural vegetation in LCRAS might be inaccurate.[3]

[3] For more information on LCRAS, see appendix A.

CHAPTER II

LITERATURE REVIEW

USBR is in need of a simpler, less expensive, and updated method of mapping natural riparian vegetation for LCRAS. It is likely that such a method can be developed using remote sensing imagery. However, USBR's resources of person-hours, processing power, and data storage are not unlimited. To develop a new remote sensing-based mapping method, one must define the goals of the project and determine the optimal type of imagery which can achieve those goals.

2.1 Optimal Spatial Resolution for Remote Sensing Applications

The optimal spatial resolution for any remote sensing study is highly dependent on the user's needs. The satellite sensors available to the general public have not been shown to have adequate spatial resolution[1] for every application. Some tasks may require high-resolution imagery from aircraft (aerial photography) to resolve the elements being studied. Other applications may not require such detail and data density. Ramsey and Laine (1997) found that Landsat TM imagery (30 m resolution) was sufficient to detect

[1] For a brief discussion of spatial and spectral resolution in digital imagery see appendix B.

changes in homogeneous regions of wetland vegetation in Southern Louisiana, but the same satellite imagery was not adequate in detecting changes in mixed vegetated areas. Because much of the wetlands being studied in that region consist of mixed vegetation, the authors concluded that Landsat image resolution was not sufficient for their ultimate goal of detecting changes in the vegetation pre- and post- Hurricane Andrew (*Id*). In South Africa, Riyad, et al. (2008) found that they required pixel sizes between 1.75 m and 2.3 m to accurately map insect infestations in commercially grown pine trees. High-resolution aerial photography was required for this study, as few satellites can achieve a resolution of 2.3 m. Quickbird is the only commercial satellite which approaches this resolution, at 2.4 m per pixel (Xie et al., 2008). Nijland, et al. (2009) needed resolutions of 55 m to map leaf area index (LAI) and 95 m to map above ground biomass in an area of heterogeneous natural vegetation in the Mediterranean. Though the authors' original imagery consisted of high resolution (5 m) aerial imagery, they found that degrading the imagery to the resolutions stated above were more accurate in mapping LAI and above-ground biomass. Menges et al. (2001) also note that the nature of the subject being mapped may affect the optimal image resolution. While mapping canopy density in the tropics of Northern Australia, they found that the height of the dominant vegetation type affected the optimal image resolution needed. ***These studies all emphasize that the optimal resolution of remotely sensed imagery will depend on the goal of the project and the environment being examined.***

2.2 Species Level Vegetation Mapping Using Remote Sensing Imagery

When the goal of a remote sensing project is to map vegetation at the species level, high resolution imagery (either high spectral or high spatial resolution[2]) is usually required. Xie et al. (2008) state that the Ikonos and Quickbird satellites (with resolutions of 4 m and 2.4 m, respectively) are well-suited for species level vegetation mapping, due to their relatively high spatial resolutions. The authors also note that the Hyperion sensor aboard NASA's EO-1 satellite may also be used for species level classification, because despite its rather low spatial resolution of 30 m, it collects data in 220 spectral bands. This suggests that hyperspectral[3] resolution may compensate for low spatial resolution. Hirano et al. (2003) explored this concept by mapping species level vegetation in the Florida Everglades using imagery from the Airborne Visible/Infrared Imaging Spectrometer (AVIRIS)[4]. Hirano et al. (2003) found that AVIRIS imagery could be used to identify vegetation species in the Everglades with varying success (between 40% and 100% accuracy, depending on the specific species.) This implies that hyperspectral resolution may not always be sufficient to overcome deficiencies in spatial resolution.

Considering spatial resolution only for species level vegetation mapping, Harman (2005), Wang et al. (2007), and Becker et al. (2007) had variable success at creating species level vegetation maps using high-resolution imagery. Harman (2005) was able to map the location of invasive species in Hawai'i using Quickbird (2.4 m) and Ikonos (4 m) imagery. Wang et al. (2007) used Quickbird to detect change in vegetation species along the Fire Island National Seashore and achieved an accuracy of 82%. Becker et al. (2007),

[2] See appendix B.
[3] See appendix B.
[4] AVIRIS is an aircraft mounted sensor that has collected data over North America, Europe, and parts of South America. It has a medium spatial resolution of 20 m and a hyperspectral resolution of 1 nm in 224 bands.

however, found that a spatial resolution of less than 2 m was necessary to map vegetation species in a Great Lakes coastal wetland with at least 85% accuracy.

2.3 Disadvantages of High Resolution Imagery

There are disadvantages in relying on high resolution imagery for species identification. Image availability often decreases as the spatial resolution of the image increases. Despite a published revisit time of 1 – 3.5 days for Quickbird, the latitude of the satellite's flight path strongly influences the image quality (Xie et al. 2008; Harman 2005). Due to Quickbird's altitude and high resolution sensors, the swath width is much narrower than other spaceborne sensors, and distortion at the edges of a Quickbird image are extreme (Harman 2005.) Thus, Quickbird images are often only usable if the study area falls close to the nadir. This limits the frequency of usable, available Quickbird images. Furthermore, Quickbird and Ikonos are commercial satellites, meaning that data from these platforms are not available for free. It must be purchased from the parent company, and this raises the cost of employing such imagery to map vegetation. Landsat and ASTER imagery may have much lower resolution than Quickbird and Ikonos, but both Landsat and ASTER are government run programs, and most of the resulting imagery is free to the public.

The availability of aerial photography is less frequent than spaceborne imagery, as aircraft are not in constant flight. The cost of planning, fuel, and pilot hours all must be considered when acquiring aerial imagery (Neale 2005). Furthermore, high resolution imagery increases the density of the data set, making it more expensive to store and process (Xie et al. 2008). One must also consider the extra person-hours required to analyze high resolution imagery, due to the increased data density. ***Thus, when trying to***

perform species-level classification using remotely-sensed data, there must be a balance between the spatial resolution needed to achieve the goals of the study and the resources (money, computing power, and time) available to the researcher. Though the literature suggests that high-resolution imagery is required to map vegetation at the species level, the cost of doing so can be prohibitive.

2.4 Vegetation Mapping in the Lower Colorado River Riparian Zone

Natural vegetation mapping in the Lower Colorado River riparian zone dates to the early and mid-1970s. Anderson and Ohmart (1976) sought to assess wildlife habitat in the region. They found that natural vegetation stands could be classified based on the quality of the habitat they provided for wildlife. Essentially, they discovered that habitat quality changed based on the dominant type of vegetation present, the overall height characteristics of the vegetation (such as all tall species, all short species, or a mixture of species), and canopy density. Using aerial photos and extensive ground surveys, they drew boundaries around stands of vegetation that had similar qualities (one type of dominant vegetation and/or similar density throughout), thereby dividing the region into polygons which could be independently classified. The original maps made by Anderson and Ohmart (1976) were updated, using the same classification scheme and methods, several times in the 1980s and ‘90s (Anderson and Ohmart, 1976, 1985; Younker and Andersen, 1986; Ohmart et al. 1988; CH2MHILL 1999). USBR began incorporating data from the maps into the Lower Colorado River Accounting System (LCRAS) when the first LCRAS report was published in 1994 (USBR 2008). The maps were digitized and updated in 1997 when an independent contractor hired by USBR created an Arc Info coverage map of the polygons and detected changes in the vegetation by interpreting

aerial photographs (CH2MHILL 1999). USBR conducts change detection analyses every year to see if dominant species or polygon boundaries have changed in the previous year, but USBR has made no major operational changes to the way it classifies natural vegetation in the Lower Colorado River riparian zone since 1976.

Other efforts to map the natural vegetation in the Lower Colorado River riparian zone have been carried out by Nagler et al. (2005.) Nagler et al. (2005) evaluated the existing Anderson-Ohmart classification system and tested methods to improve it. They combined high-resolution aerial digital photographs, oblique angle film aerial photos, and NDVI information from Landsat ETM+ and MODIS satellite imagery. By adding the oblique angle photos and NDVI data, they were able to map specimens of Cottonwood (*Populus fremontii*), willow (*Salix gooddingii*), and marsh vegetation (mostly cattails, *Typha domengensis*) at the species level with greater than 90% accuracy. The Andersen-Ohmart classification scheme allows these species to be identified only they constitute a pre-set percentage of a given stand of vegetation. For example, in the original Anderson-Ohmart classification scheme, Cottonwood must comprise 10% of the vegetation in a given polygon before it is counted as present. Nagler et al. (2005) could not, however, distinguish other prominent species from each other, including saltcedar (*Tamarix ramosissima*), arrowweed (*Pluchea sericea*), and mesquite (*Prosopis spp.*) Because these species may exercise different rates of ET, USBR would require that they be differentiated on a vegetation map used in LCRAS. Nagler et al. (2005) showed that their method was better than Anderson-Ohmart classification for delineating some species of natural vegetation in the Lower Colorado River riparian zone, but not all species of

interest could be discerned. Thus, this study may not represent adequate improvements to the Anderson-Ohmart system already employed by LCRAS.

CHAPTER III

OBJECTIVES

Until very recently, no full species-specific, high-resolution map had ever been made of the natural vegetation in the Lower Colorado River riparian zone. A map of this nature has now been made, but the process required the use of expensive, high-resolution aerial imagery, copious computer resources (in terms of both data storage and processing), and extensive person-hours. Furthermore, this map will be difficult to update in the future, as new high-resolution aerial imagery (with matching spatial resolution to the original map) will need to be acquired for accurate change detection.

The objective of this study is to develop a new method of mapping natural vegetation in the Lower Colorado River riparian zone. The new method must meet the following criteria:

- It must provide more or equally accurate and detailed information about the riparian vegetation than the current Anderson-Ohmart method
- The method must be inexpensive, both in terms of money, processing time, and data storage

- A majority of the data (excluding information gathered for error-assessment, and the existing high-resolution map) must come from low-resolution remote sensing platforms, or other easy to access sources.

We suspect that Landsat TM 5 satellite imagery, used in conjunction with the newly-created high-resolution map will be sufficient for our purposes. Within the context of mapping vegetation at the species level, Landsat TM 5 imagery is considered low-resolution data (30 m pixels.) Moreover, Landsat imagery is available free of charge from the United States Geological Survey. Also, only two Landsat TM 5 tiles are needed to get coverage of the entire study area, in seven spectral bands. Once these two tiles are stitched together and subsetted to the riparian zone, the resulting image is a 14 megabyte ERDAS Imagine .img file. For contrast, the 0.33 m resolution aerial photographs, with just three spectral bands, needed to produce the high-resolution map total several hundred gigabytes. Furthermore, the revisit time for Landsat TM 5 is 16 days, meaning that imagery of the entire study region is available as frequently as every 16 days (weather dependent.)

Using Landsat TM 5 clearly lowers the cost of mapping the riparian vegetation in the Lower Colorado River Basin. However, the relatively large 30 m pixels in Landsat imagery are likely incapable of adequately resolving certain vegetation species and/or other features of interest. Instead, we will focus on defining commonly occurring heterogeneous riparian species assemblages. At the very least, we hope to equal previous mapping efforts of the area (Anderson-Ohmart methods), but accomplish the task faster and cheaper than has been done in the past. This would require that we can identify large

stands of nearly homogeneous species (salt cedar, mesquite, arrowweed) and/or overall vegetation density without relying on extensive field surveys.

Ideally, we would like to show that our method, or the products of our method, can be used to predict coverage of vegetation species as they shift over the next several years. To confirm any predictions, however, would require an in situ error assessment, which is beyond the scope of this study. USBR will be in a position to test this in the future.

CHAPTER IV

MATERIALS AND METHODS

The basic approach of our method was to develop a set of spectral signatures which accurately discerned the most commonly occurring assemblages of riparian species in the Lower Colorado River Basin. A spectral-based mapping method has the advantage of not being dependent upon the physical location of objects on the ground. Thus, even if the locations of plant species shift over time, we predict that they will still have the same spectral emissions[1].

This method produced two products, to be used in concert with one another. The first product was a set of spectral signatures that can be used to group similar pixels in Landsat images of the Lower Colorado River Basin. The second product was a set of "zone" definitions which detail what the spectral signatures physically represent on the Earth's surface.

[1] Spectral signatures are likely to be consistent over time provided that they are measured during the same season, under similar atmospheric conditions. Dramatic changes in plant health and introduction of new dominating species may also alter spectral signatures. Such changes have not occurred in the Lower Colorado River Basin in the past forty years.

Landsat TM 5 images were used as the primary data source for developing the spectral signatures. A recently-developed high-resolution map of the riparian vegetation and other relevant ground cover types was used to define the signatures in the Landsat image. In other terms, the high-resolution map allowed us to ascertain what mix of vegetation species and other ground cover types were represented by the signatures in the Landsat image.

The high-resolution map used in this study was made from aerial photographs of the region, taken in mid-June 2004. Thus, the Landsat scenes were chosen based on the time of acquisition (June 16, 2004), which most closely corresponded to the time of year when the aerial photographs were taken. This was done to minimize differences associated with sun angle, seasonal vegetation cycles, and atmospheric conditions.

Using imagery from 2004 precluded us from performing an independent in situ error assessment of the final results. Instead, we divided our study area into three primary regions (CRIT North, CRIT South, and Cibola), developed an initial set of signatures for one of the regions, and then used the other two regions to test the robustness of the signatures across the river basin in general. In situ field error assessment (ground-truthing) is generally carried out as a final test of any remote sensing mapping project. However, to accomplish this for our study, we would need to wait until 2011, when new imagery is available and in situ field assessment could be carried out simultaneously. This task is beyond the scope of our study, but USBR will be in a position to carry out this assessment in the future.

4.1 Data Preparation

The data consisted of two Landsat TM 5 scenes with seven spectral bands and a spatial resolution of 30 m, and a high-resolution vegetation map of the area, with 0.33 m pixels and 10 ground cover classes. Refer to Figures 4-1 and 4-2. All Landsat images were stitched together and georeferenced to the 0.33 m pixel aerial photographs of the study area, using the ERDAS Imagine image processing software's geometric correction tool.

For ease of processing, and for comparison tests, the area of interest was divided into three sub-regions: CRIT North, CRIT South, and Cibola. Refer to Figure 4-1. Each region was extracted from both the Landat TM 5 image and the high-resolution map, using the same AOI file in ERDAS. The AOI files closely trimmed the images to the boundaries of the riparian vegetation, excluding as much agricultural vegetation as possible.

When preparing the Landsat TM 5 image for use in our study, we discovered that a thin layer of cloud cover had obscured most of the CRIT South sub-region. Refer to Figure 4-1. For this reason, we opted not to use CRIT South in developing or testing our products.

4.2 Methods

This study can be divided into three primary procedures:

I. **Product Development.** This involved developing the products which characterize the species assemblages found in one sub-region of the Lower Colorado River Basin

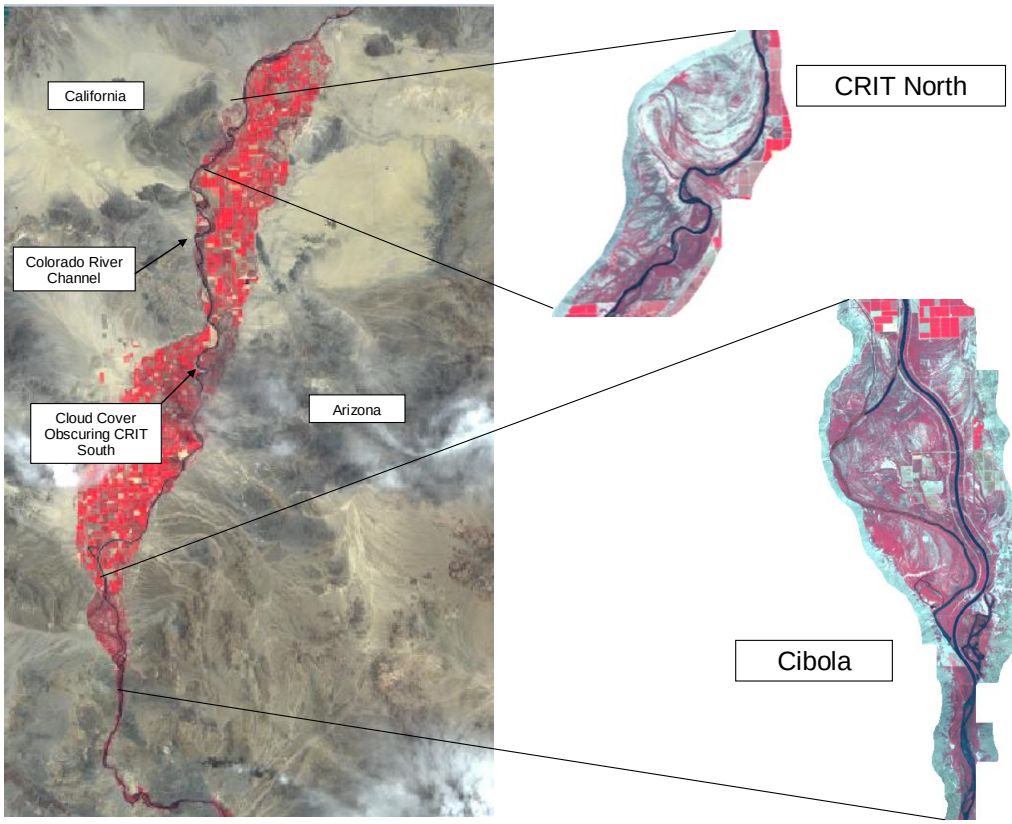

Figure 4-1. False-color Landsat TM 5 image from Lower Colorado River. The image above was extracted from a mosaic of two Landsat TM 5 scenes, both acquired by the satellite on June 16, 2004. The area includes three primary large sub-regions of riparian vegetation: CRIT North, CRIT South, and Cibola. CRIT South was partially obscured by cloud cover in this image, thus it was not used in this study. Note the sub-regions of CRIT North and Cibola to the right of the main image.

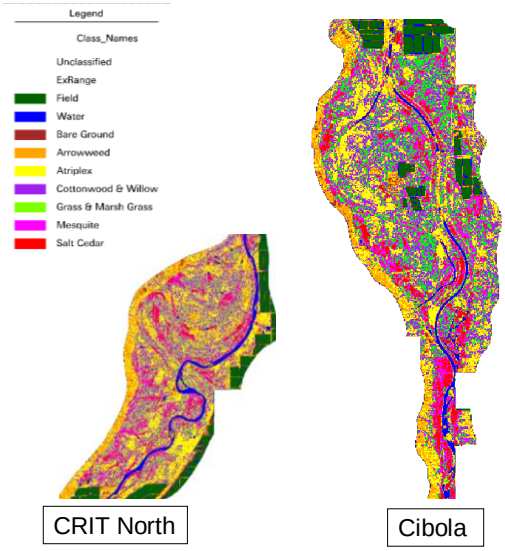

Figure 4-2. High-resolution ground cover map: CRIT North and Cibola.

II. **Product Testing.** The validity of the products were tested on a different sub-region

III. **Sensitivity Testing.** The sensitivity of the methodology was tested by repeating parts I and II using the same Landsat image and a *different, MORE ACCURATE* high-resolution ground cover map.

Each of these procedures involves several steps and processes. Refer to Figures 4-3, 4-4, and 4-5 for a summary of these steps, their order, and the section number in which each process is described in the text.

4.2.1 Methods I: Developing the Products in CRIT North

The first part of this study involves describing (characterizing) the riparian species assemblages found in one sub-region of the study area on the Landsat image. A combination of spectral-based classifications and statistical methods were used to accomplish this. The results produced two products:

1. a set of ***spectral signatures*** which can be used to identify and group similar pixels together into zones in a Landsat image, and
2. a set of ***zone definitions*** which describe the actual distribution of riparian vegetation species and other ground cover types represented by each zone.

CRIT North was chosen as the target sub-region for developing these products.

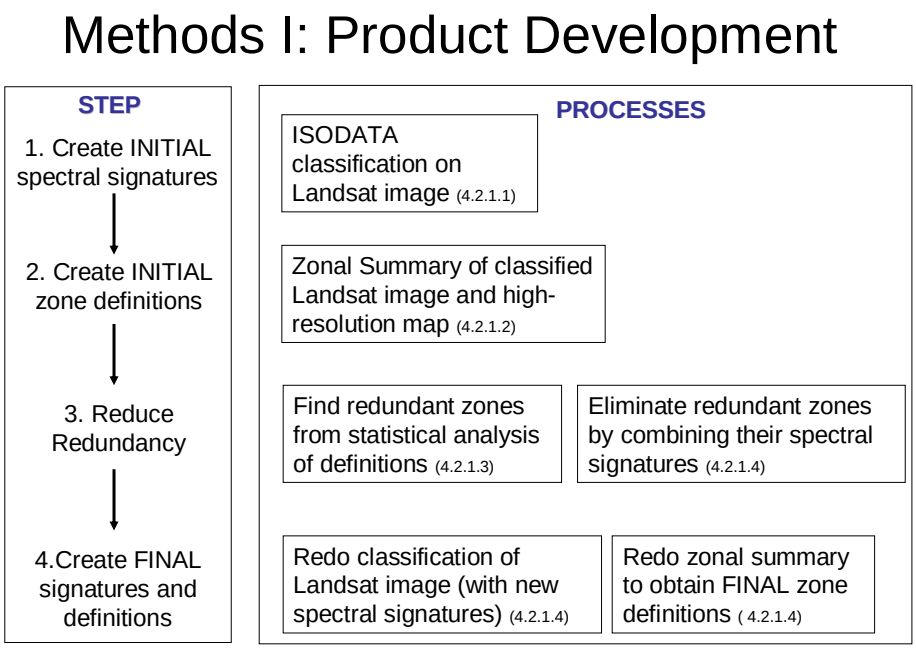

Figure 4-3. Summary of steps and processes of Methodology Part I: Product Development.

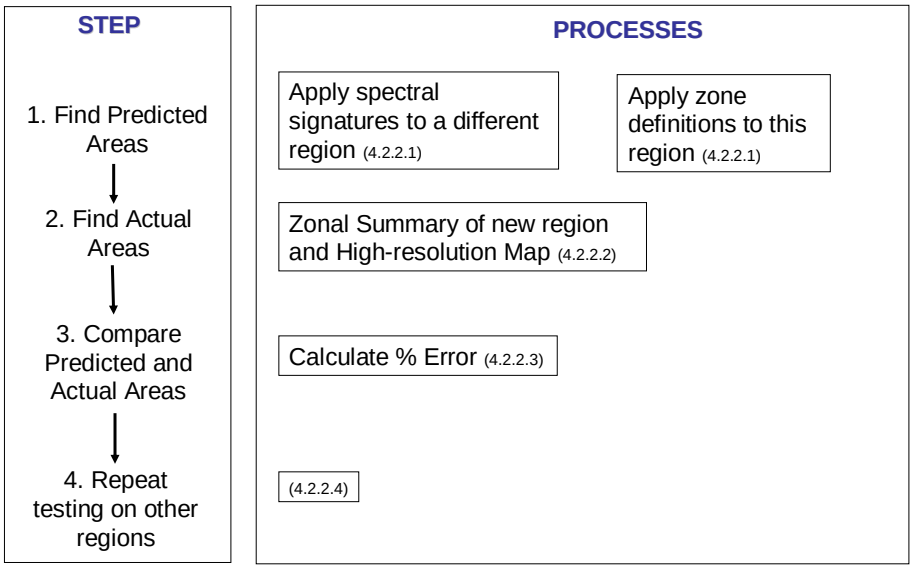

Figure 4-4. Summary of steps and processes of Methodology Part II: Product Testing.

Figure 4-5. Summary of Methodology Part III: Sensitivity Testing.

4.2.1.1 Developing Initial Spectral Signatures

A simple classification algorithm was applied to the Landsat image of CRIT North. We chose the ERDAS Imagine ISODATA[2] unsupervised classification algorithm. The ISODATA algorithm is a derivation of a statistical clustering procedure called *k-means*, optimized for digital pixel clustering. ISODATA quantitatively and iteratively places the pixels from a digital image into groups which exhibit similar spectral signatures. (NOTE: this is only a labeling procedure. ISODATA does not involve physically moving the pixels into contiguous clumps. Pixels belonging to the same group do not need to be next to one another. They must only have similar spectral characteristics.) The user may define the desired number of groups, the number of iterations, and the desired convergence threshold. The algorithm then decides which pixels should be grouped together. We ran the algorithm on CRIT North to develop a set of 50 clusters at a convergence threshold of .990. Fifty clusters were thought to be sufficient to capture the variability in vegetation species and other ground cover, while not being overly taxing to the computer. The resulting spectral definitions (also known as signatures) of the 50 clusters were saved into a separate signature file for use in the analysis. Refer to Figure 4-6 for examples of spectral signature plots. Refer to Figure 4-7 to see the ISODATA classified Landsat image of CRIT North.

4.2.1.2 Developing Initial Zone Definitions

The ISODATA algorithm provides a method of grouping similar pixels, but it does not provide any information as to what each group physically represents on the Earth's surface. To get an idea of this, we performed a zonal summary analysis of the

[2] The Iterative Self-Organizing Data Analysis Technique (ISODATA) is one of the simplest and most common algorithms used to cluster pixels in remotely-sensed data (including medical imaging). The ISODATA algorithm in ERDAS Imagine uses spectral information from the image to cluster pixels.

classified CRIT North image using the high-resolution vegetation map. A zonal summary analysis essentially involves overlaying an image with large "zones" on another image which provides detailed information about the contents of those zones. In our case, the pixels from each of the 50 clusters in the Landsat image represented the zones, and the high-resolution map provided details about their contents. Refer to Figure 4-8 for a more visual explanation of the "overlaying" zonal summary analysis procedure.

The zonal summary resulted in a count of the number of small pixels from the high-resolution map found within the boundaries of each cluster (hereafter called "zones") from the Landsat map. Each small pixel from the high-resolution map had previously been labeled as a particular type of ground cover. Thus, the zonal summary provided a count of the number of pixels of each ground cover type comprising each of the 50 zones in the Landsat image. From this information, we calculated the percent coverage of each type of ground cover comprising each zone. Refer to Table 4-1 and Table 4-2.

For example, zone 29 from the Landsat image of CRIT North contained 12,432,073 total pixels when overlaid with the high-resolution map. Of those pixels, 1,911,792 represent saltcedar, about 15.4% of the total for that zone. Thus zone 29 should, on average, contain 15.4% saltcedar wherever it is found in the Landsat image. This exercise was carried out for each zone and ground cover type combination, resulting in a complete set of 50 zone definitions.

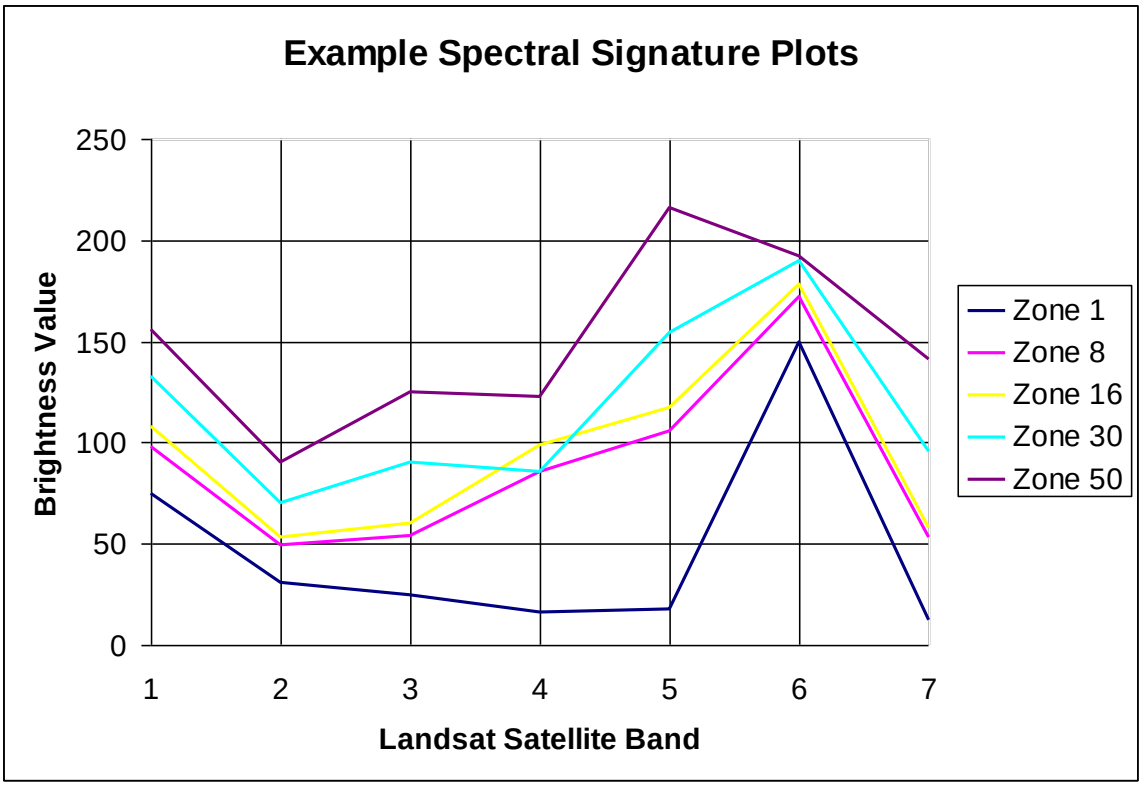

Figure 4-6. Example Spectral Signature Plots. The chart above is a plot of the spectral signatures for five of the fifty zones created from the ISODATA classification of CRIT North. Each Landsat satellite band (x-axis) is sensitive to electro-magnetic emissions in a specific part of the spectrum. The brightness values (y-axis) represent the intensity of radiation picked up by the sensor in each band. The collection of brightness values from all the bands for one zone defines that zone's spectral signature. For example, all of the image pixels lumped into zone 1 by the ISODATA classification have an average brightness value of 75 in band 1 and an average brightness value of 31 in band 2, 25 in band 3, 16 in band 4, etc. . These signatures may be used to cluster pixels in other images based on their spectral characteristics.

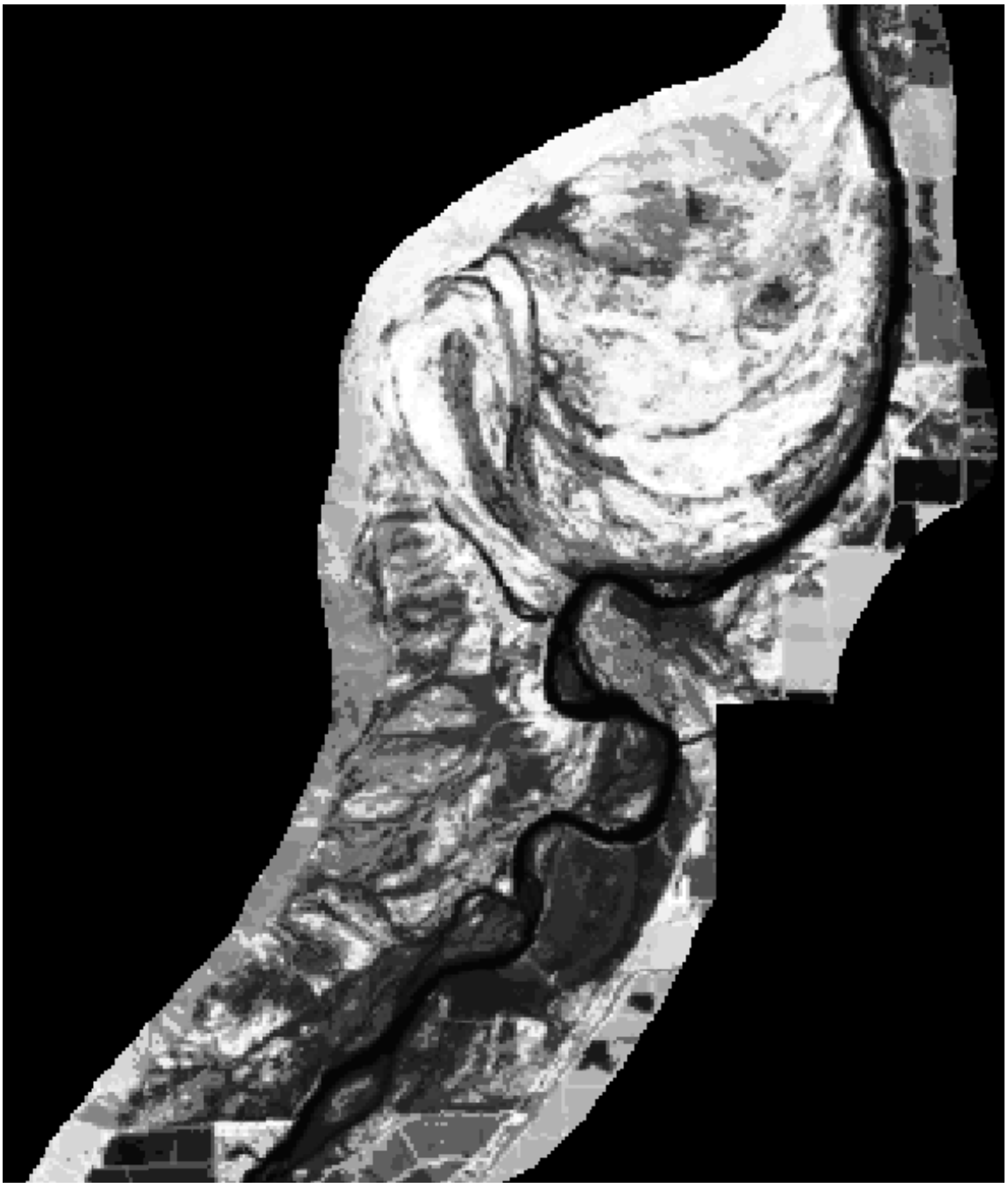

Figure 4-7. ISODATA classified Landsat image of CRIT North. The pixels in the image above have been clustered into fifty groups, or zones. Each zone is represented by a different shade of gray.

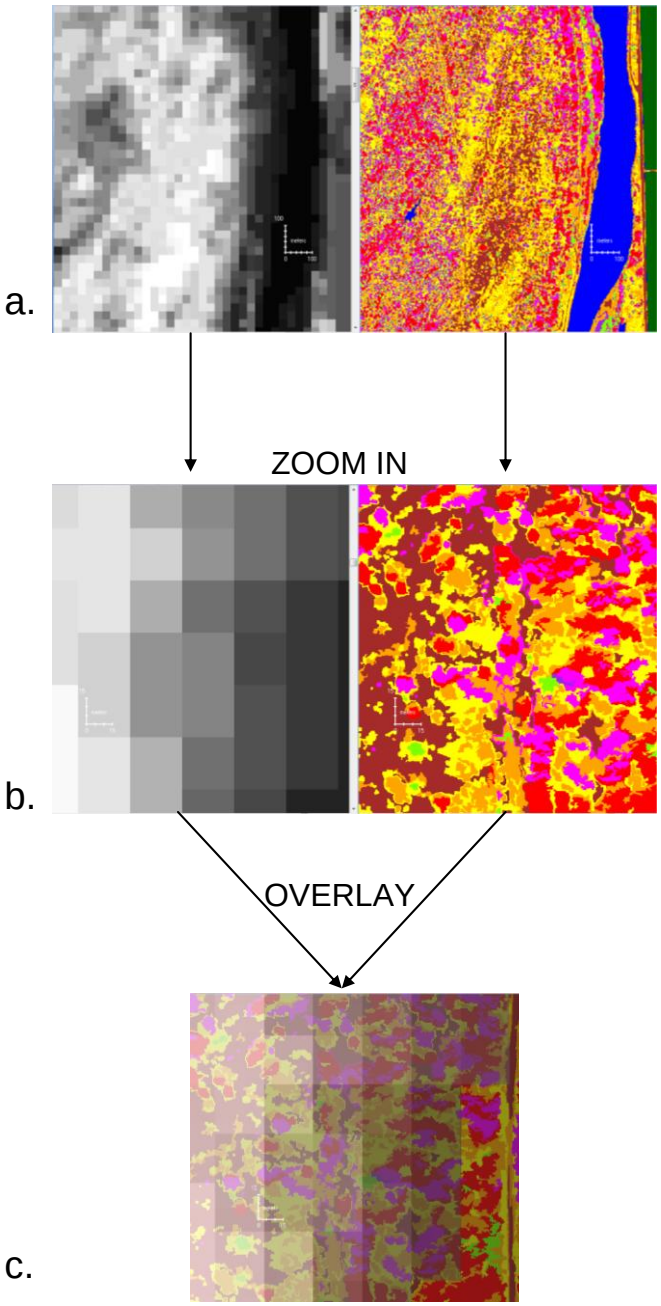

Figure 4-8. Overlaying for zonal summary analysis. In parts a and b of the figure at left, the image on the left is a portion of the ISODATA classified image of CRIT North. On the left is the corresponding portion of the high-resolution map. As one zooms in on the images, the difference in spatial resolution between the ISODATA classified image (30 m) and the high-resolution map (0.33 m) become apparent. In part c, the two images from part b have been overlain. The overlay allows one to determine which pixels from the high-resolution image correspond to the pixels in the ISODATA classified image. A zonal summary is the count of all high-resolution pixels (by class) which reside within the boundaries of a particular zone from the ISODATA classification.

Table 4-1: Initial Pixel Counts from CRIT North Zonal Summary

Zone	CLUSTER TOTAL	Unclass.	ExR	Field	Water	Bare Ground	Arrowweed	Atriplex	Cottonwood & Willow	Grass & Marsh	Mesquite	Saltcedar
0	471436435	471309244	0	36142	0	29001	33057	22886	0	388	1976	3741
1	14097308	4199	0	0	13515060	64689	166761	95736	20576	80502	43006	106779
2	4847144	171171	0	4550674	0	48759	57968	14146	383	650	884	2509
3	6326678	2186	0	0	4315110	204193	543890	248714	100053	244526	218990	449016
4	6679691	3352	0	0	2524196	297089	1127610	537787	234144	508928	522322	924263
5	10134112	2927	0	547035	352368	70359	1413921	1880206	210502	544653	2759400	2352741
6	5711096	111517	0	5542723	0	11567	11519	17938	365	3	10017	5447
7	16821139	1372	0	10701	463659	264841	3871240	3378508	439509	1224089	3536605	3630615
8	14007581	1244	0	177495	140245	309599	1924441	2112906	461508	1198198	3858888	3823057
9	11792105	5667	0	0	567146	291048	4321088	2665225	99496	1062191	1243205	1537039
10	6988106	5945	0	1281078	7387	51216	323369	403611	292792	414875	2603565	1604268
11	7383527	5757	0	0	638821	103733	2212591	1148874	63366	675460	1209524	1325401
12	11941075	5828	0	5595	343325	353177	3292132	2785552	194260	868125	1938256	2154825
13	14094863	18197	0	9604	276021	419746	3014790	2970396	371079	1067105	2823824	3124101
14	4813559	13264	0	262851	68531	475971	883481	1141600	112168	256208	691557	907928
15	6968324	206274	0	5904908	15318	258833	251346	171804	30854	8806	46937	73244
16	9426130	20925	0	229313	33239	137799	760734	1308762	642817	413110	3282520	2596911
17	8718692	54000	0	0	334176	290038	2715745	2337549	42456	457068	1392999	1094661
18	2884525	1635	0	142764	258403	368445	437799	435062	114393	119543	475360	531121
19	9207797	161247	0	7720839	38907	442013	410262	259304	12185	11109	67536	84395
20	6400624	108943	0	267245	35986	340152	713582	1275303	408986	172176	1716728	1361523
21	12398802	8272	0	124667	113330	794006	2242934	3743174	390404	260345	2557982	2163688
22	10812775	93543	0	226362	102813	599235	2427820	2984490	203739	462348	1750907	1961518
23	10739272	2568	0	2290	186604	406310	1727249	2477775	353074	427861	2778741	2376800
24	9840891	22325	0	9361	183551	925932	1793968	2765937	230246	273979	1848805	1786787
25	9868833	18113	0	0	233580	523188	2554715	3424665	88222	329912	1406296	1290142
26	6973673	366649	0	0	51156	1511465	3301549	1221080	10994	69114	225097	216569
27	8963182	51540	0	494	259907	867236	2564521	3085903	30051	176305	1015574	911651
28	5020467	48216	0	111256	22701	778348	856916	1116890	310974	90872	874623	809671
29	12432073	22212	0	35497	154830	1036301	2384007	4030582	298219	228355	2330278	1911792
30	9651197	260681	0	7990	150293	2544572	3267425	2261037	26136	109868	503231	519964
31	9584726	15820	0	150204	154328	1122323	2140089	3269363	136405	184408	1185031	1226755
32	5237229	147004	0	3962728	4742	428233	329088	225325	12199	19043	48532	60335
33	7787611	87151	0	551508	65645	1618082	1516490	2171969	160878	72109	832328	711451
34	12830520	162602	0	18872	227703	1457231	3837588	4447084	50569	183648	1206787	1238436
35	7779215	324813	0	6663271	19378	332967	174930	135458	25261	5540	47741	49856
36	3897507	0	0	0	399432	50799	1320427	678855	6104	99285	411700	930905
37	10802778	8364	0	9154	95395	1258612	2239550	3378126	196215	151896	1855534	1609932
38	13641297	131840	0	182622	107764	1972505	4299035	4518383	53708	160592	1101750	1113098
39	7796470	242197	0	6378531	14629	467911	330806	227212	20612	3955	32252	78365
40	2002953	60795	0	226560	833	822085	291945	197161	68107	10864	156062	168541
41	5835203	29039	0	715039	43762	1999900	1161551	1248730	45803	21000	295116	275263
42	11474132	319206	0	0	118388	2617508	4042373	2816417	21793	69250	745019	724178
43	7509059	87835	0	1145000	111154	538655	2042080	2172417	16694	67509	566314	761401
44	11673516	17453	0	70989	56264	2082768	2674701	3583970	213871	116173	1597324	1260003
45	15468534	99785	0	2819	76333	2324852	4535357	5015396	72592	103071	1732709	1505620
46	11718737	114666	0	0	63924	3075586	3352780	2934317	89842	72437	1046316	968869
47	12949493	90331	0	366764	7388	3366862	3471191	4077824	11299	30099	723868	803867
48	20194783	119431	0	49	52466	4657518	5462396	6265869	62735	90309	1837253	1646757
49	17526017	259556	0	0	9107	6349627	4541506	4134873	33715	52476	1060514	1084643
50	9597169	58733	0	15236	4	3867650	2537237	2158869	8644	15308	514153	421335

Table 4-2: Initial Zone Definitions (percent coverage by ground cover type) in CRIT North

Zone	CLUSTER TOTAL	Unclass.	ExR	Field	Water	Bare Ground	Arrowweed	Atriplex	Cottonwood & Willow	Grass & Marsh	Mesquite	Saltcedar
0	99.97	0.00	0.01	0.00	0.01	0.01	0.00	0.00	0.00	0.00	0.00	99.97
1	0.03	0.00	0.00	95.87	0.46	1.18	0.68	0.15	0.57	0.31	0.76	0.03
2	3.53	0.00	93.88	0.00	1.01	1.20	0.29	0.01	0.01	0.02	0.05	3.53
3	0.03	0.00	0.00	68.20	3.23	8.60	3.93	1.58	3.86	3.46	7.10	0.03
4	0.05	0.00	0.00	37.79	4.45	16.88	8.05	3.51	7.62	7.82	13.84	0.05
5	0.03	0.00	5.40	3.48	0.69	13.95	18.55	2.08	5.37	27.23	23.22	0.03
6	1.95	0.00	97.05	0.00	0.20	0.20	0.31	0.01	0.00	0.18	0.10	1.95
7	0.01	0.00	0.06	2.76	1.57	23.01	20.08	2.61	7.28	21.02	21.58	0.01
8	0.01	0.00	1.27	1.00	2.21	13.74	15.08	3.29	8.55	27.55	27.29	0.01
9	0.05	0.00	0.00	4.81	2.47	36.64	22.60	0.84	9.01	10.54	13.03	0.05
10	0.09	0.00	18.33	0.11	0.73	4.63	5.78	4.19	5.94	37.26	22.96	0.09
11	0.08	0.00	0.00	8.65	1.40	29.97	15.56	0.86	9.15	16.38	17.95	0.08
12	0.05	0.00	0.05	2.88	2.96	27.57	23.33	1.63	7.27	16.23	18.05	0.05
13	0.13	0.00	0.07	1.96	2.98	21.39	21.07	2.63	7.57	20.03	22.16	0.13
14	0.28	0.00	5.46	1.42	9.89	18.35	23.72	2.33	5.32	14.37	18.86	0.28
15	2.96	0.00	84.74	0.22	3.71	3.61	2.47	0.44	0.13	0.67	1.05	2.96
16	0.22	0.00	2.43	0.35	1.46	8.07	13.88	6.82	4.38	34.82	27.55	0.22
17	0.62	0.00	0.00	3.83	3.33	31.15	26.81	0.49	5.24	15.98	12.56	0.62
18	0.06	0.00	4.95	8.96	12.77	15.18	15.08	3.97	4.14	16.48	18.41	0.06
19	1.75	0.00	83.85	0.42	4.80	4.46	2.82	0.13	0.12	0.73	0.92	1.75
20	1.70	0.00	4.18	0.56	5.31	11.15	19.92	6.39	2.69	26.82	21.27	1.70
21	0.07	0.00	1.01	0.91	6.40	18.09	30.19	3.15	2.10	20.63	17.45	0.07
22	0.87	0.00	2.09	0.95	5.54	22.45	27.60	1.88	4.28	16.19	18.14	0.87
23	0.02	0.00	0.02	1.74	3.78	16.08	23.07	3.29	3.98	25.87	22.13	0.02
24	0.23	0.00	0.10	1.87	9.41	18.23	28.11	2.34	2.78	18.79	18.16	0.23
25	0.18	0.00	0.00	2.37	5.30	25.89	34.70	0.89	3.34	14.25	13.07	0.18
26	5.26	0.00	0.00	0.73	21.67	47.34	17.51	0.16	0.99	3.23	3.11	5.26
27	0.58	0.00	0.01	2.90	9.68	28.61	34.43	0.34	1.97	11.33	10.17	0.58
28	0.96	0.00	2.22	0.45	15.50	17.07	22.25	6.19	1.81	17.42	16.13	0.96
29	0.18	0.00	0.29	1.25	8.34	19.18	32.42	2.40	1.84	18.74	15.38	0.18
30	2.70	0.00	0.08	1.56	26.37	33.86	23.43	0.27	1.14	5.21	5.39	2.70
31	0.17	0.00	1.57	1.61	11.71	22.33	34.11	1.42	1.92	12.36	12.80	0.17
32	2.81	0.00	75.66	0.09	8.18	6.28	4.30	0.23	0.36	0.93	1.15	2.81
33	1.12	0.00	7.08	0.84	20.78	19.47	27.89	2.07	0.93	10.69	9.14	1.12
34	1.27	0.00	0.15	1.77	11.36	29.91	34.66	0.39	1.43	9.41	9.65	1.27
35	4.18	0.00	85.65	0.25	4.28	2.25	1.74	0.32	0.07	0.61	0.64	4.18
36	0.00	0.00	0.00	10.25	1.30	33.88	17.42	0.16	2.55	10.56	23.88	0.00
37	0.08	0.00	0.08	0.88	11.65	20.73	31.27	1.82	1.41	17.18	14.90	0.08
38	0.97	0.00	1.34	0.79	14.46	31.51	33.12	0.39	1.18	8.08	8.16	0.97
39	3.11	0.00	81.81	0.19	6.00	4.24	2.91	0.26	0.05	0.41	1.01	3.11
40	3.04	0.00	11.31	0.04	41.04	14.58	9.84	3.40	0.54	7.79	8.41	3.04
41	0.50	0.00	12.25	0.75	34.27	19.91	21.40	0.78	0.36	5.06	4.72	0.50
42	2.78	0.00	0.00	1.03	22.81	35.23	24.55	0.19	0.60	6.49	6.31	2.78
43	1.17	0.00	15.25	1.48	7.17	27.19	28.93	0.22	0.90	7.54	10.14	1.17
44	0.15	0.00	0.61	0.48	17.84	22.91	30.70	1.83	1.00	13.68	10.79	0.15
45	0.65	0.00	0.02	0.49	15.03	29.32	32.42	0.47	0.67	11.20	9.73	0.65
46	0.98	0.00	0.00	0.55	26.25	28.61	25.04	0.77	0.62	8.93	8.27	0.98
47	0.70	0.00	2.83	0.06	26.00	26.81	31.49	0.09	0.23	5.59	6.21	0.70
48	0.59	0.00	0.00	0.26	23.06	27.05	31.03	0.31	0.45	9.10	8.15	0.59
49	1.48	0.00	0.00	0.05	36.23	25.91	23.59	0.19	0.30	6.05	6.19	1.48
50	0.61	0.00	0.16	0.00	40.30	26.44	22.49	0.09	0.16	5.36	4.39	0.61

4.2.1.3 Eliminating Redundancy and Developing Final Spectral Signatures

By this point in the methodology we had produced initial versions of both products: a set of spectral signatures from the ISODATA classification, and the set of corresponding zone definitions to characterize the signatures on the Earth's surface.

Having defined the zones in CRIT North in terms of actual ground cover and species assemblages, the next step was to numerically evaluate those zonal definitions and eliminate redundancy. We used a hierarchical statistical clustering procedure, called Ward's clustering, to accomplish this. Ward's clustering is based on evaluating data variance. The algorithm operates by establishing *n* number of clusters (of one data point each) and then iteratively combining the data into fewer clusters in such a way that the minimum of information is lost (maximum variance is preserved) at each iteration. Eventually, all the data are grouped into one cluster, effectively ignoring all variance and uniqueness in the data set. This process can be plotted as a tree which begins at the "leaves" (each data point in its own cluster), combines the "leaves" into "branches" (similar data points are grouped together), and eventually reaches the "trunk" (all the data are placed in one all-inclusive cluster.) Refer to Figure 4-9 for an example tree plot.

Figure 4-10 depicts a Ward's clustering tree for 9 clusters, lettered A through I. At the start of the clustering procedure, all 9 clusters are separate from each other; they are the "leaves" of the tree. The first leaves to be joined are G and H. This means that combing G and H removes the least amount of variance among all the clusters. Clusters B and C are combined next, followed by E and F, and then EF and GH. Eventually, all the clusters are combined at the "trunk", the base of the tree plot.

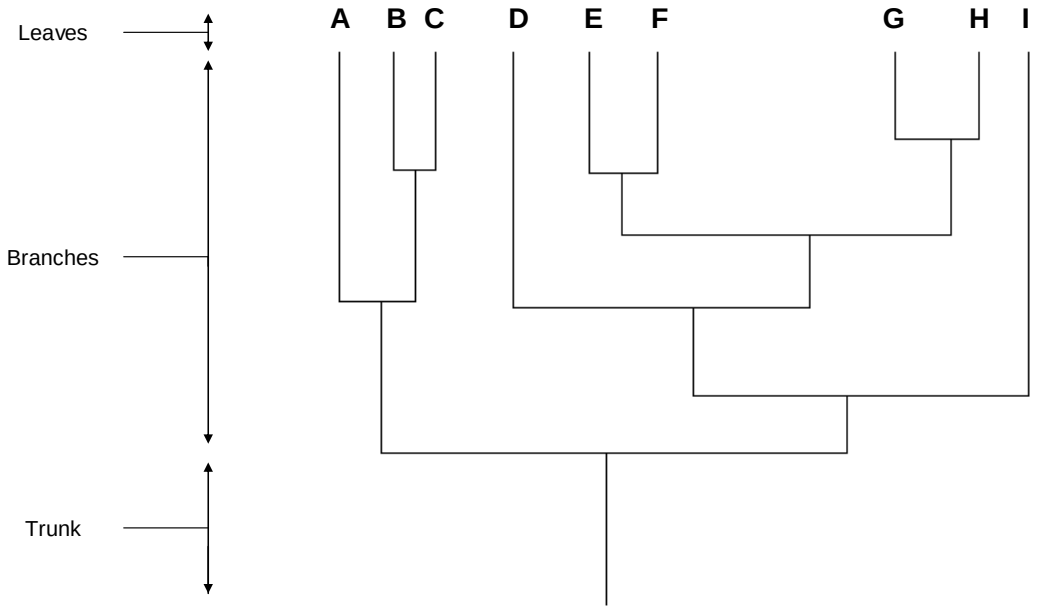

Figure 4-9. Example Ward's clustering tree plot.

We used the SAS software package to conduct the Ward's clustering analysis. After each iteration of the algorithm, SAS calculates the R square, which represents the proportion of variance of the data represented by the clusters at that step. R square values decrease after each iteration, as data are clustered together. SAS also provides statistical measures (cubic clustering criterion, pseudo F, and pseudo t^2) which estimate an appropriate number of clusters. These statistics can be used in conjunction with the R square values to:

1. estimate how many clusters are needed to adequately account for the variance in the data, and
2. determine which data points can be combined while minimizing the loss of useful information.

In our case, each data "point" was a single zone definition, or the set of numbers which described the percent ground cover type within each zone, as determined from the zonal analysis of CRIT North. A Ward's cluster is a grouping of those zones, based on the parameters of the Ward's clustering algorithm. A Ward's clustering analysis was performed on the zone definitions from CRIT North to establish candidate clusters. The pseudo t^2 statistic was used to identify a proper number of clusters. Refer to Figure 4-10, which plots the pseudo t^2 plot for the Ward's clustering analysis of CRIT North. In Figure 4-10 the number of clusters one step to the right of a peak in the plot may be considered a candidate number of clusters. This plot indicates that 18 clusters is an appropriate number. The Ward's tree plot clustering results from CRIT North were used to determine which zones should be clumped together. See Figure 4-11. This information was used in the next step to combine zones.

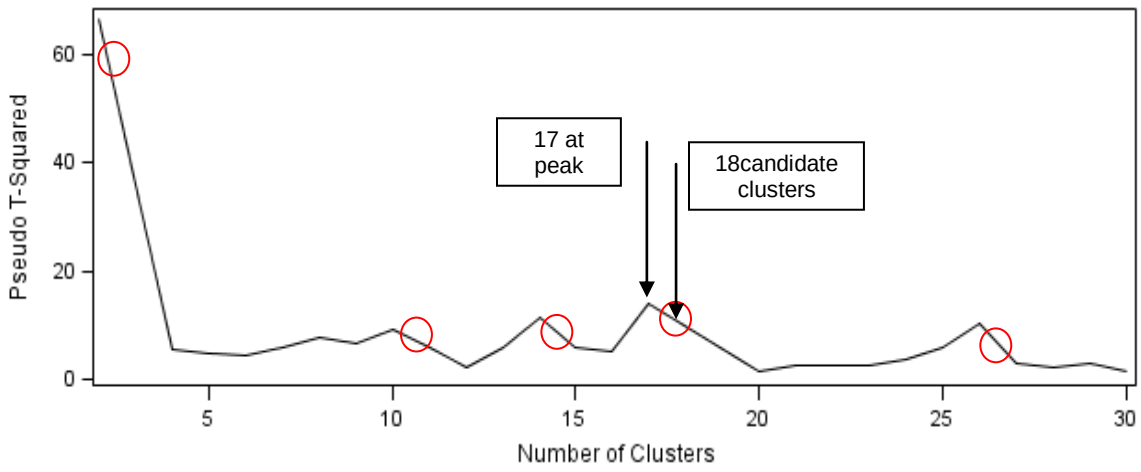

Figure 4-10. Pseudo t^2 plotted against number of clusters. The plot above is from the Ward's clustering analysis of the initial zone definitions from CRIT North. Red circles highlight possible final numbers of clusters for this data set. The plot indicates that 18 is an appropriate number of clusters (one step to the right of the peak at 17 clusters.)

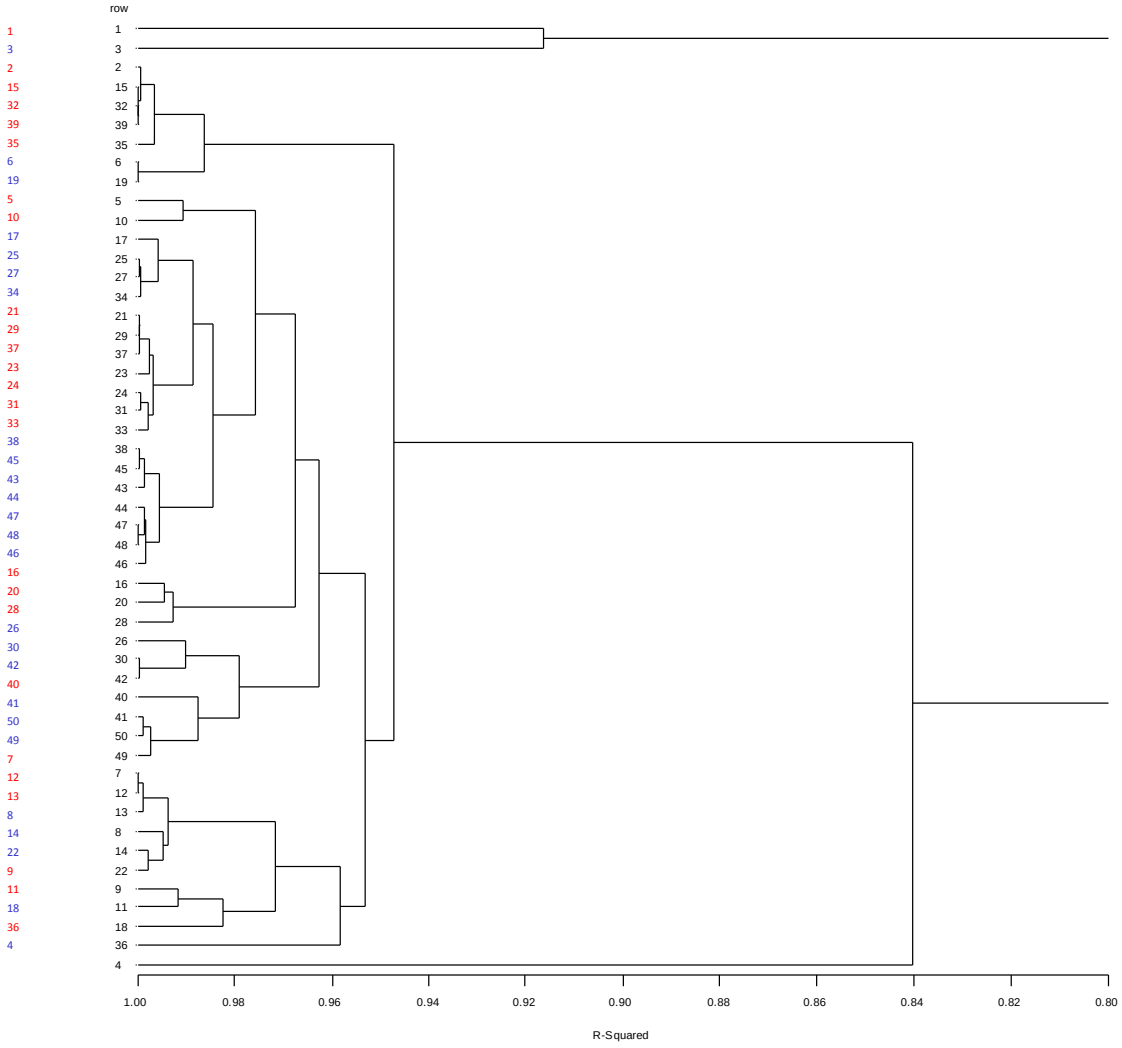

Figure 4-11. Ward's clustering tree plot. The plot above shows the hierarchical clustering of zones for the CRIT North initial zone definitions. At left, the color-coded numbers indicate which zones should be combined, based on the clustering algorithm. For example, the algorithm suggests that zone 1 and zone 3 should remain independent, but zones 2, 15, 32, 39, and 35 should be combined into a single zone. This process resulted in 18 final zones, from the initial 50.

4.2.1.4 Developing Final Spectral Signatures and Zone Definitions

The Ward's clustering procedure discovered redundant zones by examining the zone definitions. To combine zones, we combined their corresponding spectral using the ERDAS Imagine Signature Editor. The Signature Editor merges spectral signatures together, and outputs new, more inclusive spectral signatures in their place. The resulting set of new signatures was the final version of this product from our study.

The new signature file contained fewer zones with slightly different spectral definitions than the original 50 zone file. This new set of signatures was used to re-classify the original CRIT North Landsat image, by placing the image pixels into groups as defined by the new signatures. This type of classification is called "supervised", because the classes are defined by a priori knowledge of the area. Refer to Figure 4-12 to see the reclassified CRIT North Landsat image, using the final set of spectral signatures. A new zonal summary with the high-resolution map was carried out on this newly-classified Landsat image, and the resulting zone definitions (percent coverage of ground cover type) were saved for testing. This set of zone definitions was the final version of this product. Refer to Table 4-3 for the final zone definitions.

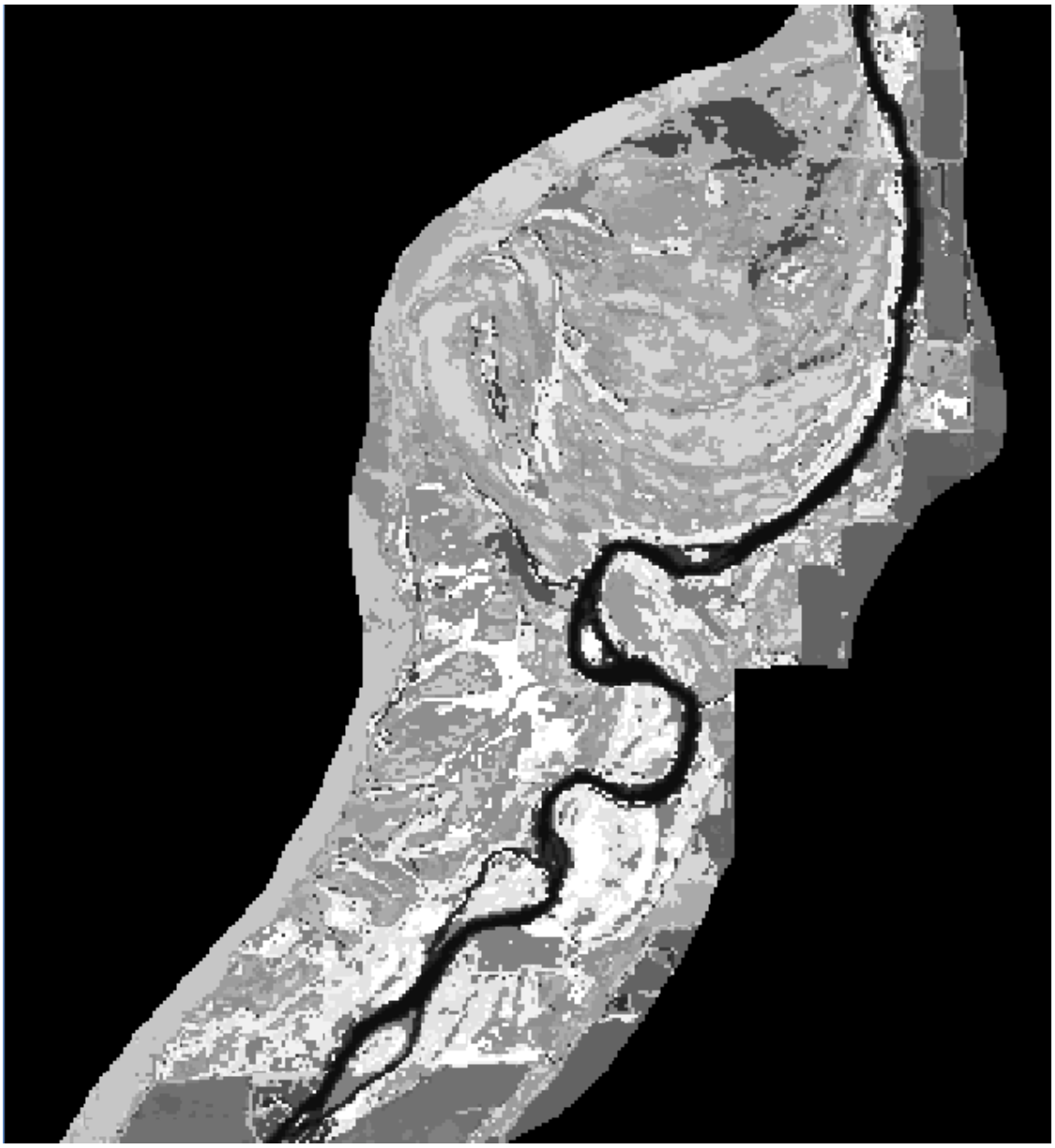

Figure 4-12. Reclassified Landsat image of CRIT North. The image above was created by applying the final 18 spectral signatures to the Landsat image of CRIT North. The zones are represented in 18 shades of gray.

Table 4-3: Final Zone Definitions (percent coverage by ground cover type) for CRIT North

Zone	Unclass	ExR.	Field	Water	Bare Ground	Arrowweed	Atriplex	Cottonwood & Willow	Grass & Marsh	Mesquite	Saltcedar
0	99.97	0.00	0.01	0.00	0.01	0.01	0.00	0.00	0.00	0.00	0.00
1	0.03	0.00	0.00	96.39	0.43	1.06	0.58	0.13	0.47	0.28	0.64
2	0.04	0.00	0.00	70.17	2.79	8.19	3.65	1.48	3.87	3.10	6.70
3	0.06	0.00	1.93	36.17	5.70	16.83	8.33	3.05	7.08	7.77	13.07
4	0.18	0.00	5.97	7.57	12.24	15.31	15.91	3.81	4.02	16.10	18.89
5	0.00	0.00	0.00	7.28	2.39	32.42	24.48	0.22	2.25	10.92	20.04
6	2.31	0.00	9.57	1.08	39.67	17.09	10.45	3.18	1.04	7.07	8.55
7	3.98	0.00	82.66	0.17	5.59	3.85	2.30	0.23	0.10	0.37	0.74
8	1.74	0.00	89.36	0.16	3.31	2.54	1.96	0.03	0.06	0.36	0.48
9	0.04	0.00	8.85	1.46	0.61	10.22	14.05	3.43	5.81	31.40	24.11
10	0.45	0.00	0.03	2.21	7.65	28.37	34.40	0.51	2.81	12.41	11.17
11	0.24	0.00	0.68	1.30	10.54	19.28	30.05	2.42	1.99	17.93	15.57
12	0.65	0.00	1.89	0.44	17.22	27.20	31.93	0.58	0.71	10.25	9.14
13	0.77	0.00	3.44	0.41	5.98	11.00	18.14	6.26	2.92	28.72	22.36
14	3.50	0.00	0.03	1.01	24.06	38.49	22.09	0.19	0.80	4.79	5.03
15	0.99	0.00	2.11	0.15	36.15	25.32	23.65	0.22	0.27	5.71	5.44
16	0.04	0.00	0.00	1.92	2.04	23.28	21.48	2.08	7.59	20.44	21.14
17	0.10	0.00	0.52	0.84	4.75	18.62	22.28	2.86	6.04	20.85	23.12
18	0.05	0.00	0.00	5.43	1.41	34.31	20.65	1.06	9.14	13.10	14.84

4.2.2 Methods II: Testing Spectral Signatures and Zone Definitions

As stated previously, to truly evaluate how well the signatures and zone definitions developed in the previous steps depict actual ground cover in CRIT North, we would need to ground-truth the results. However, by employing the high-resolution map from 2004 as the basis of our zonal definitions, we eliminated ground-truthing as a method of error assessment for this study. We simply could not go back in time to field check CRIT North in 2004. Instead, we tested whether or not our signatures and zonal definitions could predict the area covered by each riparian vegetation species and ground cover type in the other two sub-regions of our study area. These predictions were compared to actual areal ground coverage, calculated from the high-resolution map.

The entire testing procedure completed twice. One execution tested the final spectral signatures and zonal definitions (18 final zones) as developed in Methods I. The second execution tested the initial spectral signatures and zonal definitions (50 original zones). Refer to Figures 4-13 and 4-14 for the classified Landsat images of Cibola using the 18 zones defined in Methods I and using the 50 initial zones identified early in Methods I. The testing results were compared between the two runs, to check the usefulness of reducing redundancy in the zones.

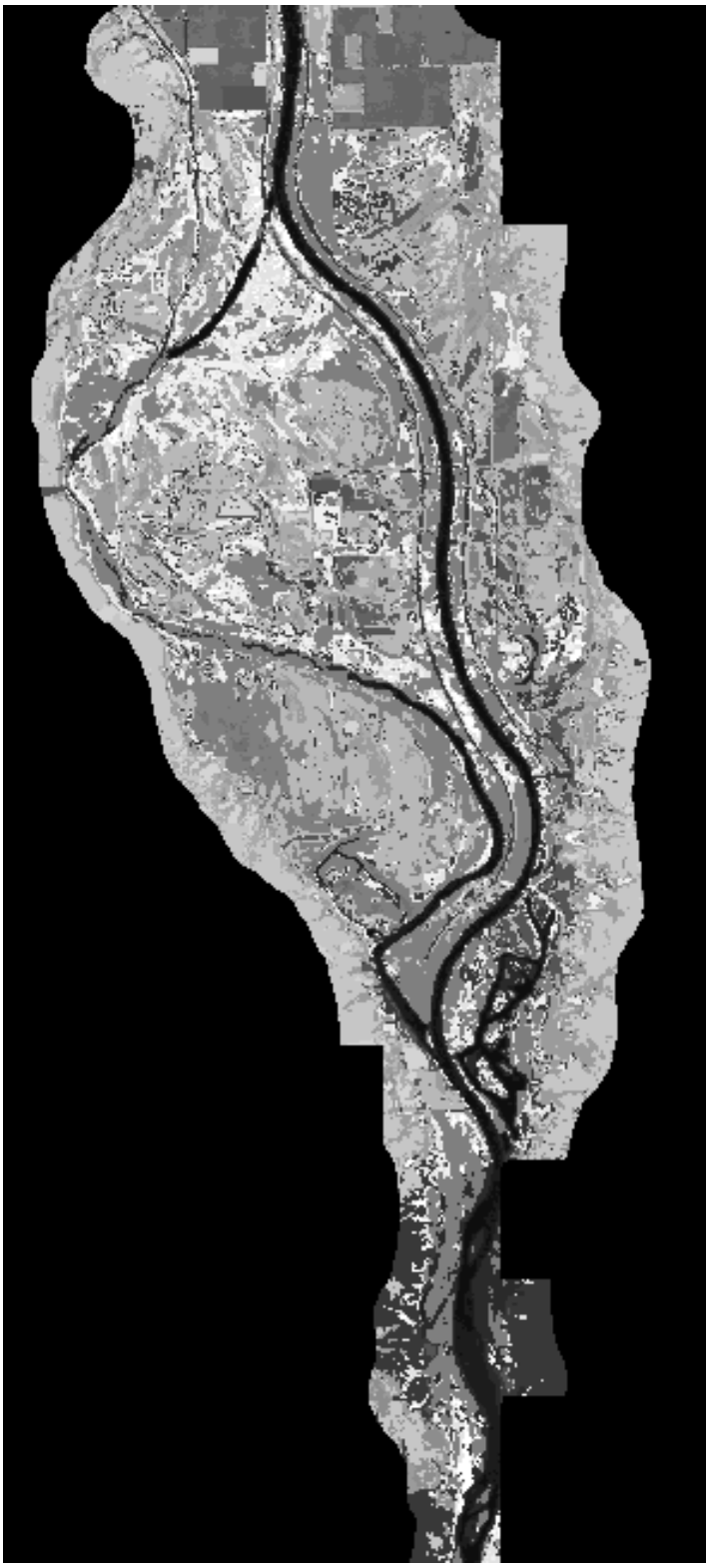

Figure 4-13. Classified Landsat image of Cibola, 18 zones. The image above depicts the Landsat image of Cibola, classified by the 18 spectral signatures developed in Methods I on CRIT North.

Figure 4-14. Classified Landsat image of Cibola, 50 zones. The image above depicts the Landsat image of Cibola, classified by the initial 50 spectral signatures developed in Methods I on CRIT North.

4.2.2.1 Predicting Areal Coverage of Ground Cover Types in Cibola

Beginning with the Cibola sub-region, we classified the Landsat image of Cibola using the final spectral signature file developed for CRIT North. We then multiplied the histogram (pixel count) from each zone by 900 m^2, which is the area of a single Landsat pixel. This provided the area covered by each zone in Cibola. Finally, we split the area of each zone into the proportion of each ground cover type as defined by the zone definitions from CRIT North (the definitions being tested.) The predicted areal coverages are reported in chapter 5.

4.2.2.2 Calculating Actual Areal Coverage of Ground Cover Types in Cibola

To calculate the actual areal coverages, we conducted a zonal analysis of Cibola by overlaying the Cibola Landsat image (classified by the signatures from CRIT North) with the corresponding area of the high-resolution map. This zonal analysis resulted in the ACTUAL percent coverage of each ground cover type comprising each of the zones.

The zonal analysis also provided a count of the number of pixels from the high-resolution map falling within each zone in Cibola. These pixel counts were converted to areas by multiplying them by 0.0929 m^2 (the area of one pixel in the high-resolution map.) Finally, these areas were divided into the proportions of each ground cover type from the zonal analysis of Cibola. The actual areal coverages are reported in chapter 5.

4.2.2.3 Comparing Predicted Areas to Actual Areas

The areas of all the ground cover types in Cibola, as predicted by the zone definitions from CRIT North, were compared to the actual areas as calculated from a direct zonal analysis of Cibola. To do this, we calculated the percent difference between the predicted area and the actual area. The percent difference was calculated for each type

of ground cover, and for each type of ground cover within each zone. By calculating the percent difference, we were able to determine if our spectral signatures and zone definitions developed from CRIT North led to over- or under-prediction of area in Cibola. The percent error results are reported in chapter 5.

4.2.2.4 Repeat Testing procedure on Other Sub-regions

As mentioned previously, the Landsat image from June 16, 2004 was partially obscured by cloud cover in the CRIT South region, thus we could not repeat the testing procedure on this sub-region. However, with a complete high-resolution map of the entire Lower Colorado River Basin, the testing procedure could potentially be done on any sub-region in the riparian zone.

4.2.3 Methods III: Sensitivity Testing

The final part of this study was to repeat the study (all of Methods I and II) with the same Landsat image, but a different, more accurate high-resolution map. The intention was to check if the percent error in predicted versus actual species coverage was *sensitive to differences in the accuracy of the high-resolution map*. A change in the percent errors would indicate that the method does exhibit sensitivity to changes in the high-resolution map, thus implying that the method is not regionally or image dependent. If this is the case, it would indicate that the method could be used to predict areal species coverage in future Landsat images, without the need of a new, labor-intensive high-resolution map.

The testing procedure in the sensitivity run was done only once, on the final spectral signatures and zone definitions, after completing a Ward's clustering analysis.

In addition to using a new high-resolution map, the sensitivity run also used pre-

defined polygon vectors to force-classify the agricultural fields in the Landsat image after the ISODATA classification was completed for CRIT North, and after the supervised classification of Cibola. The polygon vectors consisted of outlines of the existing agricultural fields in each region. The pixels from the Landsat images which corresponded to the areas covered by the field polygons were reassigned to a single zone, representing the fields. Force-classifying the fields reduce inaccuracies in the analysis caused by different field types and conditions. For example, recently irrigated fields are often misclassified as water, while dry, fallow fields look like bare ground. By using our a priori knowledge to classify the fields, we eliminate these errors. The pre-defined polygon vectors had already been created by USBR in 1994, and these files are regularly updated for the annual reports of ET produced by USBR. Thus, force-classifying the fields add very little burden to the methods employed in this study.

The following series of figures and tables detail the development of products from the sensitivity run, using a more accurate, updated high-resolution map. Figure 4-15 shows the updated high-resolution map. The most noticeable changes from the old map are the prominent stands of saltcedar dominating both CRIT North and Cibola in the new map. Figure 4-16 is the ISODATA classification of CRIT North with the fields force-classified. Tables 4-4 and 4-5 show the initial zone definitions, found from the zonal summary of the CRIT ISODATA classification and the new high-resolution map. Figures 4-17 and 4-18 show the results of the Ward's clustering analysis executed on the zone definitions. Table 4-6 shows the final zone definitions (percent coverage only shown.) Figure 4-19 is the final classified Landsat image of CRIT North, using the final set of spectral signatures and the field polygon vectors. Figure 4-20 is the Cibola classified

Landsat image, made from the final zone definitions, with the fields force-classified. The percent errors from the sensitivity run are reported in chapter 5.

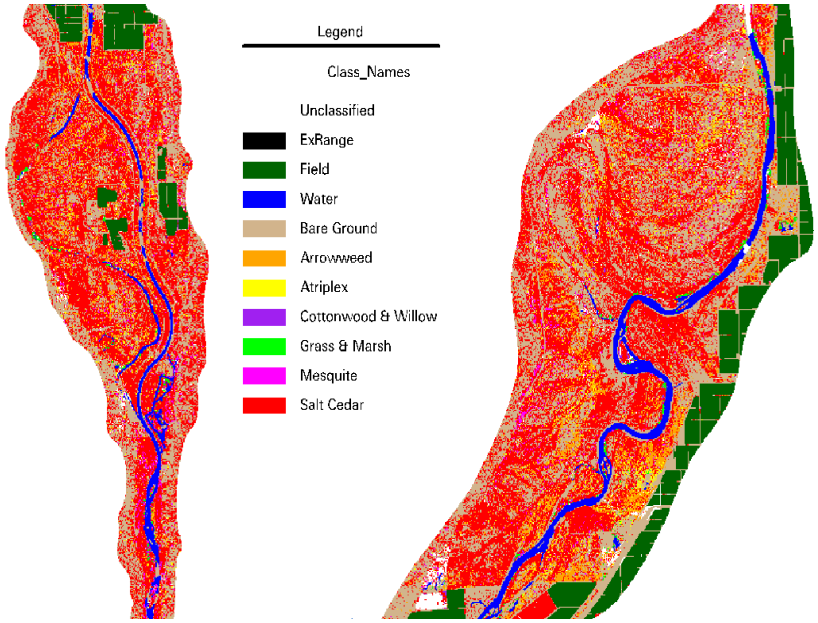

Figure 4-15. Newly updated high-resolution map, sensitivity run. The high-resolution maps above of Cibola (left) and CRIT North (right) were used as the basis for zonal summary analyses in the sensitivity run. Note the greater extent of saltcedar in the new maps compares to the old map, from Figure 4-3.

Figure 4-16. ISODATA Classification of CRIT North, sensitivity run. In the image above, the ISODATA procedure was carried out on the Landsat image of CRIT North. The fields were force-classified from existing polygon vectors of the fields.

Table 4-4: Initial Pixel Counts from CRIT North Zonal Summary, Sensitivity Run

Zone	CLUSTER TOTAL	Unclass.	ExR.	Field	Water	Bare Ground	Arrowweed	Atriplex	Cottonwood & Willow	Grash & Marsh	Mesquite	Saltcedar
0	460623197	460531089	0	0	0	47092	1293	219	72	3	1522	41907
1	14174336	704759	0	0	12636770	509861	30643	9718	6265	77860	5024	193436
2	51241281	566226	0	50491045	0	134787	576	0	97	0	725	47825
3	6259648	326941	0	0	3636902	1191791	74953	33798	25169	196713	39729	733652
4	6495742	243909	0	0	1778522	1961755	142985	74603	81562	369451	51805	1791150
5	10557916	220634	0	0	405123	743559	767276	399215	149242	342780	244292	7285795
6	1391471	1106772	0	0	0	88704	1869	717	30907	0	2693	159809
7	14965267	296111	0	0	176988	1198070	1650861	759593	95954	248991	318256	10220443
8	11879429	182218	0	0	324078	2110190	2352515	797798	69811	208339	130593	5703887
9	11245550	212602	0	0	155980	1355176	2581223	548211	3885	104682	198320	6085471
10	5955452	382540	0	0	23922	198729	100838	129258	21256	32196	267494	4799219
11	15992561	389369	0	0	90453	1671087	1593669	589297	51990	243906	401331	10961459
12	8978541	449804	0	0	531	713338	242393	329537	39839	9073	484944	6709082
13	15392394	327939	0	0	65901	2449195	1708604	596064	14743	80673	352625	9796650
14	2931400	66061	0	0	404780	1085550	101552	47247	18172	87573	58496	1061969
15	1796719	433708	0	0	0	610257	8816	9611	23023	0	3600	707704
16	2718450	199126	0	0	2477	1098370	33938	16083	3128	2305	13942	1349081
17	7212868	115364	0	0	134707	1055077	1866838	476972	276	37265	108143	3418226
18	11522838	299496	0	0	67557	2458332	1546855	531290	6401	53468	257428	6302011
19	10508314	280667	0	0	11630	2317198	504638	362966	16639	41252	198186	6775138
20	2143859	295430	0	0	0	1013468	29427	9999	5885	1035	4381	784234
21	6688889	387085	0	0	46828	970630	170171	234963	28142	10464	334431	4506175
22	10402449	198978	0	0	29663	3738036	1024637	417329	4362	24359	156284	4808801
23	10504684	366137	0	0	27265	2108205	544980	471659	8428	21065	288125	6668820
24	8445540	213736	0	0	0	2124097	187924	295220	4458	1983	232506	5385616
25	7969472	208485	0	0	33484	2115419	1510575	447039	488	13715	137953	3502314
26	7387976	229635	0	0	93385	2332598	336652	296558	13231	13310	188438	3884169
27	9090943	411299	0	0	6396	4478916	571277	172888	930	0	79812	3369425
28	5280567	252496	0	0	18594	2508170	171830	109733	15306	5435	77271	2121732
29	12102716	296789	0	0	29131	4760675	1452946	642044	1124	11640	195290	4713077
30	11364130	362953	0	0	7694	6453161	598410	286810	751	542	160045	3493764
31	12014358	314326	0	0	47644	3861961	543082	543932	8941	15589	285290	6393593
32	1000390	411189	0	0	7292	424633	3470	4779	1137	2068	2894	142928
33	1778880	101233	0	0	21310	1030965	24352	21119	10396	0	45694	523811
34	12956163	446202	0	0	2034	6995423	682914	418772	9	0	216223	4194586
35	12233304	275954	0	0	29214	5939766	926098	513544	1661	6968	240216	4299883
36	1277910	304487	0	0	0	817609	10847	7366	674	1914	4887	130126
37	11139447	322385	0	0	23543	4021907	377633	466199	7878	5558	295576	5618768
38	7068918	180791	0	0	0	1811844	1072984	456751	0	0	141097	3405451
39	1960003	115720	0	0	0	1375797	31898	11848	8240	252	9601	406647
40	861039	57690	0	0	0	555181	5346	5531	11092	0	13476	212723
41	7460127	159527	0	0	1189	5035494	305159	253268	603	1041	137956	1565890
42	12593066	439646	0	0	1867	6504410	465837	429014	3052	1347	290600	4457293
43	6784334	177491	0	0	0	2328530	770546	474009	0	767	185077	2847914
44	13693395	304652	0	0	3571	7421129	654650	478290	3812	5798	252389	4569104
45	14464121	267915	0	0	447	7502865	862770	628638	1349	880	394060	4805197
46	6494860	204767	0	0	2427	3795567	121513	195447	11820	2287	152651	2008381
47	16641367	135838	0	0	0	10574547	322192	377929	24	0	500432	4730405
48	21729424	438590	0	0	2994	12024521	699272	728502	9302	1679	664704	7159860
49	17133861	343257	0	0	0	11180738	288025	370864	1463	0	353549	4595965
50	10179059	76028	0	0	0	7872065	115767	183867	556	0	201953	1728823

Table 4-5: Final Zone Definitions (percent coverage by ground cover type) in CRIT North, Sensitivity Run

Zone		Unclass.	ExR	Field	Water	Bare Ground	Arrowweed	Atriplex	Cottonwood & Willow	Grass & Marsh	Mesquite	Saltcedar
0		99.98	0.00	0.00	0.00	0.01	0.00	0.00	0.00	0.00	0.00	0.01
1		4.97	0.00	0.00	89.15	3.60	0.22	0.07	0.04	0.55	0.04	1.36
2		1.11	0.00	98.54	0.00	0.26	0.00	0.00	0.00	0.00	0.00	0.09
3		5.22	0.00	0.00	58.10	19.04	1.20	0.54	0.40	3.14	0.63	11.72
4		3.75	0.00	0.00	27.38	30.20	2.20	1.15	1.26	5.69	0.80	27.57
5		2.09	0.00	0.00	3.84	7.04	7.27	3.78	1.41	3.25	2.31	69.01
6		79.54	0.00	0.00	0.00	6.37	0.13	0.05	2.22	0.00	0.19	11.48
7		1.98	0.00	0.00	1.18	8.01	11.03	5.08	0.64	1.66	2.13	68.29
8		1.53	0.00	0.00	2.73	17.76	19.80	6.72	0.59	1.75	1.10	48.01
9		1.89	0.00	0.00	1.39	12.05	22.95	4.87	0.03	0.93	1.76	54.11
10		6.42	0.00	0.00	0.40	3.34	1.69	2.17	0.36	0.54	4.49	80.59
11		2.43	0.00	0.00	0.57	10.45	9.97	3.68	0.33	1.53	2.51	68.54
12		5.01	0.00	0.00	0.01	7.94	2.70	3.67	0.44	0.10	5.40	74.72
13		2.13	0.00	0.00	0.43	15.91	11.10	3.87	0.10	0.52	2.29	63.65
14		2.25	0.00	0.00	13.81	37.03	3.46	1.61	0.62	2.99	2.00	36.23
15		24.14	0.00	0.00	0.00	33.97	0.49	0.53	1.28	0.00	0.20	39.39
16		7.32	0.00	0.00	0.09	40.40	1.25	0.59	0.12	0.08	0.51	49.63
17		1.60	0.00	0.00	1.87	14.63	25.88	6.61	0.00	0.52	1.50	47.39
18		2.60	0.00	0.00	0.59	21.33	13.42	4.61	0.06	0.46	2.23	54.69
19		2.67	0.00	0.00	0.11	22.05	4.80	3.45	0.16	0.39	1.89	64.47
20		13.78	0.00	0.00	0.00	47.27	1.37	0.47	0.27	0.05	0.20	36.58
21		5.79	0.00	0.00	0.70	14.51	2.54	3.51	0.42	0.16	5.00	67.37
22		1.91	0.00	0.00	0.29	35.93	9.85	4.01	0.04	0.23	1.50	46.23
23		3.49	0.00	0.00	0.26	20.07	5.19	4.49	0.08	0.20	2.74	63.48
24		2.53	0.00	0.00	0.00	25.15	2.23	3.50	0.05	0.02	2.75	63.77
25		2.62	0.00	0.00	0.42	26.54	18.95	5.61	0.01	0.17	1.73	43.95
26		3.11	0.00	0.00	1.26	31.57	4.56	4.01	0.18	0.18	2.55	52.57
27		4.52	0.00	0.00	0.07	49.27	6.28	1.90	0.01	0.00	0.88	37.06
28		4.78	0.00	0.00	0.35	47.50	3.25	2.08	0.29	0.10	1.46	40.18
29		2.45	0.00	0.00	0.24	39.34	12.01	5.30	0.01	0.10	1.61	38.94
30		3.19	0.00	0.00	0.07	56.79	5.27	2.52	0.01	0.00	1.41	30.74
31		2.62	0.00	0.00	0.40	32.14	4.52	4.53	0.07	0.13	2.37	53.22
32		41.10	0.00	0.00	0.73	42.45	0.35	0.48	0.11	0.21	0.29	14.29
33		5.69	0.00	0.00	1.20	57.96	1.37	1.19	0.58	0.00	2.57	29.45
34		3.44	0.00	0.00	0.02	53.99	5.27	3.23	0.00	0.00	1.67	32.38
35		2.26	0.00	0.00	0.24	48.55	7.57	4.20	0.01	0.06	1.96	35.15
36		23.83	0.00	0.00	0.00	63.98	0.85	0.58	0.05	0.15	0.38	10.18
37		2.89	0.00	0.00	0.21	36.11	3.39	4.19	0.07	0.05	2.65	50.44
38		2.56	0.00	0.00	0.00	25.63	15.18	6.46	0.00	0.00	2.00	48.17
39		5.90	0.00	0.00	0.00	70.19	1.63	0.60	0.42	0.01	0.49	20.75
40		6.70	0.00	0.00	0.00	64.48	0.62	0.64	1.29	0.00	1.57	24.71
41		2.14	0.00	0.00	0.02	67.50	4.09	3.39	0.01	0.01	1.85	20.99
42		3.49	0.00	0.00	0.01	51.65	3.70	3.41	0.02	0.01	2.31	35.39
43		2.62	0.00	0.00	0.00	34.32	11.36	6.99	0.00	0.01	2.73	41.98
44		2.22	0.00	0.00	0.03	54.19	4.78	3.49	0.03	0.04	1.84	33.37
45		1.85	0.00	0.00	0.00	51.87	5.96	4.35	0.01	0.01	2.72	33.22
46		3.15	0.00	0.00	0.04	58.44	1.87	3.01	0.18	0.04	2.35	30.92
47		0.82	0.00	0.00	0.00	63.54	1.94	2.27	0.00	0.00	3.01	28.43
48		2.02	0.00	0.00	0.01	55.34	3.22	3.35	0.04	0.01	3.06	32.95
49		2.00	0.00	0.00	0.00	65.26	1.68	2.16	0.01	0.00	2.06	26.82
50		0.75	0.00	0.00	0.00	77.34	1.14	1.81	0.01	0.00	1.98	16.98

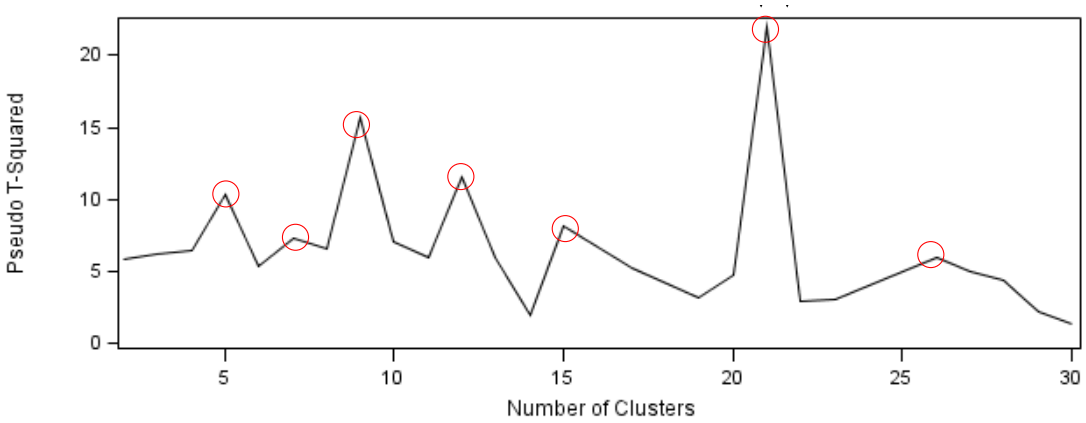

Figure 4-17. Pseudo t^2 plotted against number of clusters, sensitivity run. The plot above is from the Ward's clustering analysis of the initial zone definitions from CRIT North The plot indicates that 22 is an appropriate number of clusters (one step to the right of the peak at 21.)

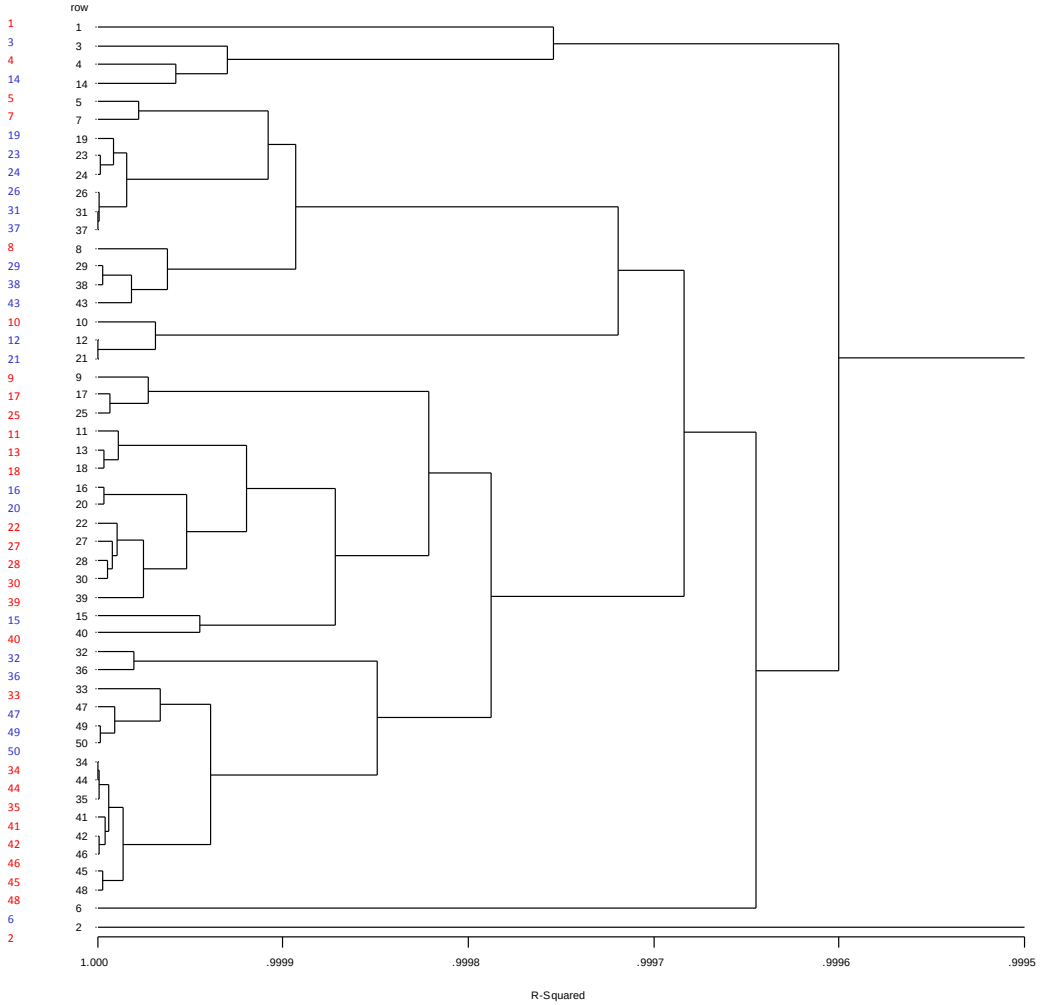

Figure 4-18. Ward's clustering tree plot, sensitivity run.

Figure 4-19. Reclassified Landsat image of CRIT North, sensitivity run. The image above was created by applying the final 22 spectral signatures to the Landsat image of CRIT North. The zones are represented in 22 shades of gray. Fields were force-classified.

Table 4-6. Final Zone Definitions (percent coverage by ground cover type) in CRIT North, Sensitivity Run

Zone		Unclass.	ExR.	Field	Water	Bare Ground	Arrowweed	Atriplex	Cottonwood &Willow	Grash/marsh	Mesquite	Saltcedar
0		99.98	0.00	0.00	0.00	0.01	0.00	0.00	0.00	0.00	0.00	0.01
1		5.06	0.00	0.00	89.93	3.08	0.20	0.06	0.03	0.44	0.04	1.16
2		1.07	0.00	98.58	0.00	0.26	0.00	0.00	0.00	0.00	0.00	0.09
3		5.04	0.00	0.00	59.55	18.55	1.20	0.52	0.39	3.08	0.57	11.11
4		4.13	0.00	0.00	27.10	29.91	2.25	1.13	1.33	5.46	0.82	27.86
5		79.89	0.00	0.00	0.00	5.17	0.13	0.04	2.51	0.00	0.19	12.07
6		1.52	0.00	0.00	1.51	15.05	20.11	6.54	0.57	1.69	1.38	51.64
7		7.01	0.00	0.00	0.15	3.05	2.10	2.36	0.35	0.48	4.65	79.86
8		2.95	0.00	0.00	10.42	40.33	4.89	1.66	0.76	2.75	1.71	34.52
9		25.78	0.00	0.00	0.06	36.31	0.47	0.41	1.15	0.02	0.17	35.63
10		6.35	0.00	0.00	1.03	53.73	2.01	2.02	0.40	0.08	3.20	31.18
11		7.70	0.00	0.00	0.00	63.88	0.62	0.57	1.16	0.40	1.56	24.12
12		1.54	0.00	0.00	1.34	6.58	9.65	4.61	0.88	2.09	2.32	70.99
13		2.74	0.00	0.00	0.16	26.61	4.03	4.08	0.09	0.13	2.50	59.68
14		2.65	0.00	0.00	0.16	36.27	11.81	5.62	0.01	0.06	1.98	41.45
15		4.86	0.00	0.00	0.18	10.28	2.63	3.61	0.35	0.12	4.75	73.21
16		1.77	0.00	0.00	1.22	17.21	22.83	5.66	0.02	0.56	1.71	49.01
17		2.32	0.00	0.00	0.38	15.25	10.92	4.10	0.14	0.81	2.27	63.81
18		8.96	0.00	0.00	0.04	46.36	1.12	0.44	0.17	0.06	0.25	42.59
19		3.66	0.00	0.00	0.25	51.61	6.28	2.66	0.06	0.08	1.27	34.13
20		35.18	0.00	0.00	0.34	54.89	0.41	0.28	0.17	0.19	0.26	8.28
21		1.30	0.00	0.00	0.00	65.43	1.97	2.36	0.01	0.00	2.59	26.33
22		2.46	0.00	0.00	0.03	54.65	4.41	3.60	0.03	0.02	2.24	32.55

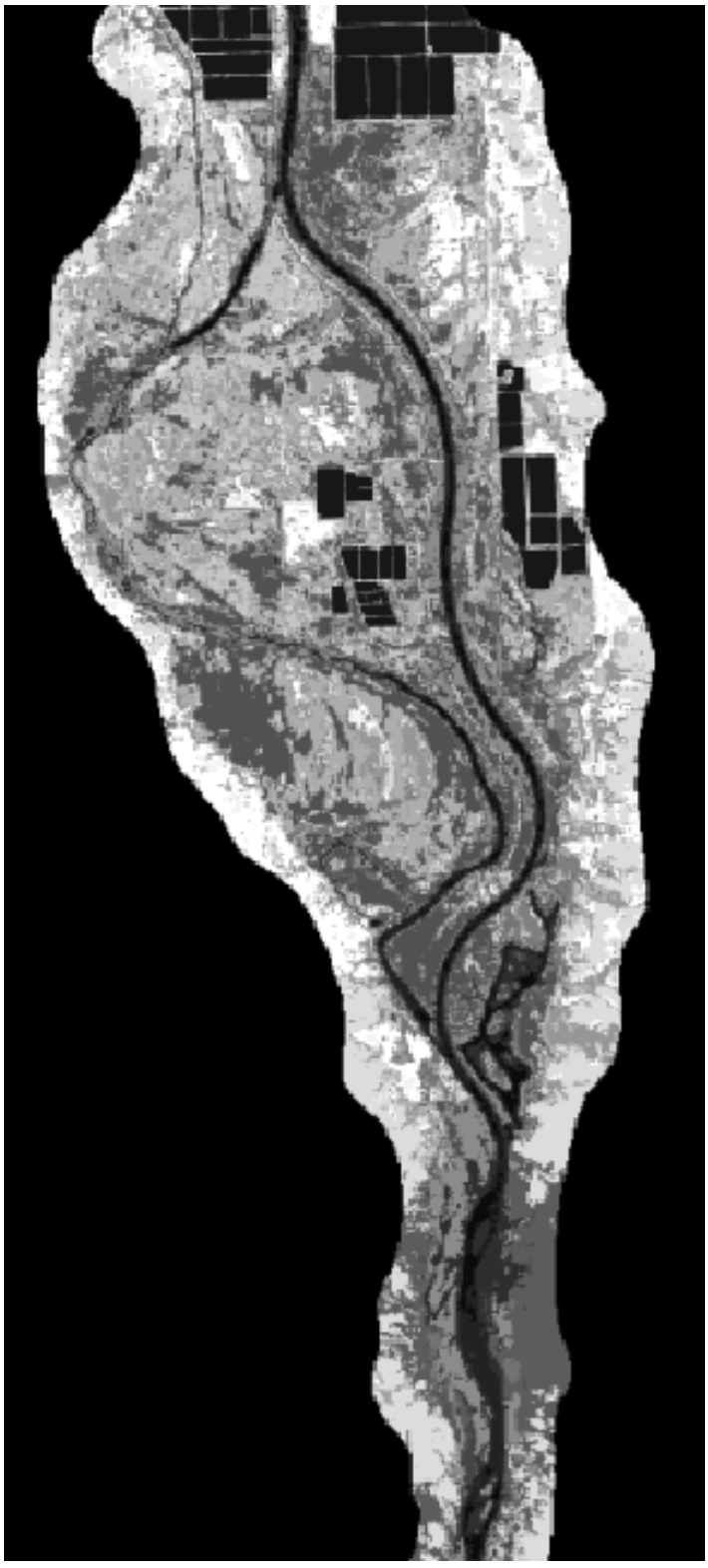

Figure 4-20. Classified Landsat image of Cibola, sensitivity run. The image above depicts the Landsat image of Cibola, classified by the 22 spectral signatures developed from CRIT North. Fields are force-classified.

CHAPTER V

RESULTS

The results reported in this chapter consist of the percent error calculations (as described in section 4.2.2 Methods II) between predicted and actual coverage of various ground cover classes in Cibola. The testing procedure outlined in section 4.2.2 was executed three times, each time on a specific set of spectral signatures and zone definitions. Those sets were as follows:

1. Set of **18** spectral signatures and zone definitions
    - Using ORIGINAL high-resolution map; after Ward's clustering
2. Set of **50** spectral signatures and zone definitions
    - Using ORIGINAL high-resolution map; NO Ward's clustering
3. Set of **22** spectral signatures and zone definitions (Sensitivity Run)
    - Using UPDATED high-resolution map; after Ward's clustering

For ease of discussion, the results (percent errors) from each of these sets will be referred to by number (1, 2, or 3) as listed above. The results for each set are presented separately.

5.1 Set 1 Results

Table 5-1 shows the predicted area covered by each ground cover class within each zone, and the regional total area (for Cibola) covered by each ground cover type across all the zones, as predicted by the signatures and definitions from set 1. All predicted areas are reported in square meters.

Table 5-2 shows the actual area covered by each ground cover class within each zone, and the regional total area (for Cibola) covered by each ground cover type across all the zones, using the spectral signatures from set 1. All actual areas are reported in square meters.

Table 5-3 shows the percent error in predicted versus actual areas for Cibola, using the signatures and definitions from set 1. Regional total errors vary considerably across ground cover types, from an error of -0.82% for saltcedar, to an error of 72.05% for grass & marsh. Errors within zones also vary. For example, in zone 9 fields were over-predicted by 3,900%, but in zone 7 fields were under-predicted by just 6.7%.

5.2 Set 2 Results

Tables 5-4, 5-5, and 5-6 present the predicted areas, actual areas, and percent errors, respectively, for set 2 in Cibola. In Table 5-6, regional total percent errors generally increased in magnitude from Table 5-3. There was no ground cover class for which there was an improvement in percent error in set 2 over set 1. Refer to Table 5-10 for a comparison of regional total percent errors among all three sets of results.

5.3 Set 3 Results

Tables 5-7, 5-8, and 5-9 present the predicted areas, actual areas, and percent errors, respectively, for set 3 in Cibola. In Table 5-9, from the regional total percent error

for most ground cover classes showed improvement in set 3 over sets 1 and 2. In some cases these improvements were large. For example, the percent error for cottonwood & willow improved from 43.75% in set 1 and 45.73% in set 2 to 9.17% in set 3. Fields, which were over predicted by 8.57% in set 1 and 22.6% in set 2, were under predicted by just 1.07% in set 3. Grass & marsh, bare ground, and unclassified pixels were the only classes which saw an increase in the magnitude of percent error from sets 1 and 2 to set 3. Refer to Table 5-10 for a comparison of the regional total percent errors for all three sets.

Table 5-1. Predicted Areas (m^2) by Zone and Ground Cover Type, Cibola Set 1

Zone		Unclass.	ExR.	Field	Water	Bare Ground	Arrowweed	Atriplex	Cottonwood & Willow	Grass & Marsh	Mesquite	Saltcedar
0		74927280	0	5746	0	4610	5255	3638	0	62	314	595
1		598	0	0	2019571	8922	22215	12087	2716	9772	5854	13465
2		1057	0	0	2012732	80055	234913	104821	42557	111143	88818	192205
3		1817	0	57369	1073572	169333	499556	247240	90462	210283	230684	387884
4		12923	0	419277	532273	860016	1075824	1118287	267923	282231	1131653	1327693
5		0	0	0	0	0	0	0	0	0	0	0
6		69431	0	287249	32366	1191031	513096	313840	95444	31257	212120	256567
7		118072	0	2454241	5184	166109	114306	68153	6856	3078	11096	22005
8		37211	0	1915639	3532	70943	54521	41971	671	1373	7616	10324
9		6856	0	1478022	244010	101822	1706036	2346062	572995	969868	5242713	4025715
10		7483	0	418	36360	125944	467230	566520	8397	46327	204418	183904
11		21017	0	60921	115854	939078	1717905	2677544	215942	177451	1597744	1387444
12		23416	0	67862	15949	619402	978193	1148273	20801	25438	368451	328614
13		120757	0	536622	63290	933229	1716345	2830163	977012	455100	4480527	3488456
14		314968	0	2776	91095	2162740	3460444	1986274	16635	71939	430586	452643
15		24853	0	52649	3810	903702	632944	591341	5486	6641	142787	135986
16		1314	0	0	69041	73382	838679	773721	74890	273485	736509	761680
17		6936	0	34573	56162	316667	1241379	1485336	190945	402293	1389860	1541248
18		596	0	0	63128	16406	398626	239956	12370	106178	152231	172410
Region Sum		75696582	0	7373365	6437930	8743392	15677466	16555227	2602103	3183916	16433981	14688839

Table 5-2. Actual Areas (m^2) by Zone and Ground Cover Type, Cibola Set 1

Zone		Unclass.	ExR	Field	Water	Bare Ground	Arrowweed	Atriplex	Cottonwood & Willow	Grass & Marsh	Mesquite	Saltcedar
0		74059540	0	178	0	6564	9523	2136	241	364	650	1589
1		2506	0	0	1613986	82491	184901	128273	11485	8773	22793	36015
2		13301	0	0	1806572	156842	279714	247429	32723	35703	122095	167423
3		17529	0	0	527947	150344	341715	233900	153379	196008	550406	791148
4		110312	0	61420	99752	822694	2199965	1599382	113337	105145	954450	946409
5		0	0	0	0	0	0	0	0	0	0	0
6		7193	0	485818	10662	669535	508778	713608	26397	13820	323817	238286
7		12109	0	2630459	809	91864	91372	45045	14776	6726	18012	28393
8		13803	0	1712884	8980	53887	82116	53993	32052	11753	45700	123175
9		6347	0	36937	201666	175438	2401327	2792426	725674	579714	4379920	5369221
10		19684	0	21288	14487	116318	676626	497383	6056	31497	107743	153804
11		46095	0	398523	40636	1275730	2292258	2570303	107434	89967	1093510	979943
12		55986	0	369726	8983	909190	849903	809688	18182	20177	277572	257799
13		2368	0	745007	29058	1226759	2628632	4680525	338690	153077	2860039	2916196
14		327331	0	32885	74898	2117132	3725047	1506818	30743	183298	241010	725801
15		44648	0	185983	2322	1207763	490677	355913	5422	5831	105136	88305
16		5470	0	872	26057	60456	1262042	799028	70798	182573	531712	656503
17		5506	0	109477	30421	293427	1846612	2063364	105063	150594	893867	1155655
18		2077	0	0	43283	17534	495718	180910	17684	75556	152234	174790
Region Sum		74751806	0	6791457	4540520	9433971	20366925	19280123	1810137	1850578	12680666	14810456

Table 5-3. Percent Error (%) by Zone and Ground Cover Type, Cibola Set 1											
Zone	Unclass.	ExR.	Field	Water	Bare Ground	Arrowweed	Atriplex	Cottonwood & Willow	Grass & Marsh	Mesquite	Saltcedar
0	1.17	0.00	3122.86	0.00	-29.77	-44.81	70.37	-100.00	-83.06	-51.67	-62.58
1	-76.15	0.00	0.00	25.13	-89.18	-87.99	-90.58	-76.35	11.38	-74.32	-62.61
2	-92.06	0.00	0.00	11.41	-48.96	-16.02	-57.64	30.05	211.30	-27.26	14.80
3	-89.64	0.00	0.00	103.35	12.63	46.19	5.70	-41.02	7.28	-58.09	-50.97
4	-88.28	0.00	582.64	433.59	4.54	-51.10	-30.08	136.39	168.42	18.57	40.29
5	0.00	0.00	0.00	0.00	0.00	0.00	0.00	0.00	0.00	0.00	0.00
6	865.32	0.00	-40.87	203.56	77.89	0.85	-56.02	261.57	126.17	-34.49	7.67
7	875.08	0.00	-6.70	540.99	80.82	25.10	51.30	-53.60	-54.25	-38.40	-22.50
8	169.58	0.00	11.84	-60.66	31.65	-33.60	-22.27	-97.91	-88.32	-83.34	-91.62
9	8.02	0.00	3901.42	21.00	-41.96	-28.95	-15.98	-21.04	67.30	19.70	-25.02
10	-61.98	0.00	-98.04	150.98	8.28	-30.95	13.90	38.66	47.08	89.73	19.57
11	-54.41	0.00	-84.71	185.10	-26.39	-25.06	4.17	101.00	97.24	46.11	41.58
12	-58.17	0.00	-81.65	77.56	-31.87	15.09	41.82	14.40	26.07	32.74	27.47
13	5000.53	0.00	-27.97	117.81	-23.93	-34.71	-39.53	188.47	197.30	56.66	19.62
14	-3.78	0.00	-91.56	21.63	2.15	-7.10	31.82	-45.89	-60.75	78.66	-37.64
15	-44.34	0.00	-71.69	64.07	-25.18	28.99	66.15	1.19	13.91	35.81	54.00
16	-75.98	0.00	-100.00	164.96	21.38	-33.55	-3.17	5.78	49.79	38.52	16.02
17	25.97	0.00	-68.42	84.62	7.92	-32.78	-28.01	81.74	167.14	55.49	33.37
18	-71.32	0.00	0.00	45.85	-6.43	-19.59	32.64	-30.05	40.53	0.00	-1.36
Regional Total	1.26	0.00	8.57	41.79	-7.32	-23.02	-14.13	43.75	72.05	29.60	-0.82

Table 5-4. Predicted Areas (m^2) by Zone and Ground Cover Type, Cibola Set 2												
Zone		Unclass.	ExR.	Field	Water	Bare Ground	Arrowweed	Atriplex	Cottonw. & Wil.	Grass & Marsh	Mesquite	Saltcedar
0		74927280	0	5746	0	4610	5255	3638	0	62	314	595
1		624	0	0	2008664	9614	24785	14229	3058	11965	6392	15870
2		38044	0	1011408	0	10837	12884	3144	85	144	196	558
3		991	0	0	1956324	92574	246581	112758	45361	110860	99283	203569
4		1542	0	0	1161108	136658	518691	247377	107704	234102	240264	425153
5		1493	0	278956	179687	35879	721016	958794	107344	277741	1407131	1199759
6		21985	0	1092707	0	2280	2271	3536	72	1	1975	1074
7		205	0	1596	69164	39506	577471	503970	65561	182597	527553	541577
8		268	0	38204	30186	66638	414218	454783	99335	257901	830589	822877
9		386	0	0	38611	19814	294177	181447	6774	72313	84637	104641
10		10043	0	2164179	12479	86521	546281	681837	494626	700866	4398311	2710157
11		135	0	0	15028	2440	52052	27028	1491	15890	28454	31181
12		575	0	552	33872	34844	324800	274821	19166	85649	191227	212594
13		1325	0	699	20092	30554	219454	216222	27012	77677	205553	227411
14		7973	0	158004	41195	286113	531073	686232	67426	154010	415705	545769
15		44305	0	1268293	3290	55594	53986	36901	6627	1891	10081	15732
16		8917	0	97716	14164	58719	324167	557695	273920	176036	1398760	1106606
17		3729	0	0	23078	20030	187545	161428	2932	31564	96198	75596
18		3611	0	315325	570739	813791	966974	960929	252662	264037	1049936	1173096
19		7928	0	379594	1913	21732	20170	12749	599	546	3320	4149
20		85478	0	209683	28235	266887	559884	1000617	320895	135091	1346964	1068266
21		889	0	13393	12175	85300	240958	402128	41941	27969	274803	232444
22		10978	0	26566	12066	70327	284932	350263	23911	54262	205489	230206
23		377	0	336	27414	59691	253749	364008	51870	62857	408223	349174
24		6278	0	2633	51619	260395	504508	777849	64751	77050	519929	502488
25		1057	0	0	13633	30536	149107	199883	5149	19255	82079	75300
26		104953	0	0	14643	432654	945062	349532	3147	19784	64434	61992
27		1123	0	11	5663	18896	55879	67239	655	3842	22128	19864
28		45257	0	104429	21308	730587	804334	1048355	291892	85296	820954	759988
29		1873	0	2994	13058	87400	201063	339932	25151	19259	196532	161237
30		79977	0	2451	46110	780678	1002450	693689	8019	33708	154392	159526
31		1392	0	13216	13578	98746	188293	287651	12001	16225	104263	107934
32		20109	0	542061	649	58578	45016	30822	1669	2605	6639	8253
33		15380	0	97326	11585	285547	267619	383293	28391	12725	146883	125552
34		3638	0	422	5095	32607	85871	99509	1132	4109	27003	27712
35		3570	0	73235	213	3660	1923	1489	278	61	525	548
36		0	0	0	0	0	0	0	0	0	0	0
37		1484	0	1624	16920	223241	397231	599182	34803	26942	329118	285555
38		2853	0	3952	2332	42685	93032	97779	1162	3475	23842	24088
39		503	0	13254	30	972	687	472	43	8	67	163
40		67419	0	251247	924	911662	323756	218644	75528	12048	173067	186906
41		5092	0	125394	7674	350716	203697	218986	8032	3683	51754	48272
42		70857	0	0	26279	581028	897316	625181	4838	15372	165378	160751
43		737	0	9606	933	4519	17133	18226	140	566	4751	6388
44		2379	0	9676	7669	283899	364585	488526	29152	15835	217729	171749
45		2676	0	76	2047	62358	121648	134524	1947	2765	46475	40384
46		21355	0	0	11905	572798	624422	546488	16732	13491	194866	180442
47		2254	0	9151	184	84006	86609	101745	282	751	18061	20057
48		2065	0	1	907	80536	94454	108347	1085	1562	31769	28475
49		8850	0	0	311	216509	154856	140990	1150	1789	36161	36984
50		2390	0	620	0	157411	103264	87865	352	623	20926	17148
Region Sum		75654602	0	8326334	6534757	8703580	15117190	15882734	2637849	3328859	16691086	14515809

Table 5-5. Actual Areas (m^2) by Zone and Ground Cover Type, Cibola Set 2

Zone		Unclass.	ExR.	Field	Water	Bare Ground	Arrowweed	Atriplex	Cottonw. & Willow	Grass & Marsh	Mesquite	Saltcedar
0		74059540	0	178	0	6564	9523	2136	241	364	650	1589
1		2506	0	0	1613986	82491	184901	128273	11485	8773	22793	36015
2		3549	0	1054942	0	428	3999	1051	647	425	225	1231
3		13301	0	0	1806572	156842	279714	247429	32723	35703	122095	167423
4		18171	0	0	544783	147740	332944	225261	172794	198981	596705	828739
5		4974	0	0	144941	56868	643096	464707	326995	324453	1617102	1576083
6		5571	0	1111723	0	276	648	285	579	516	1405	1415
7		2522	0	0	30979	27755	694500	412557	68812	166999	521450	579003
8		2190	0	2251	13025	59632	846395	822962	52474	76458	481890	652538
9		1782	0	0	19643	12881	343440	135757	12777	46284	109074	119486
10		286	0	34210	37104	131713	1778069	2426759	404490	235946	2812694	3926896
11		224	0	0	10789	2913	76797	38674	365	8160	10302	25355
12		2218	0	0	9297	28698	510952	301712	11052	44036	104632	162573
13		1334	0	2439	6189	25152	332070	286561	15037	27084	124863	203323
14		1191	0	104195	8329	197619	793546	997198	35326	56171	312170	382821
15		9426	0	1171141	3004	44177	80956	46342	22531	12809	32400	70671
16		24	0	18680	8230	125872	700769	1109469	112766	57840	905716	972414
17		13656	0	11718	7850	27533	281293	129139	3089	32853	23014	71225
18		111350	0	23369	97664	716372	1971289	1372795	106713	83091	945445	928754
19		2055	0	200132	4234	55726	55316	51884	9747	4261	29194	36166
20		402	0	95632	11432	395963	865015	1726359	102850	52870	897128	867429
21		2531	0	15535	5263	127978	314195	490338	17562	14441	167340	174856
22		2839	0	167679	3415	71645	304963	425934	15115	18725	119767	137097
23		11515	0	24246	8998	95429	482454	450656	24004	20870	227338	228180
24		25816	0	15353	22158	407649	888147	739047	32863	32382	298913	300415
25		3326	0	7174	4366	35696	235721	196913	1930	7484	33071	49475
26		74826	0	892	44063	164000	1013375	306025	7105	108214	25825	245590
27		4545	0	911	702	20272	92507	52278	861	2973	7258	12870
28		4802	0	604766	9688	667452	755717	1341716	81517	31639	653395	555707
29		4005	0	9531	3120	113699	269188	328439	14223	10128	163918	130778
30		96301	0	1794	22660	598134	1238059	566651	15401	37660	101437	273759
31		1093	0	25301	1722	102522	225702	280079	6430	9158	97267	92666
32		3630	0	592035	2802	41433	30081	18338	3793	1043	6615	7126
33		1962	0	276178	1110	246721	277295	327204	9910	13203	118638	98105
34		6111	0	2686	568	38853	90731	87413	1222	1931	27442	29830
35		1166	0	72336	0	1939	3658	1708	126	145	891	701
36		0	0	0	0	0	0	0	0	0	0	0
37		16583	0	113823	5762	339534	482815	493794	22961	15276	228255	194384
38		6067	0	22582	480	57348	76560	80461	1057	1940	21393	24633
39		0	0	5572	0	5982	1293	689	421	0	750	1518
40		5012	0	367535	9053	516504	383176	519503	18091	9183	226048	163480
41		6990	0	181323	1262	364745	185963	170070	6493	4950	49694	43080
42		103570	0	9906	3737	978612	888869	374125	4894	9698	63801	103367
43		1198	0	2695	0	23597	20692	11050	1	149	536	779
44		6644	0	219871	3727	356515	305674	373117	11067	11141	173788	125128
45		13230	0	9226	1055	101172	116109	107871	1903	1652	23225	38330
46		56771	0	100527	6263	861708	562049	362581	5455	9575	109195	105126
47		5906	0	70568	0	129412	59875	42058	206	254	4940	5999
48		11637	0	901	0	121962	94210	76945	1190	908	16758	23194
49		13247	0	19821	496	299857	126515	85486	510	1151	27003	23004
50		4209	0	20081	0	240386	56103	42326	332	630	15215	10127
Region Sum		74751806	0	6791457	4540520	9433971	20366925	19280123	1810137	1850578	12680666	14810456

Table 5-6. Percent Error (%) by Zone and Ground Cover Type, Cibola Set 2

Zone	Unclass.	ExR.	Field	Water	Bare Ground	Arrowweed	Atriplex	Cottonw. & Willow	Grass & Marsh	Mesquite	Saltcedar
0	1.17	0.00	3122.86	0.00	-29.77	-44.81	70.37	-100.00	-83.06	-51.67	-62.58
1	-75.10	0.00	0.00	24.45	-88.35	-86.60	-88.91	-73.37	36.37	-71.96	-55.94
2	972.01	0.00	-4.13	0.00	2434.71	222.16	199.12	-86.85	-65.97	-12.79	-54.72
3	-92.55	0.00	0.00	8.29	-40.98	-11.85	-54.43	38.62	210.51	-18.68	21.59
4	-91.51	0.00	0.00	113.13	-7.50	55.79	9.82	-37.67	17.65	-59.73	-48.70
5	-69.99	0.00	0.00	23.97	-36.91	12.12	106.32	-67.17	-14.40	-12.98	-23.88
6	294.65	0.00	-1.71	0.00	725.89	250.60	1142.33	-87.56	-99.89	40.55	-24.10
7	-91.89	0.00	0.00	123.26	42.34	-16.85	22.16	-4.72	9.34	1.17	-6.46
8	-87.78	0.00	1597.39	131.76	11.75	-51.06	-44.74	89.30	237.31	72.36	26.10
9	-78.35	0.00	0.00	96.57	53.83	-14.34	33.66	-46.99	56.24	-22.40	-12.42
10	3414.42	0.00	6226.16	-66.37	-34.31	-69.28	-71.90	22.28	197.04	56.37	-30.98
11	-39.46	0.00	0.00	39.29	-16.21	-32.22	-30.11	308.19	94.73	176.19	22.98
12	-74.08	0.00	0.00	264.35	21.42	-36.43	-8.91	73.41	94.50	82.76	30.77
13	-0.69	0.00	-71.34	224.65	21.48	-33.91	-24.55	79.64	186.80	64.62	11.85
14	569.18	0.00	51.64	394.61	44.78	-33.08	-31.18	90.87	174.18	33.17	42.56
15	370.02	0.00	8.30	9.52	25.84	-33.31	-20.37	-70.59	-85.23	-68.88	-77.74
16	36673.16	0.00	423.11	72.11	-53.35	-53.74	-49.73	142.91	204.35	54.44	13.80
17	-72.69	0.00	-100.00	193.98	-27.25	-33.33	25.00	-5.09	-3.92	318.00	6.14
18	-96.76	0.00	1249.35	484.39	13.60	-50.95	-30.00	136.77	217.77	11.05	26.31
19	285.70	0.00	89.67	-54.82	-61.00	-63.54	-75.43	-93.85	-87.18	-88.63	-88.53
20	21139.06	0.00	119.26	146.99	-32.60	-35.27	-42.04	212.00	155.52	50.14	23.15
21	-64.89	0.00	-13.79	131.35	-33.35	-23.31	-17.99	138.81	93.67	64.22	32.93
22	286.64	0.00	-84.16	253.33	-1.84	-6.57	-17.77	58.20	189.79	71.57	67.91
23	-96.72	0.00	-98.61	204.66	-37.45	-47.40	-19.23	116.09	201.19	79.57	53.03
24	-75.68	0.00	-82.85	132.96	-36.12	-43.20	5.25	97.04	137.94	73.94	67.26
25	-68.22	0.00	-100.00	212.26	-14.45	-36.74	1.51	166.84	157.29	148.19	52.20
26	40.26	0.00	-100.00	-66.77	163.81	-6.74	14.22	-55.71	-81.72	149.50	-74.76
27	-75.29	0.00	-98.82	706.64	-6.79	-39.60	28.62	-23.92	29.21	204.90	54.35
28	842.55	0.00	-82.73	119.94	9.46	6.43	-21.86	258.07	169.59	25.64	36.76
29	-53.23	0.00	-68.59	318.47	-23.13	-25.31	3.50	76.84	90.15	19.90	23.29
30	-16.95	0.00	36.67	103.49	30.52	-19.03	22.42	-47.94	-10.49	52.20	-41.73
31	27.36	0.00	-47.77	688.33	-3.68	-16.57	2.70	86.64	77.17	7.19	16.48
32	453.93	0.00	-8.44	-76.85	41.38	49.65	68.08	-56.01	149.77	0.36	15.82
33	683.76	0.00	-64.76	943.65	15.74	-3.49	17.14	186.49	-3.62	23.81	27.98
34	-40.46	0.00	-84.28	797.02	-16.08	-5.36	13.84	-7.42	112.83	-1.60	-7.10
35	206.21	0.00	1.24	0.00	88.75	-47.44	-12.82	120.72	-57.88	-41.14	-21.86
36	0.00	0.00	0.00	0.00	0.00	0.00	0.00	0.00	0.00	0.00	0.00
37	-91.05	0.00	-98.57	193.65	-34.25	-17.73	21.34	51.58	76.37	44.19	46.90
38	-52.98	0.00	-82.50	385.34	-25.57	21.52	21.52	9.91	79.18	11.45	-2.21
39	0.00	0.00	137.87	0.00	-83.75	-46.83	-31.43	-89.83	0.00	-91.06	-89.27
40	1245.13	0.00	-31.64	-89.80	76.51	-15.51	-57.91	317.50	31.20	-23.44	14.33
41	-27.15	0.00	-30.85	508.25	-3.85	9.54	28.76	23.71	-25.61	4.14	12.05
42	-31.59	0.00	-100.00	603.31	-40.63	0.95	67.11	-1.16	58.51	159.21	55.52
43	-38.47	0.00	256.46	0.00	-80.85	-17.20	64.94	25026.63	281.04	786.20	719.75
44	-64.19	0.00	-95.60	105.76	-20.37	19.27	30.93	163.42	42.14	25.28	37.26
45	-79.77	0.00	-99.18	94.14	-38.36	4.77	24.71	2.30	67.36	100.11	5.36
46	-62.38	0.00	-100.00	90.08	-33.53	11.10	50.72	206.72	40.90	78.46	71.64
47	-61.84	0.00	-87.03	0.00	-35.09	44.65	141.92	36.81	196.10	265.63	234.33
48	-82.25	0.00	-99.91	0.00	-33.97	0.26	40.81	-8.86	72.03	89.58	22.77
49	-33.19	0.00	-100.00	-37.41	-27.80	22.40	64.93	125.23	55.40	33.92	60.77
50	-43.20	0.00	-96.91	0.00	-34.52	84.06	107.59	5.81	-1.10	37.54	69.34
Regional Total	1.21	0.00	22.60	43.92	-7.74	-25.78	-17.62	45.73	79.88	31.63	-1.99

Table 5-7. Predicted Areas (m^2) by Zone and Ground Cover Type, Cibola Set 3												
Zone		Unclass.	ExR.	Field	Water	Bare Ground	Arrowweed	Atriplex	Cottonw. & Willow	Grash & Marsh	Mesquite	Saltcedar
0		69545581	0	0	0	7111	195	33	11	0	230	6328
1		107523	0	0	1912198	65580	4292	1271	717	9343	758	24611
2		72822	0	6698372	0	17604	76	0	13	0	96	5929
3		143690	0	0	1697091	528610	34109	14774	11015	87810	16190	316750
4		134696	0	0	883908	975805	73331	36924	43441	178257	26833	908845
5		22241	0	0	0	1440	37	12	698	0	54	3360
6		22223	0	0	22084	220601	294831	95909	8358	24804	20237	757053
7		894355	0	0	19190	389693	267951	301653	44170	60683	593361	10195297
8		220679	0	0	778451	3013170	365486	124328	56656	205470	128002	2579181
9		52441	0	0	125	73869	963	840	2332	45	343	72497
10		273301	0	0	44114	2311346	86510	87049	17156	3645	137506	1341235
11		42561	0	0	0	353117	3400	3126	6399	2217	8615	133361
12		104612	0	0	90710	446248	654633	312640	59605	142093	157404	4816465
13		214963	0	0	12431	2089997	316567	320277	6941	9878	196472	4687625
14		27891	0	0	1656	381485	124181	59143	53	643	20854	435940
15		546610	0	0	20493	1155006	296118	405522	39639	13589	534007	8229167
16		19220	0	0	13303	186997	248122	61534	175	6111	18592	532565
17		111077	0	0	18317	730609	522918	196431	6556	38671	108893	3055893
18		48103	0	0	202	248782	5994	2371	938	331	1334	228544
19		465134	0	0	32021	6559484	797821	337489	8154	9923	161132	4337456
20		5310	0	0	52	8284	61	42	26	28	39	1249
21		19091	0	0	0	958664	28923	34609	89	0	38015	385796
22		182523	0	0	2309	4048098	326548	266968	2428	1712	165786	2410961
Region Sum		73276647	0	6698372	5548655	24771601	4453067	2662944	315570	795254	2334753	45466108

Table 5-8. Actual Areas (m^2) by Zone and Ground Cover Type, Cibola Set 3											
Zone	Unclass.	ExR.	Field	Water	Bare Ground	Arrowweed	Atriplex	Cottonw. & Willow	Grass & Marsh	Mesquite	Saltcedar
0	69537777	0	0	0	12162	245	198	0	0	324	8784
1	18177	0	0	1809519	249143	3553	1591	1260	6119	2105	34826
2	4400	0	6771147	71	12727	348	118	0	0	259	5841
3	61282	0	0	1907302	531881	21484	10401	17946	35646	35304	228793
4	105300	0	0	425348	619648	118024	34115	73680	128914	169705	1587307
5	8207	0	0	710	8414	267	186	1725	0	1138	7192
6	30110	0	0	10587	124268	275659	53296	6602	22296	35483	907797
7	133106	0	0	13542	753984	537832	339172	43059	42435	421533	10481691
8	167861	0	0	36275	2855859	487374	240429	22478	17745	173572	3469829
9	12466	0	0	186	106303	2965	2209	1682	411	2995	74235
10	67017	0	0	7422	2197589	141584	119763	7463	1138	120066	1639822
11	4061	0	0	2	375677	13056	9934	12	0	11664	138392
12	111447	0	0	74133	366400	504486	124940	82134	131949	379895	5009026
13	176037	0	0	1716	2979523	508828	322456	5757	398	224216	3636222
14	15976	0	0	155	385085	135104	40980	158	165	12567	461658
15	140146	0	0	4111	2413669	731108	493335	13247	4225	373216	7067093
16	15936	0	0	3182	230067	243668	43000	418	1317	6805	542227
17	73736	0	0	3971	761824	783892	235024	3405	4060	89677	2833778
18	15703	0	0	2747	286186	8705	10055	3462	563	16174	193004
19	400323	0	0	11023	6175670	467949	247605	3112	13409	185155	5204367
20	1782	0	0	0	8735	112	163	0	0	442	3857
21	28996	0	0	0	1191540	15575	14302	102	0	14180	200492
22	225130	0	0	200	4784169	182569	127678	1367	16	141117	1945087
Region Sum	71354975	0	6771147	4312201	27430524	5184387	2470949	289067	410805	2417595	45681321

Table 5-9. Percent Error (%) by Zone and Ground Cover Type, Cibola Set 3

Zone	Unclass.	ExR.	Field	Water	Bare Ground	Arrowweed	Atriplex	Cottonw. & Willow	Grass & Marsh	Mesquite	Saltcedar
0	0.01	0.00	0.00	0.00	-41.53	-20.39	-83.28	0.00	0.00	-29.15	-27.95
1	491.53	0.00	0.00	5.67	-73.68	20.78	-20.11	-43.08	52.68	-64.02	-29.33
2	1554.98	0.00	-1.07	-100.00	38.31	-78.06	-100.00	0.00	0.00	-62.89	1.51
3	134.47	0.00	0.00	-11.02	-0.61	58.76	42.04	-38.62	146.34	-54.14	38.44
4	27.92	0.00	0.00	107.81	57.48	-37.87	8.23	-41.04	38.28	-84.19	-42.74
5	171.01	0.00	0.00	-100.00	-82.88	-86.34	-93.80	-59.57	0.00	-95.24	-53.29
6	-26.19	0.00	0.00	108.60	77.52	6.95	79.95	26.59	11.25	-42.97	-16.61
7	571.91	0.00	0.00	41.70	-48.32	-50.18	-11.06	2.58	43.00	40.76	-2.73
8	31.47	0.00	0.00	2045.94	5.51	-25.01	-48.29	152.05	1057.88	-26.25	-25.67
9	320.69	0.00	0.00	-33.17	-30.51	-67.53	-61.97	38.67	-89.16	-88.56	-2.34
10	307.81	0.00	0.00	494.39	5.18	-38.90	-27.32	129.88	220.39	14.53	-18.21
11	947.99	0.00	0.00	-100.00	-6.00	-73.96	-68.53	55450.47	596590.75	-26.14	-3.64
12	-6.13	0.00	0.00	22.36	21.79	29.76	150.23	-27.43	7.69	-58.57	-3.84
13	22.11	0.00	0.00	624.55	-29.85	-37.78	-0.68	20.58	2384.22	-12.37	28.91
14	74.58	0.00	0.00	966.37	-0.93	-8.08	44.32	-66.36	290.99	65.94	-5.57
15	290.03	0.00	0.00	398.50	-52.15	-59.50	-17.80	199.23	221.62	43.08	16.44
16	20.61	0.00	0.00	318.07	-18.72	1.83	43.10	-58.14	364.01	173.21	-1.78
17	50.64	0.00	0.00	361.32	-4.10	-33.29	-16.42	92.55	852.46	21.43	7.84
18	206.33	0.00	0.00	-92.64	-13.07	-31.15	-76.42	-72.90	-41.25	-91.75	18.41
19	16.19	0.00	0.00	190.50	6.21	70.49	36.30	162.04	-26.00	-12.97	-16.66
20	197.98	0.00	0.00	0.00	-5.16	-45.28	-73.97	0.00	0.00	-91.15	-67.62
21	-34.16	0.00	0.00	0.00	-19.54	85.70	141.99	-12.14	0.00	168.10	92.42
22	-18.93	0.00	0.00	1055.30	-15.39	78.86	109.09	77.62	10801.14	17.48	23.95
Regional Total	2.69	0.00	-1.07	28.67	-9.69	-14.11	7.77	9.17	93.58	-3.43	-0.47

Table 5-10. Percent Error (%) by Set, Comparison											
Set	Unclass.	ExR.	Field	Water	Bare Ground	Arrowweed	Atriplex	Cottonw. & Willow	Grass & Marsh	Mesquite	Saltcedar
1 (18 zones)	1.26	0	8.57	41.79	-7.32	-23.02	-14.13	43.75	72.05	29.6	-0.82
2 (50 zones)	1.21	0	22.6	43.92	-7.74	-25.78	-17.62	45.73	79.88	31.63	-1.99
3 (22 zones)	2.69	0	-1.07	28.67	-9.69	-14.11	7.77	9.17	93.58	-3.43	-0.47

The table above places the percent error in predicted versus actual area in Cibola by ground cover class for each set of products next to one another. Note that most classes see an improvement in percent error with the third set, which employed the more accurate high-resolution map. The exceptions are bare ground, grass & marsh, and the unclassified pixels.

CHAPTER VI

DISCUSSION

6.1 Did the Study Meet the Objectives?

In Chapter three we stated that the objective of our study was to develop a method of mapping riparian vegetation in the Lower Colorado River Basin which meets the following criteria:

- It must provide more or equally accurate and detailed information about the riparian vegetation than the current Anderson-Ohmart method
- The method must be inexpensive, both in terms of money, processing time, and data storage
- A majority of the data (excluding information gathered for error-assessment, and the existing high-resolution map) must come from low-resolution remote sensing platforms, or other easy to access sources.

The last two objectives were met by this study. All data used in the study were obtained for free (Landsat satellite images are free from the USGS, and the polygon vectors of the fields are reusable and easily updateable, as the field boundaries rarely change),

processing time was maximized by developing ERDAS scripts and models which automated the processes, and the file sizes involved were far below those needed to perform a high-resolution mapping study.

To meet the first objective, we stated that we would need to be able to identify large stands of nearly homogeneous species (salt cedar, mesquite, arrowweed) and/or overall vegetation density without relying on extensive field surveys. Our results suggest that we at least partially met this objective. Of the three tests we performed, set three achieved percent errors of -0.47% for saltcedar and -3.43% for mesquite; both are low rates of error. We did not reach as low a percent error for arrowweed, reaching -14.11% for the best set. Refer to Table 5-10.

This suggests that some ground cover classes are more difficult than others to map. There are several factors that could contribute to this. The classes with the highest percent error rates (arrowweed at -14.11%, water at 28.67%, and grass & marsh at 93.58%, refer to Table 5-10) are present in relatively small amounts in Cibola. From the actual areas of each class in Cibola, we are able to calculate that arrowweed comprises just 3.12% of the total area of ground cover in Cibola. Water comprises 2.59% of the ground cover, and grass & marsh are present in only 0.25% of the image. Because the relative amounts of these classes are low, it could be that the resolution of Landsat imagery (30 m^2) is too coarse to accurately discern these classes, especially if the arrowweed, water, and grass & marsh are present in very small patches.

Saltcedar, on the other hand, comprises 27.47% of the Cibola region, and we were able to predict its coverage well, with a percent error of -0.47%. This is likely attributable to the large, homogeneous stands of saltcedar present throughout both CRIT North and

Cibola. Larger, contiguous stands of one class of ground cover are easier to resolve in Landsat imagery.

The high percentage of unclassified pixels may contribute to inaccuracies in predicting other ground cover classes. Much of the unclassified portion of the image is located at the perimeter and beyond to the background of the useful pixels in the CRIT North and Cibola imagery, though a few unclassified pixels are present in the interior of the image. Refer to Figure 6-1. The background unclassified pixels in Cibola actually comprise 42.9% of the area of the image, far more than any other ground cover class. This high contribution of background area may influence the statistics of the entire region, without contributing any useful information to the final products. This provides an argument for ignoring the unclassified pixels in the development of zone definitions and for the Ward's clustering analysis. Ward's clustering, in particular, is sensitive to outliers. Thus, ignoring unclassified pixels may eliminate a potentially large source of unnecessary influence and error.

Ultimately, the products developed in this study are intended to predict the area covered by various ground cover types in the Lower Colorado River riparian zone, for use in the evapo-transpiration estimates in the LCRAS reports produced by USBR. Thus, the user of the products is in the best position to determine if they are accurate enough to estimate water loss due to ET by the riparian vegetation. The coverage of the species present most abundantly in the Lower Colorado River, saltcedar, was predicted with the greatest accuracy, which is promising for use in LCRAS. Moreover, the existing Anderson-Ohmart mapping method often ignores the presence of small stands of vegetation imbedded within large stands of another species. The method in this study

provides at the very least an estimation of the area covered by such imbedded small stands of vegetation.

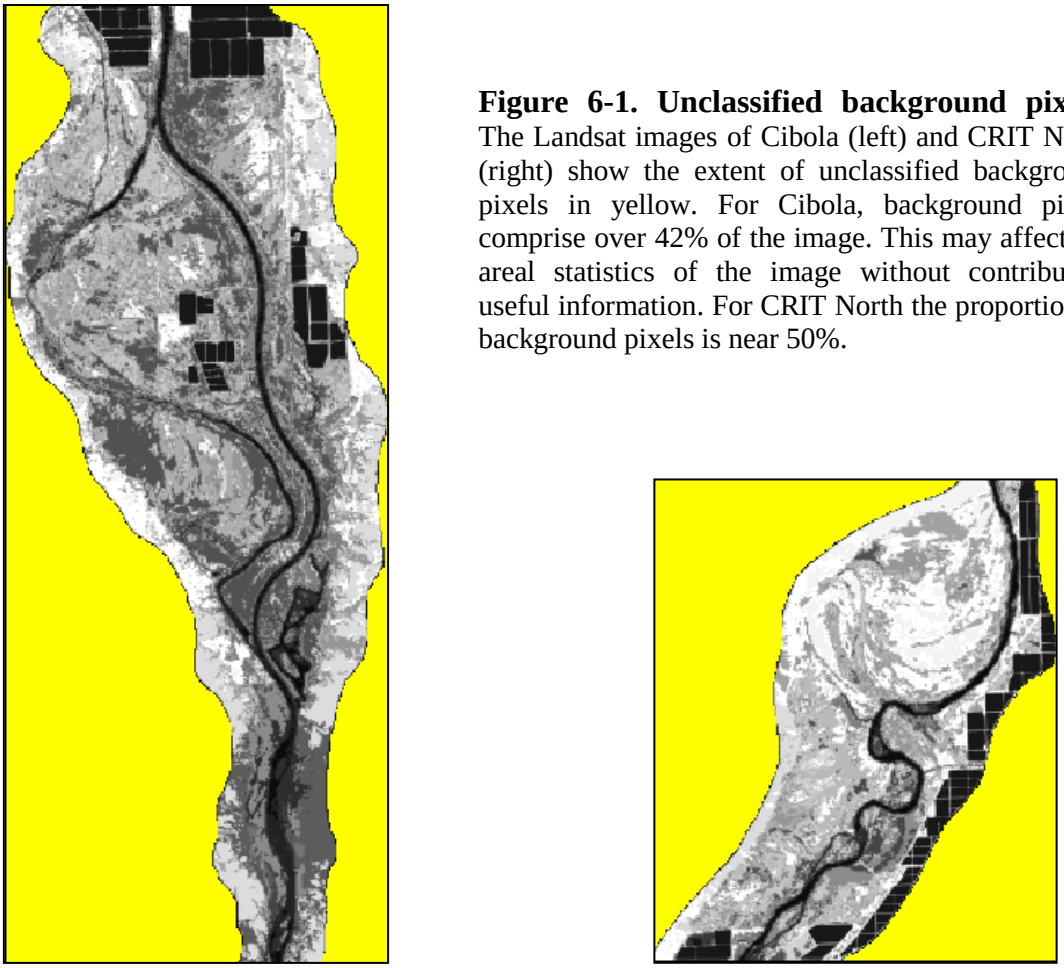

Figure 6-1. Unclassified background pixels. The Landsat images of Cibola (left) and CRIT North (right) show the extent of unclassified background pixels in yellow. For Cibola, background pixels comprise over 42% of the image. This may affect the areal statistics of the image without contributing useful information. For CRIT North the proportion of background pixels is near 50%.

6.2 Validity of the Ward's Clustering Procedure

The first two sets of spectral signatures and zone definitions tested were developed using the same Landsat image, region, and high-resolution map. The difference between the two sets of products was that the Ward's clustering procedure was performed on the first set of products, but not the second set.

The Ward's clustering procedure was carried out on the initial zone definitions under the assumption that 50 zones provided more than enough degrees of freedom to

capture the variability in the image, and reducing the number of zones would make the final products easier to use and interpret without losing useful information. Thus, the first set of products involved the reduction of the original 50 zones to 18 zones. Percent error rates were relatively high for certain key classes using this first product set, namely mesquite, arrowweed and water. See Table 5-10. For that reason, we returned to the original 50 zones and tested their validity. In almost every class, the percent errors increased in magnitude when all 50 zones were tested. See Table 5-10.

This outcome suggests that performing the Ward's clustering analysis does not remove useful information from the zone definitions. In fact, reducing the number of zones improved the accuracy of the method. It is possible that using too many zones to classify the Landsat images of CRIT North and Cibola led to over-fragmentation of the images. If we imagine "fragments" as being the average size of contiguous groups of pixels of the same zone, the smaller the fragments in the Landsat classifications, the more closely the fragments must line-up with corresponding features in the high-resolution map when overlain. Each fragment "line-up" with its corresponding high-resolution feature has error associated with it, and more fragments may mean compounded error. With larger fragments (which we achieve with fewer zones) we may be delineating less detail, but it is easier to get a composite average of the features lying within that fragment. With larger fragments, small features do not need to line up exactly with the corresponding features in the high-resolution map for accurate area prediction.

6.3 Method Sensitivity to Accuracy of the High-Resolution Map

The third set of products produced by this study was made using a newer, more accurate high-resolution map. The purpose of this was to test if the method improved

when using a better high-resolution. From Table 5-10, the method improved significantly when using the new high-resolution map.

One reason for the improvement may be the nature of the two high-resolution maps. The original map was much more fragmented into heterogeneous mixtures of vegetation species, though the newer map showed that the Lower Colorado River Basin is actually dominated by large, more homogeneous stands of a single species: saltcedar. In the Landsat image, therefore, the spectral signature of saltcedar should heavily dominate the image, and this influence should be reflected in the final zone definitions. This suggests that the method may not be suitable for identifying heterogeneous mixtures of vegetation species.

6.4 Suggestions for Future Work

To truly evaluate the validity of this method, a map of the predicted areas should be made while simultaneously field-checking the results. Random pixels could be selected from the map, located in the field, and surveyed directly for percent ground cover of the classes represented in that pixel. This will only be possible in the future, when another field season arrives.

Field checking the products in a future field season will also check if the method in this study is image-specific, or if the products developed from imagery acquired on one day are useable on imagery from a different day. Possible variations in imagery from one day to the next (or from year to year, around the same time in the growing season) could be due to atmospheric conditions, climate (dry vs. wet conditions, leading to changes in vegetation health), or any other outside contributor which would lead to the detection of spectral signatures in one image that are not present in another.

For example, regions of the Lower Colorado River Basin experienced a wild-fire in 2005, but the products in this study were developed from 2004 imagery. The lack of burned areas in 2004 would mean that the influence of this ground-cover type was not accounted for by our products. This could be corrected by updating the high-resolution map, and producing a new set of spectral signatures and zone definitions. The difficulty of updating the high-resolution map, however, depends on the extant of the areas burned.

This brings up the question of how long a given set of spectral signatures and zone definitions will remain valid for use in predicting ground coverage for LCRAS. For the most part, the changes in the Lower Colorado River riparian zone proceed slowly, on the order of decades. However, shifting climates, expanding saltcedar and arrowweed, and bio control studies[1], all have the potential to create rapid changes. This would require more frequent updating of the products.

This study provides the framework for further development and testing of riparian vegetation mapping methods which improve upon Anderson-Ohmart. The method is not dependent on annual extensive field surveys or high-resolution imagery collection. It has so far been shown to accurately predict areal coverage of the most predominant vegetation species in the region. Moreover, the method is relatively simple to automate and execute, and it employs imagery available for free. USBR may find that the method is faster, less expensive, and more detailed than what is already employed by LCRAS to map riparian vegetation. The benefits of this method have the potential to streamline

[1] In an effort to control the spread of saltcedar, a beetle (*Diorhabda elongata*) intended to preferentially defoliate saltcedar, was released in the Western U.S. in 2001. The beetles are slowly approaching the Lower Colorado River Basin from the North.

mapping procedures in LCRAS, leaving USBR with more resources to carry out its mission of managing water in the Western United States.

CHAPTER VII

LOW RESOLUTION VEGETATION MAPPING IN THE LOWER COLORADO RIVER BASIN

Amundsen, K. J. and Clapham, W. B.

ABSTRACT

In the Western United States, monitoring water usage is a complex task carried out by the U.S. Bureau of Reclamation (USBR). It may be argued that USBR's greatest challenge is equitably distributing the waters of the Colorado River, particularly the Lower Colorado River, where water rights have been established and contested several times. To help meet the demands of water management in the Lower Colorado River Basin, USBR estimates the amount of water lost from the basin each year via evapo-transpiration by riparian vegetation in the Lower Colorado River riparian zone. Key components of those estimates include maps of the vegetation itself, which provide a measure of the acreage covered by each dominant species.

Previous mapping efforts have relied extensively on costly in-situ field measurements using the Anderson-Ohmart Classification scheme (which was developed

for habitat evaluation, not species identification) and data-dense high resolution aerial photographs. This study employs low resolution Landsat imagery and simple classification and clustering algorithms to identify heterogeneous species assemblages in the Lower Colorado River as possible alternatives to Anderson-Ohmart and/or high resolution aerial photographs.

Our results show that the method developed here is able to identify heterogeneous riparian species assemblages, but certain vegetative species can be mapped with greater accuracy than others. Pending an error assessment to be carried out in a future field season, we believe our method to be an inexpensive, relatively simple update to USBR's existing mapping procedures.

INTRODUCTION

The U.S. Bureau of Reclamation (USBR), of the Department of the Interior is tasked with overseeing the equitable distribution of water resources, located either on the surface or below the ground, in the Western United States. This task includes monitoring and accounting for the use of all water taken from the Colorado River (*Arizona v. California*, 547 U.S. 150, 2006).

The Lower Colorado River riparian zone is a particular area of interest to USBR, because water from the Lower Colorado River supports industry, agriculture, and urban use in Nevada, Arizona, California, and Mexico. However, Arizona and California have repeatedly disagreed over interpretation of the *Colorado River Compact of 1922* (Norviel et al. 1922), the original document delineating water allotments to the interested parties. In 1964 the U.S. Supreme Court entered a decree (*Arizona v. California, 376 U.S. 340, 1964)* which, among other things, ordered the Secretary of the Interior to more closely

monitor how much water was being drawn from the Colorado River at several points of diversion and to provide its findings in an annual report. The Secretary tasked USBR to carry out this function (Dwyer, 2010). The resulting reports, called the "Compilation of Records in Accordance with Article V of the Decree of the Supreme Court of the United States in Arizona v. California Dated March 9, 1964", also known as Decree Accounting reports, have been published annually since 1964. They are reviewed by the Department of the Interior to ensure that the states in the Lower Colorado River Basin do not exceed their legal water allotment.

As part of the water monitoring effort, USBR developed the Lower Colorado River Accounting System (LCRAS). LCRAS is used to estimate the amount of water lost from the Lower Colorado River via evapo-transpiration (ET) by agricultural and natural riparian vegetation and direct evaporation from open water sources. LCRAS has been shown to accurately predict ET rates and water loss via agricultural vegetation, but riparian vegetation ET rates have proven to be more difficult to estimate (Bureau of Reclamation, 2008).

Part of the problem stems from the outdated vegetation mapping procedure used by LCRAS to find coverage of various riparian species. This mapping procedure, the Anderson-Ohmart method, was originally developed in the 1970s (Anderson and Ohmart, 1976; 1985). The current mapping method used by LCRAS is still based on Anderson-Ohmart, which requires extensive field evaluation and high-resolution aerial photographs to map stands of riparian vegetation in the Lower Colorado River riparian zone. Aerial photography can be expensive to acquire and process, and extensive field work is time-consuming. Moreover, the Anderson-Ohmart method was developed for the purpose of

evaluating habitat suitability of the riparian zone for birds and other wildlife. Thus, the Anderson-Ohmart method places priority on vegetation density and plant height, rather than specific species and plant identification. For LCRAS, it is more important to identify the coverage of specific species, as each species exercises a different rate of ET (Bureau of Reclamation, 2008).

Until very recently, no full species-specific, high-resolution map had ever been made of the natural vegetation in the Lower Colorado River riparian zone. A map of this nature has now been made, but the process required the use of expensive, high-resolution aerial imagery, copious computer resources (in terms of both data storage and processing), and extensive person-hours. Furthermore, this map will be difficult to update in the future, as new high-resolution aerial imagery (with matching spatial resolution to the original map) will need to be acquired for accurate change detection.

The objective of this study is to develop a new method of mapping natural vegetation in the Lower Colorado River riparian zone. The new method must meet the following criteria:

- It must provide more or equally accurate and detailed information about the riparian vegetation than the current Anderson-Ohmart method
- The method must be inexpensive, both in terms of money, processing time, and data storage
- A majority of the data (excluding information gathered for error-assessment, and the existing high-resolution map) must come from low-resolution remote sensing platforms, or other easy to access sources.

MATERIALS AND METHODS

We chose to use Landsat TM 5 imagery as our primary data source for this study. Within the context of mapping vegetation at the species level, Landsat TM 5 imagery is considered low-resolution data (30 m pixels.) Moreover, Landsat imagery is available free of charge from the United States Geological Survey. Also, only two Landsat TM 5 tiles are needed to get coverage of our entire study area, in seven spectral bands. Once these two tiles are stitched together and subsetted to the riparian zone, the resulting image is a 14 megabyte ERDAS Imagine .img file, a very manageable data set. Furthermore, the revisit time for Landsat TM 5 is 16 days, meaning that imagery of the entire study region is available as frequently as every 16 days (weather dependent.)

This study also made use of the high-resolution riparian vegetation map of the Lower Colorado River, recently produced from high-resolution aerial photographs of the riparian taken in mid-June 2004. The Landsat images employed in this study were chosen to correspond to the same time that the aerial photographs were taken.

All Landsat images were stitched together and georeferenced to the 0.33 m pixel aerial photographs of the study area, using the ERDAS Imagine image processing software's geometric correction tool.

For ease of processing, and for comparison tests, the area of interest was divided into three sub-regions: CRIT North, CRIT South, and Cibola.. Each region was extracted from both the Landat TM 5 image and the high-resolution map, using the same AOI file in ERDAS. The AOI files closely trimmed the images to the boundaries of the riparian vegetation, excluding as much agricultural vegetation as possible.

When preparing the Landsat TM 5 image for use in our study, we discovered that a thin layer of cloud cover had obscured most of the CRIT South sub-region. For this reason, we opted not to use CRIT South in developing or testing our products. Refer to Figure 1 and Figure 2 for the Landsat image and corresponding high resolution maps of the areas of interest.

The disadvantage of using imagery from 2004 is that we could not obtain in situ information to test our results. However, it was decided that the best products would be produced by using Lansdat images taken simultaneously with the aerial photographs. In lieu of field-checking the results, the CRIT North region was used exclusively to develop the products, and the Cibola region was used to test the products.

This study produced two products, to be used in concert, to map riparian vegetation and ground cover in the Lower Colorado River Basin. The first product is a set of spectral signatures, which is used to group similar pixels in a Landsat image. The second product is a set of zonal definitions, which detail the coverage of each ground cover class found within each group of pixels defined by the spectral signatures. The spectral signatures were obtained by employing the ISODATA unsupervised classification algorithm in ERDAS Imagine. The ISODATA algorithm was run to produce a set of 50 spectral clusters. The resulting classified Landsat image was then overlain with the high-resolution map, and a zonal analysis was performed. Refer to Figure 3. The zonal analysis told us the percent coverage of each ground class (from the high-resolution map) which comprised each of the fifty clusters in the Landsat classification. Refer to Table 1.

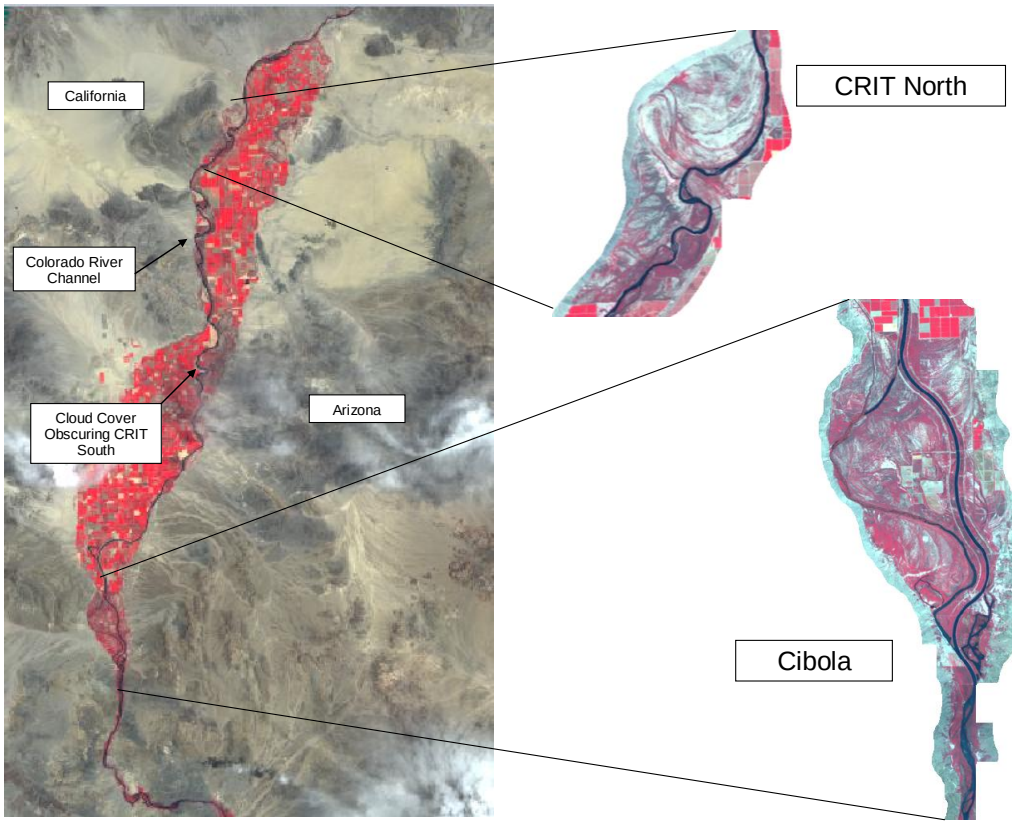

Figure 1. False-color Landsat TM 5 image from Lower Colorado River. The image above was extracted from a mosaic of two Landsat TM 5 scenes, both acquired by the satellite on June 16, 2004. The area includes three primary large sub-regions of riparian vegetation: CRIT North, CRIT South, and Cibola. CRIT South was partially obscured by cloud cover in this image, thus it was not used in this study. Note the sub-regions of CRIT North and Cibola to the right of the main image.

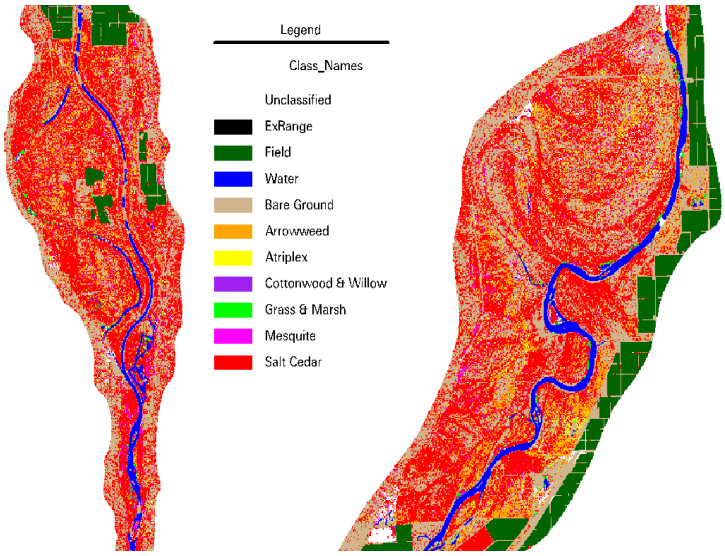

Figure 2. High-resolution ground cover map: CRIT North and Cibola.

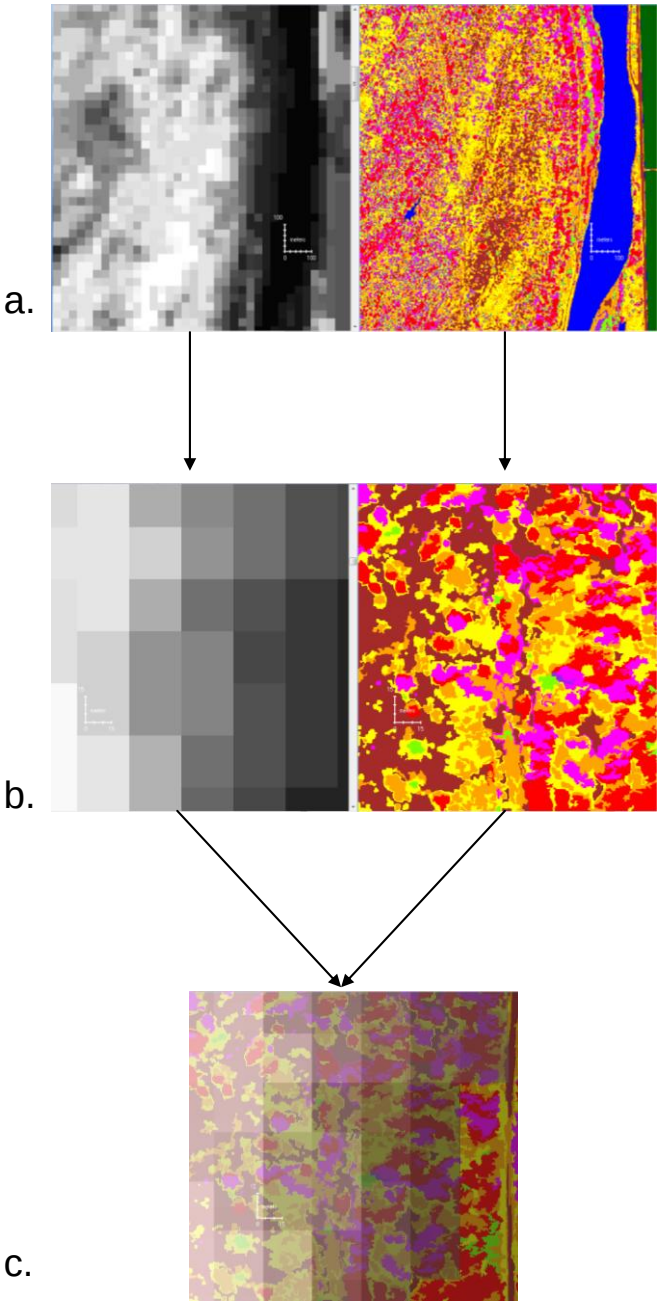

Figure 3. Overlaying for zonal summary analysis. In parts a and b of the figure above, the image on the left is a portion of the ISODATA classified image of CRIT North. On the left is the corresponding portion of the high-resolution map. As one zooms in on the images, the difference in spatial resolution between the ISODATA classified image (30 m) and the high-resolution map (0.33 m). In part c, the two images from part b have been overlain. The overlay allows one to determine which pixels from the high-resolution image correspond to the pixels in the ISODATA classified image. A zonal summary is the count of all high-resolution pixels (by class) which reside within the boundaries of a particular zone from the ISODATA classification.

Table 1: Initial 50 Zone Definitions (percent coverage by ground cover type) in CRIT North

Zone		Unclass.	ExR	Field	Water	Bare Ground	Arrowweed	Atriplex	Cottonwood & Willow	Grass & Marsh	Mesquite	Saltcedar
0		99.98	0.00	0.00	0.00	0.01	0.00	0.00	0.00	0.00	0.00	0.01
1		4.97	0.00	0.00	89.15	3.60	0.22	0.07	0.04	0.55	0.04	1.36
2		1.11	0.00	98.54	0.00	0.26	0.00	0.00	0.00	0.00	0.00	0.09
3		5.22	0.00	0.00	58.10	19.04	1.20	0.54	0.40	3.14	0.63	11.72
4		3.75	0.00	0.00	27.38	30.20	2.20	1.15	1.26	5.69	0.80	27.57
5		2.09	0.00	0.00	3.84	7.04	7.27	3.78	1.41	3.25	2.31	69.01
6		79.54	0.00	0.00	0.00	6.37	0.13	0.05	2.22	0.00	0.19	11.48
7		1.98	0.00	0.00	1.18	8.01	11.03	5.08	0.64	1.66	2.13	68.29
8		1.53	0.00	0.00	2.73	17.76	19.80	6.72	0.59	1.75	1.10	48.01
9		1.89	0.00	0.00	1.39	12.05	22.95	4.87	0.03	0.93	1.76	54.11
10		6.42	0.00	0.00	0.40	3.34	1.69	2.17	0.36	0.54	4.49	80.59
11		2.43	0.00	0.00	0.57	10.45	9.97	3.68	0.33	1.53	2.51	68.54
12		5.01	0.00	0.00	0.01	7.94	2.70	3.67	0.44	0.10	5.40	74.72
13		2.13	0.00	0.00	0.43	15.91	11.10	3.87	0.10	0.52	2.29	63.65
14		2.25	0.00	0.00	13.81	37.03	3.46	1.61	0.62	2.99	2.00	36.23
15		24.14	0.00	0.00	0.00	33.97	0.49	0.53	1.28	0.00	0.20	39.39
16		7.32	0.00	0.00	0.09	40.40	1.25	0.59	0.12	0.08	0.51	49.63
17		1.60	0.00	0.00	1.87	14.63	25.88	6.61	0.00	0.52	1.50	47.39
18		2.60	0.00	0.00	0.59	21.33	13.42	4.61	0.06	0.46	2.23	54.69
19		2.67	0.00	0.00	0.11	22.05	4.80	3.45	0.16	0.39	1.89	64.47
20		13.78	0.00	0.00	0.00	47.27	1.37	0.47	0.27	0.05	0.20	36.58
21		5.79	0.00	0.00	0.70	14.51	2.54	3.51	0.42	0.16	5.00	67.37
22		1.91	0.00	0.00	0.29	35.93	9.85	4.01	0.04	0.23	1.50	46.23
23		3.49	0.00	0.00	0.26	20.07	5.19	4.49	0.08	0.20	2.74	63.48
24		2.53	0.00	0.00	0.00	25.15	2.23	3.50	0.05	0.02	2.75	63.77
25		2.62	0.00	0.00	0.42	26.54	18.95	5.61	0.01	0.17	1.73	43.95
26		3.11	0.00	0.00	1.26	31.57	4.56	4.01	0.18	0.18	2.55	52.57
27		4.52	0.00	0.00	0.07	49.27	6.28	1.90	0.01	0.00	0.88	37.06
28		4.78	0.00	0.00	0.35	47.50	3.25	2.08	0.29	0.10	1.46	40.18
29		2.45	0.00	0.00	0.24	39.34	12.01	5.30	0.01	0.10	1.61	38.94
30		3.19	0.00	0.00	0.07	56.79	5.27	2.52	0.01	0.00	1.41	30.74
31		2.62	0.00	0.00	0.40	32.14	4.52	4.53	0.07	0.13	2.37	53.22
32		41.10	0.00	0.00	0.73	42.45	0.35	0.48	0.11	0.21	0.29	14.29
33		5.69	0.00	0.00	1.20	57.96	1.37	1.19	0.58	0.00	2.57	29.45
34		3.44	0.00	0.00	0.02	53.99	5.27	3.23	0.00	0.00	1.67	32.38
35		2.26	0.00	0.00	0.24	48.55	7.57	4.20	0.01	0.06	1.96	35.15
36		23.83	0.00	0.00	0.00	63.98	0.85	0.58	0.05	0.15	0.38	10.18
37		2.89	0.00	0.00	0.21	36.11	3.39	4.19	0.07	0.05	2.65	50.44
38		2.56	0.00	0.00	0.00	25.63	15.18	6.46	0.00	0.00	2.00	48.17
39		5.90	0.00	0.00	0.00	70.19	1.63	0.60	0.42	0.01	0.49	20.75
40		6.70	0.00	0.00	0.00	64.48	0.62	0.64	1.29	0.00	1.57	24.71
41		2.14	0.00	0.00	0.02	67.50	4.09	3.39	0.01	0.01	1.85	20.99
42		3.49	0.00	0.00	0.01	51.65	3.70	3.41	0.02	0.01	2.31	35.39
43		2.62	0.00	0.00	0.00	34.32	11.36	6.99	0.00	0.01	2.73	41.98
44		2.22	0.00	0.00	0.03	54.19	4.78	3.49	0.03	0.04	1.84	33.37
45		1.85	0.00	0.00	0.00	51.87	5.96	4.35	0.01	0.01	2.72	33.22
46		3.15	0.00	0.00	0.04	58.44	1.87	3.01	0.18	0.04	2.35	30.92
47		0.82	0.00	0.00	0.00	63.54	1.94	2.27	0.00	0.00	3.01	28.43
48		2.02	0.00	0.00	0.01	55.34	3.22	3.35	0.04	0.01	3.06	32.95
49		2.00	0.00	0.00	0.00	65.26	1.68	2.16	0.01	0.00	2.06	26.82
50		0.75	0.00	0.00	0.00	77.34	1.14	1.81	0.01	0.00	1.98	16.98

We arbitrarily chose fifty as our initial number of clusters, to ensure that the algorithm sufficiently captured the variability in ground cover present in the Landsat image. Then, we performed a Ward's clustering analysis on the resulting zone definitions to reduce the number of clusters, while retaining a statistically significant amount of information in the definitions. Using the results of the Ward's clustering analysis, we combined redundant zones by merging their spectral signatures. Then, the Landsat image of CRIT North was reclassified using the reduced number of signatures, and a new zonal analysis was performed with the high-resolution map to obtain the final zone definitions. Refer to Table 2.

To test the products, we used the Cibola region in the Landsat image and the high-resolution map to:

1. ***predict the areal coverage*** of each ground cover type in Cibola, according to the products produced from CRIT North, and
2. ***find the actual areal coverage*** of each ground cover type in Cibola, as indicated by a zonal analysis of the region using the high-resolution map.

To calculate the predicted areas, the Cibola region Landsat image was classified using the spectral signatures from CRIT North. Then the histogram pixel counts from each resulting cluster were identified. The total pixel count from each cluster was multiplied by 900 m^2 (the area of one Landsat pixel.) Finally, the total area calculated for each cluster was divided into the proper percent coverage of each ground cover type, according to the zonal definitions found in CRIT North.

To find the actual areal coverage of each ground type in Cibola, we used the Landsat image of Cibola classified by the spectral signatures developed in CRIT North as

Table 2. Final Zone Definitions (percent coverage by ground cover type) in CRIT North

Zone		Unclass.	ExR.	Field	Water	Bare Ground	Arrowweed	Atriplex	Cottonwood &Willow	Grash/marsh	Mesquite	Saltcedar
0		99.98	0.00	0.00	0.00	0.01	0.00	0.00	0.00	0.00	0.00	0.01
1		5.06	0.00	0.00	89.93	3.08	0.20	0.06	0.03	0.44	0.04	1.16
2		1.07	0.00	98.58	0.00	0.26	0.00	0.00	0.00	0.00	0.00	0.09
3		5.04	0.00	0.00	59.55	18.55	1.20	0.52	0.39	3.08	0.57	11.11
4		4.13	0.00	0.00	27.10	29.91	2.25	1.13	1.33	5.46	0.82	27.86
5		79.89	0.00	0.00	0.00	5.17	0.13	0.04	2.51	0.00	0.19	12.07
6		1.52	0.00	0.00	1.51	15.05	20.11	6.54	0.57	1.69	1.38	51.64
7		7.01	0.00	0.00	0.15	3.05	2.10	2.36	0.35	0.48	4.65	79.86
8		2.95	0.00	0.00	10.42	40.33	4.89	1.66	0.76	2.75	1.71	34.52
9		25.78	0.00	0.00	0.06	36.31	0.47	0.41	1.15	0.02	0.17	35.63
10		6.35	0.00	0.00	1.03	53.73	2.01	2.02	0.40	0.08	3.20	31.18
11		7.70	0.00	0.00	0.00	63.88	0.62	0.57	1.16	0.40	1.56	24.12
12		1.54	0.00	0.00	1.34	6.58	9.65	4.61	0.88	2.09	2.32	70.99
13		2.74	0.00	0.00	0.16	26.61	4.03	4.08	0.09	0.13	2.50	59.68
14		2.65	0.00	0.00	0.16	36.27	11.81	5.62	0.01	0.06	1.98	41.45
15		4.86	0.00	0.00	0.18	10.28	2.63	3.61	0.35	0.12	4.75	73.21
16		1.77	0.00	0.00	1.22	17.21	22.83	5.66	0.02	0.56	1.71	49.01
17		2.32	0.00	0.00	0.38	15.25	10.92	4.10	0.14	0.81	2.27	63.81
18		8.96	0.00	0.00	0.04	46.36	1.12	0.44	0.17	0.06	0.25	42.59
19		3.66	0.00	0.00	0.25	51.61	6.28	2.66	0.06	0.08	1.27	34.13
20		35.18	0.00	0.00	0.34	54.89	0.41	0.28	0.17	0.19	0.26	8.28
21		1.30	0.00	0.00	0.00	65.43	1.97	2.36	0.01	0.00	2.59	26.33
22		2.46	0.00	0.00	0.03	54.65	4.41	3.60	0.03	0.02	2.24	32.55

the input to a zonal summary with the high-resolution map of Cibola. Thus, the high-resolution map served as a ground-truthing proxy for the study. This zonal summary resulted in the count of high-resolution pixels corresponding to each of the Landsat clusters in Cibola. These pixel counts were converted to the actual areal coverage of each ground cover type by multiplying the pixel counts by 0.0929 m^2 (the area of one high-resolution map pixel.)

The predicted and actual area calculations were compared by calculating the percent error.

RESULTS

The predicted and actual areal coverage of various ground cover types in Cibola are presented in Table 3 and Table 4, respectively, with the percent error in predicted versus actual areas presented in Table 5. In Table 5, positive errors indicate over-prediction, while negative numbers indicate under-prediction.

From Table 5, the percent errors in Cibola total area prediction vary considerably among the ground cover classes, ranging from 93.58% over-prediction of grass and marsh, to -0.47% under-prediction of saltcedar. Other high percent error rates are seen with water (28.67%) and arrowweed (-14.11%.) Bare ground and cottonwood and willow show moderately low percent errors (-9.69%, and 9.17%, respectively), while atriplex, mesquite, field, and unclassified pixels exhibit low to very low percent error rates (7.77%, -3.43%, -1.07%, and 2.69%, respectively.)

Table 3. Predicted Areas (m^2) by Zone and Ground Cover Type, Cibola												
Zone		Unclass.	ExR.	Field	Water	Bare Ground	Arrowweed	Atriplex	Cottonw. & Willow	Grash & Marsh	Mesquite	Saltcedar
0		69545581	0	0	0	7111	195	33	11	0	230	6328
1		107523	0	0	1912198	65580	4292	1271	717	9343	758	24611
2		72822	0	6698372	0	17604	76	0	13	0	96	5929
3		143690	0	0	1697091	528610	34109	14774	11015	87810	16190	316750
4		134696	0	0	883908	975805	73331	36924	43441	178257	26833	908845
5		22241	0	0	0	1440	37	12	698	0	54	3360
6		22223	0	0	22084	220601	294831	95909	8358	24804	20237	757053
7		894355	0	0	19190	389693	267951	301653	44170	60683	593361	10195297
8		220679	0	0	778451	3013170	365486	124328	56656	205470	128002	2579181
9		52441	0	0	125	73869	963	840	2332	45	343	72497
10		273301	0	0	44114	2311346	86510	87049	17156	3645	137506	1341235
11		42561	0	0	0	353117	3400	3126	6399	2217	8615	133361
12		104612	0	0	90710	446248	654633	312640	59605	142093	157404	4816465
13		214963	0	0	12431	2089997	316567	320277	6941	9878	196472	4687625
14		27891	0	0	1656	381485	124181	59143	53	643	20854	435940
15		546610	0	0	20493	1155006	296118	405522	39639	13589	534007	8229167
16		19220	0	0	13303	186997	248122	61534	175	6111	18592	532565
17		111077	0	0	18317	730609	522918	196431	6556	38671	108893	3055893
18		48103	0	0	202	248782	5994	2371	938	331	1334	228544
19		465134	0	0	32021	6559484	797821	337489	8154	9923	161132	4337456
20		5310	0	0	52	8284	61	42	26	28	39	1249
21		19091	0	0	0	958664	28923	34609	89	0	38015	385796
22		182523	0	0	2309	4048098	326548	266968	2428	1712	165786	2410961
Cibola Sum		73276647	0	6698372	5548655	24771601	4453067	2662944	315570	795254	2334753	45466108

Table 4. Actual Areas (m^2) by Zone and Ground Cover Type, Cibola											
Zone	Unclass.	ExR.	Field	Water	Bare Ground	Arrowweed	Atriplex	Cottonwood & Willow	Grass & Marsh	Mesquite	Saltcedar
0	69537777	0	0	0	12162	245	198	0	0	324	8784
1	18177	0	0	1809519	249143	3553	1591	1260	6119	2105	34826
2	4400	0	6771147	71	12727	348	118	0	0	259	5841
3	61282	0	0	1907302	531881	21484	10401	17946	35646	35304	228793
4	105300	0	0	425348	619648	118024	34115	73680	128914	169705	1587307
5	8207	0	0	710	8414	267	186	1725	0	1138	7192
6	30110	0	0	10587	124268	275659	53296	6602	22296	35483	907797
7	133106	0	0	13542	753984	537832	339172	43059	42435	421533	10481691
8	167861	0	0	36275	2855859	487374	240429	22478	17745	173572	3469829
9	12466	0	0	186	106303	2965	2209	1682	411	2995	74235
10	67017	0	0	7422	2197589	141584	119763	7463	1138	120066	1639822
11	4061	0	0	2	375677	13056	9934	12	0	11664	138392
12	111447	0	0	74133	366400	504486	124940	82134	131949	379895	5009026
13	176037	0	0	1716	2979523	508828	322456	5757	398	224216	3636222
14	15976	0	0	155	385085	135104	40980	158	165	12567	461658
15	140146	0	0	4111	2413669	731108	493335	13247	4225	373216	7067093
16	15936	0	0	3182	230067	243668	43000	418	1317	6805	542227
17	73736	0	0	3971	761824	783892	235024	3405	4060	89677	2833778
18	15703	0	0	2747	286186	8705	10055	3462	563	16174	193004
19	400323	0	0	11023	6175670	467949	247605	3112	13409	185155	5204367
20	1782	0	0	0	8735	112	163	0	0	442	3857
21	28996	0	0	0	1191540	15575	14302	102	0	14180	200492
22	225130	0	0	200	4784169	182569	127678	1367	16	141117	1945087
Cibola Sum	71354975	0	6771147	4312201	27430524	5184387	2470949	289067	410805	2417595	45681321

Table 5. Percent Error (%) by Zone and Ground Cover Type, Cibola											
Zone	Unclass.	ExR	Field	Water	Bare Ground	Arrowweed	Atriplex	Cottonwood & Willow	Grass & Marsh	Mesquite	Saltcedar
0	0.01	0	0	0	-41.53	-20.39	-83.28	0	0	-29.15	-27.95
1	491.53	0	0	5.67	-73.68	20.78	-20.11	-43.08	52.68	-64.02	-29.33
2	1554.98	0	-1.07	-100	38.31	-78.06	-100	0	0	-62.89	1.51
3	134.47	0	0	-11.02	-0.61	58.76	42.04	-38.62	146.34	-54.14	38.44
4	27.92	0	0	107.81	57.48	-37.87	8.23	-41.04	38.28	-84.19	-42.74
5	171.01	0	0	-100	-82.88	-86.34	-93.80	-59.57	0	-95.24	-53.29
6	-26.19	0	0	108.60	77.52	6.95	79.95	26.59	11.25	-42.97	-16.61
7	571.91	0	0	41.70	-48.32	-50.18	-11.06	2.58	43.00	40.76	-2.73
8	31.47	0	0	2045.94	5.51	-25.01	-48.29	152.05	1057.88	-26.25	-25.67
9	320.69	0	0	-33.17	-30.51	-67.53	-61.97	38.67	-89.16	-88.56	-2.34
10	307.81	0	0	494.39	5.18	-38.90	-27.32	129.88	220.39	14.53	-18.21
11	947.99	0	0	-100	-6.00	-73.96	-68.53	55450.47	596590.75	-26.14	-3.64
12	-6.13	0	0	22.36	21.79	29.76	150.23	-27.43	7.69	-58.57	-3.84
13	22.11	0	0	624.55	-29.85	-37.78	-0.68	20.58	2384.22	-12.37	28.91
14	74.58	0	0	966.37	-0.93	-8.08	44.32	-66.36	290.99	65.94	-5.57
15	290.03	0	0	398.50	-52.15	-59.50	-17.80	199.23	221.62	43.08	16.44
16	20.61	0	0	318.07	-18.72	1.83	43.10	-58.14	364.01	173.21	-1.78
17	50.64	0	0	361.32	-4.10	-33.29	-16.42	92.55	852.46	21.43	7.84
18	206.33	0	0	-92.64	-13.07	-31.15	-76.42	-72.90	-41.25	-91.75	18.41
19	16.19	0	0	190.50	6.21	70.49	36.30	162.04	-26.00	-12.97	-16.66
20	197.98	0	0	0	-5.16	-45.28	-73.97	0	0	-91.15	-67.62
21	-34.16	0	0	0	-19.54	85.70	141.99	-12.14	0	168.10	92.42
22	-18.93	0	0	1055.30	-15.39	78.86	109.09	77.62	10801.14	17.48	23.95
Cibola Total	2.69	0	-1.07	28.67	-9.69	-14.11	7.77	9.17	93.58	-3.43	-0.47

DISCUSSION

The results indicate that the spectral signatures and zone definitions produced from CRIT North have variable success at predicting (mapping) the areal coverage of various ground cover types in Cibola. This seems to be greatly dependent upon the ground cover type in question. It is important to note that each ground cover type is present in varying amounts in Cibola. Thus, the error in predicting one type may have less impact than another, simply because the first type is present in very small amounts.

Table 6 shows the areal coverage of each ground cover type in Cibola as a percentage of the total area of the region.

Table 6. Actual Percent Coverage (%) of Ground Cover Types, Cibola

Unclass	ExR.	Field	Water	Bare Ground	Arrowweed	Atriplex	Cottonwood & Willow	Grass & Marsh	Mesquite	Saltcedar
42.90	0	4.07	2.59	16.49	3.12	1.49	0.17	0.25	1.45	27.47

The ground cover type which exhibits the greatest error in predicting coverage actually comprises just 0.25% of the area in Cibola. Conversely, saltcedar, which has the lowest percent error rate in prediction, comprises 27.47% of the area in Cibola. This is the highest coverage of all the ground cover types. Another ground cover type with a high percent error is water, but water only comprises 2.59% of the area in Cibola. Bare ground presents the most problematic case, with a moderate percent error of -9.69% and a significant areal coverage of 16.49% in Cibola.

The high percent error in prediction of grass and marsh may be explained by their limited presence in Cibola. Landsat imagery most likely has too coarse a spatial resolution to distinguish the relatively weak spectral signature of grass and marsh.

Likewise, bare ground in Cibola frequently exists in patches much smaller than the size of a Landsat pixel, weakening its spectral influence in Landsat imagery.

Saltcedar is present in abundance in Cibola in large homogeneous stands. It may be inferred, therefore, that the saltcedar spectral signature presents itself very strongly in Landsat imagery. Water, confined almost exclusively to the river channels in Cibola, is also present in contiguous structures in Cibola, but the water depth varies greatly from the river bank to mid-channel. Sediments in shallow water and emergent vegetation may be obscuring the "pure" water spectral signature.

The abundance of unclassified pixels in the imagery may also contribute significant error to the area predictions. A majority of the unclassified pixels are in the "background", beyond the edges of the riparian zone, and they do not contain any spectral information. Refer to Figure 4. A small number of the unclassified pixels exist within the riparian zone of the Cibola imagery. Together, the unclassified pixels in Cibola comprise 42.9% of the image. This is by far the most coverage of any of the actual ground cover types in the image. In CRIT North unclassified pixels account for 50% of the image, and they were included in the calculations of the zone definitions and the Ward's clustering analysis. Thus, unclassified pixels exert great influence over the statistical calculation of the zone definitions, though they provide no information to the spectral signatures. Future applications of this method should probably exclude unclassified pixels from any statistical calculations.

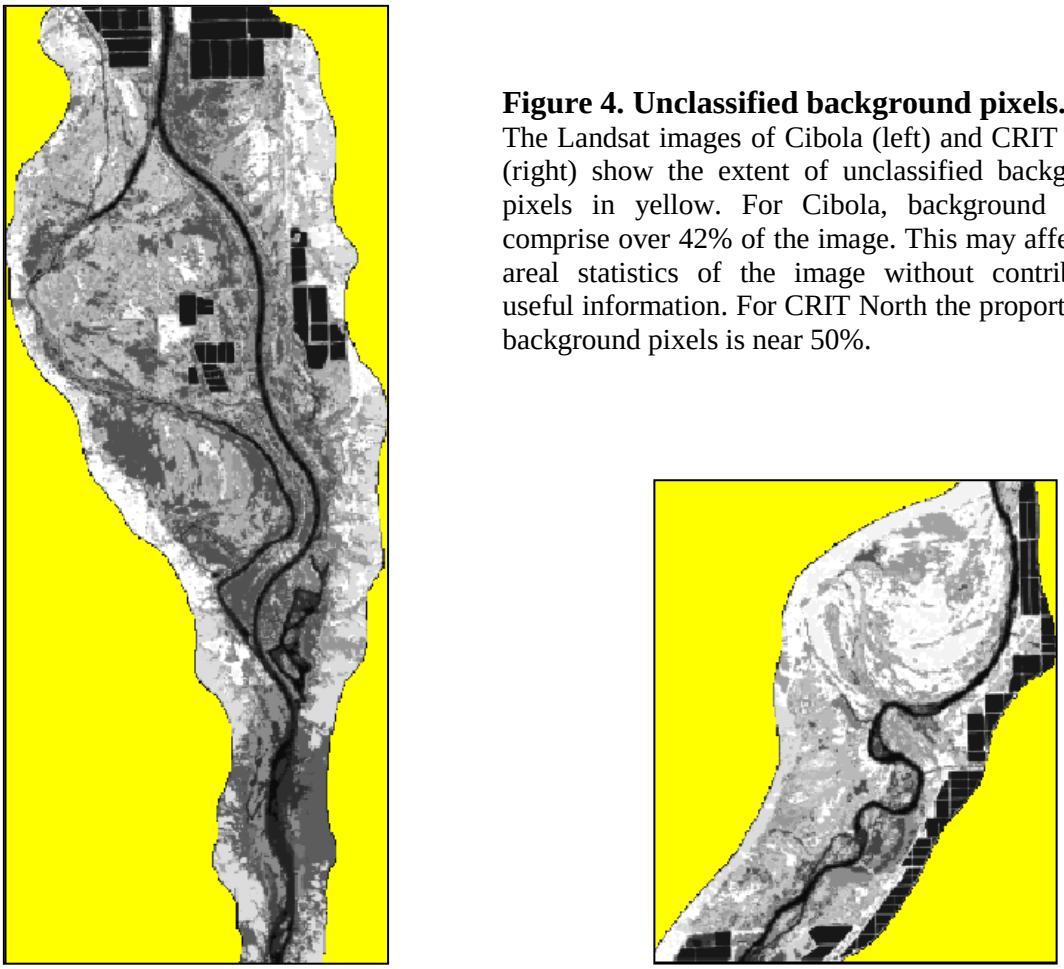

Figure 4. Unclassified background pixels.
The Landsat images of Cibola (left) and CRIT North (right) show the extent of unclassified background pixels in yellow. For Cibola, background pixels comprise over 42% of the image. This may affect the areal statistics of the image without contributing useful information. For CRIT North the proportion of background pixels is near 50%.

SUGGESTIONS FOR FUTURE WORK

To truly evaluate the validity of this method, a map of the predicted areas should be made while simultaneously field-checking the results. Random pixels could be selected from the map, located in the field, and surveyed directly for percent ground cover of the classes represented in that pixel. This will only be possible in the future, when another field season arrives.

Field checking the products in a future field season will also check if the method in this study is image-specific, or if the products developed from imagery acquired on one day are useable on imagery from a different day. Possible variations in imagery from

one day to the next (or from year to year, around the same time in the growing season) could be due to atmospheric conditions, climate (dry vs. wet conditions, leading to changes in vegetation health), or any other outside contributor which would lead to the detection of spectral signatures in one image that are not present in another.

For example, regions of the Lower Colorado River Basin experienced a wild-fire in 2005, but the products in this study were developed from 2004 imagery. The lack of burned areas in 2004 would mean that the influence of this ground-cover type was not accounted for by our products. This could be corrected by updating the high-resolution map, and producing a new set of spectral signatures and zone definitions. The difficulty of updating the high-resolution map, however, depends on the extant of the areas burned.

This brings up the question of how long a given set of spectral signatures and zone definitions will remain valid for use in predicting ground coverage for LCRAS. For the most part, the changes in the Lower Colorado River riparian zone proceed slowly, on the order of decades. However, shifting climates, expanding saltcedar and arrowweed, and bio control studies[1], all have the potential to create rapid changes. This would require more frequent updating of the products.

This study provides the framework for further development and testing of riparian vegetation mapping methods which improve upon Anderson-Ohmart. The method is not dependent on annual extensive field surveys or high-resolution imagery collection. It has so far been shown to accurately predict areal coverage of the most predominant vegetation species in the region. Moreover, the method is relatively simple to automate

[1] In an effort to control the spread of saltcedar, a beetle (*Diorhabda elongata*) intended to preferentially defoliate saltcedar, was released in the Western U.S. in 2001. The beetles are slowly approaching the Lower Colorado River Basin from the North.

and execute, and it employs imagery available for free. USBR may find that the method is faster, less expensive, and more detailed than what is already employed by LCRAS to map riparian vegetation. The benefits of this method have the potential to streamline mapping procedures in LCRAS, leaving USBR with more resources to carry out its mission of managing water in the Western United States.

WORKS CITED

Anderson, B., and Ohmart, R. (1976) Vegetation Type Maps of the Lower Colorado River from Davis Dam to the Southerly International Boundary. *U.S. Bureau of Reclamation*, Boulder City, NV.

Anderson, B., and Ohmart, R. (1985) Habitat Use by Clapper Rails in the Lower Colorado River Valley. *Condor* 87, 116-126.

Arizona v. California, 376 U.S. 340, 1964

Arizona v. California, 547 U.S. 150, 2006

Bureau of Reclamation. (2008) "Lower Colorado River Accounting System Calendar Year 2007: Demonstration of Technology Report." *NV: Bureau of Reclamation, Lower Colorado Region*. Web. 30 Mar. 2009.

Dwyer, C. (2010) "Lower Colorado River Water Accounting." *U.S. Bureau of Reclamation*. Web. 12 Jul. 2010.

Norviel, W.S., McClure, W. F., Carpenter, D. E., Scrugham, J. G., Davis, Jr., S. G., Caldwell, R.E., and Emerson, F. C. (1922) *Colorado River Compact, 1922.* Boulder, CO: University of Colorado.

WORKS CITED

Anderson, B., and Ohmart, R. (1976) Vegetation Type Maps of the Lower Colorado River from Davis Dam to the Southerly International Boundary. *U.S. Bureau of Reclamation*, Boulder City, NV.

Anderson, B., and Ohmart, R. (1985) Habitat Use by Clapper Rails in the Lower Colorado River Valley. *Condor* 87, 116-126.

Arizona v. California, 344 U.S. 919, 1964

Arizona v. California, 376 U.S. 340, 1964

Arizona v. California, 383 U.S. 268, 1966

Arizona v. California, 439 U.S. 419, 1979

Arizona v. California, 460 U.S. 605, 609, 615, 1983

Arizona v. California, 466 U.S. 144, 1984

Arizona v. California, 531 U.S. 1, 2000

Arizona v. California, 547 U.S. 150, 2006

Becker, B., Lusch, D., and Qi, J. (2007) A Classification-based Assessment of the Optimal Spectral and Spatial Resolutions for Great Lakes Coastal Wetland imagery. *Remote Sensing of Environment* 108, 111-120.

Bureau of Reclamation. (2007) "Record of Decision: Colorado River Interim Guidelines for Lower Basin Shortages and the Coordinated Operations for Lake Powell and Lake Mead." *Washington, D.C.: Bureau of Reclamation, Office of the Commissioner.* Web. 13 Mar. 2009.

Bureau of Reclamation. (2008) “Lower Colorado River Accounting System Calendar Year 2007: Demonstration of Technology Report.” *NV: Bureau of Reclamation, Lower Colorado Region*. Web. 30 Mar. 2009.

CH2MHILL (1999) Lower Colorado River 1997 Vegetation Mapping and GIS Development. *U.S. Bureau of Reclamation*, Boulder City, NV.

Dwyer, C. (2010) “Lower Colorado River Water Accounting.” *U.S. Bureau of Reclamation*. Web. 12 Jul. 2010.

ERDAS, Inc. (1999) “ERDAS Field Guide, 5th ed.” *ERDAS Inc.*, Atlanta, GA.

Harman, M. (2005) “Mapping Invasive Species in Mākaha Valley, O’ahu Using Fine Resolution Satellite Imagery.” *University of Hawai’i*. Web. 30 Apr 2010.

Hirano, A., Madden, M., Welch, R. (2003) Hyperspectral Image Data for Mapping Wetland Vegetation. *Wetlands* 23, 436-448.

McGinley, S. (2007) “Salt Cedar: Blight or Benefit? A 10 Year Study on the Lower Colorado River.” *Arizona Agriculture Experiment Station Research Report*. Web. 12 Jul. 2010.

Menges, C., Hill, G., and Ahmad, W. (2001) Use of Airborne Video Data for the Characterization of Tropical Savannas in Northern Australia: the Optimal Spatial Resolution for Remote Sensing Applications. *International Journal of Remote Sensing* 22, 727-740.

Nagler, P., Edward, G., Hursh, K., Curtis, C., Huete, A. (2005) Vegetation Mapping for Change Detection on an Arid-zone River. *Environmental Monitoring and Assessment* 109, 255-274.

Nijland, W., Addink, E., De Jong, S., and Van der Meer, F. (2009) Optimizing Spatial Image Support for Quantitative Mapping of Natural Vegetation. *Remote Sensing of Environment* 113, 771-780.

Norviel, W.S., McClure, W. F., Carpenter, D. E., Scrugham, J. G., Davis, Jr., S. G., Caldwell, R.E., and Emerson, F. C. (1922) *Colorado River Compact, 1922.* Boulder, CO: University of Colorado.

Neale, C. (2005) High Resolution Remote Sensing of Wetland, Riparian, Urban Areas and Evapo-transpiration. *Proceedings of the Conference on State-of-the Art Review of ET Remote Sensing Science and Technology*. Wilberforce: International Center for Water Resources Management.

Ohmart, R., Anderson, B., and Hunter, W. (1988) Ecology of the Lower Colorado River from Davis Dam to the Mexico-United States Boundary: a Community Profile. *National Technical Information Service*, Alexandria, VA.

Ramsey, E. W, and Laine, S. C. (1997) Comparison of Landsat Thematic Mapper and High Resolution Photography to Identify Change in Complex Coastal Wetlands. *Journal of Coastal Research* 13, 281-292.

Riyad, I., Onisimo, M., Lalit, K., and Urmilla, B. (2008) Determining the Optimal Spatial Resolution of Remotely Sensed Data for the Detection of *Sirex noctilia* Infestations in Pine Plantations in Kwazulu-Natal, South Africa. *South African Geographical Journal* 90, 22-31.

U.S. Geological Survey. (2004) "USGS Fact Sheet 2004-3062: Climatic Fluctuations, Drought, and Flow in the Colorado River Basin*." U.S. Geological Survey, Office of the Chief Scientist for Hydrology.* Web. 15 Mar. 2009.

Wang, Y., Traber, M., Milstead, B., Stevens, S. (2007) Terrestrial and Submerged Aquatic Vegetation Mapping in Fire Island National Seashore Using High Spatial Resolution Remote Sensing Data. *Marine Geodesy* 30, 77-95.

Xie, Y., Sha, Z., and Yu, M. (2008) Remote Sensing Imagery in Vegetation Mapping: a Review. *Journal of Plant Ecology* 1, 9-23.

Younker, G., and Andersen, C. (1986) Mapping Methods and Vegetation Changes Along the Lower Colorado River Between Davis Dam and the Border with Mexico. *U.S. Bureau of Reclamation*, Boulder City, NV.

APPENDICES

APPENDIX A

THE LOWER COLORADO RIVER ACCOUNTING SYSTEM (LCRAS)

A.1 Introduction

The Lower Colorado River Accounting System came about when USBR felt it needed more exact data regarding water used for agriculture in the Lower Colorado Basin. In the late 1980's the U.S. Geological Survey (USGS) began the development of LCRAS (Bureau of Reclamation, 2009). The goal was to provide estimates of water used specifically by agricultural crops in the Lower Colorado River Basin using the latest remote sensing technology available. The data from the reports were to be used to help USBR account for agricultural water usage versus other types of water consumption. In the early 1990's USBR took over further development and implementation of LCRAS. Since 1994, USBR has published annual LCRAS reports as supplements to the court mandated Decree Accounting Reports.

The scope of LCRAS has widened, since water has become scarcer in the Lower Colorado River Basin. LCRAS now provides detailed estimates of three sources of water loss from the Lower Colorado River (Bureau of Reclamation, 2008):

1. water used by crops
2. water used by natural vegetation in the riparian zone
3. water evaporated into the atmosphere from open water source

A.2 Elements of LCRAS

The Lower Colorado River Accounting System (LCRAS) uses remotely sensed data to map agricultural crops, riparian vegetation, and open water in the Lower Colorado

River region (Bureau of Reclamation, 2009). The information from the resulting maps is then combined with weather data and other information to estimate the amount of water lost to the atmosphere by evapo-transpiration (ET) of agricultural crops and riparian vegetation, and direct evaporation from open water sources (Bureau of Reclamation, 2008). LCRAS results are updated and published on a yearly basis.

LCRAS involves three key components, or processes, used to produce the final ET and evaporation water loss estimates (Bureau of Reclamation, 2008). These processes are as follows:

- Mapping the region's crops, riparian vegetation, and open water areas
- Estimating water loss via ET of crops and riparian vegetation
- Estimating water loss via evaporation from open water sources

The mapping process is critical to the overall success of LCRAS, as the ET and evaporation estimates rely heavily on the accuracy of the initial maps. The sections to follow discuss the steps involved in the LCRAS mapping procedure, followed by brief descriptions of how LCRAS estimates water loss from ET of crops and riparian vegetation and evaporation from open water sources.

Table 1 provides an example of LCRAS results from the 2007 calendar year. Note that the results are reported by vegetation or open water source type, by sub-region of the study area, and finally as a total loss of water from the Lower Colorado River Basin.

Table A-1: Water Loss Due to ET and Evaporation Estimated by LCRAS in 2007

Units: acre-feet of water per year	**Lower Colorado Basin Sub-region**				**Total**
ET/Evaporation Category	Hoover Dam to Davis Dam	Davis Dam to Parker Dam	Parker Dam to Imperial Dam	Imperial Dam to Mexico	Hoover Dam to Mexico
Agricultural ET	0	85,223	721,465	2,538,143	3,344,831
Riparian Vegetation ET	772	179,718	366,439	80,648	627,577
Maintained Open Water	0	19,695	19,090	33,784	72,569
Non-Maintained Open Water	16	1,219	5,940	1,114	8,289
Mainstem Open Water	146,810	107,586	50,096	5,495	310,831
				Total Water =	4,364,097

Table adapted from Bureau of Reclamation (2008)

A.3 The LCRAS Mapping Procedure

There are five steps used in creating the maps employed by LCRAS (Bureau of Reclamation, 2008):

1. Collect remote sensing data
2. Collect ground reference data
3. Delineate crops
4. Delineate riparian vegetation
5. Delineate open water

The steps are carried out in the general order as listed, although steps may be repeated or refined as additional data is gathered and analyzed at subsequent steps.

A.3.1 Collecting and Analyzing Remote Sensing Data

The primary source of LCRAS satellite imagery is the Landsat satellites operated by NASA and the U.S. Geological Survey. Images are collected which cover the majority of the Lower Colorado River Region, are mostly cloud-free, and capture the differential growing seasons of the various crops grown in the region. Landsat images are supplemented by other satellites when Landsat fails to fulfill the criteria listed above. The satellite images serve as the basis upon which LCRAS produces its maps. Figure 1 shows the LCRAS study area, with the blue and green portions highlighting the specific areas of concern.

Map courtesy of Bureau of Reclamation (2008).

Figure A-1. Map of the Lower Colorado River Basin, highlighting the LCRAS study area.

A.3.2 Collecting Ground Reference Data

Ground reference data, collected by scientists in the field at various times during the growing season, is used for two primary purposes. First, spectral data gathered for various crops, riparian species, and open water types are used to train remote sensing computer software to correctly classify (identify) these objects on a satellite image. Second, ground reference data are used to evaluate the accuracy of the classification performed by the computer.

Ground reference points are chosen randomly, for statistical reliability, and then are supplemented by other user-chosen points to ensure that no region of the study area is ignored. Approximately 60 to 65 percent of the ground reference data gathered for LCRAS is used for software training and classification. The remaining ground reference data is employed for accuracy assessment.

A.3.3 Delineating Crops

Crop delineation allows LCRAS users to find the acreage of each type of crop grown in the Lower Colorado River Basin. This information is necessary for accurate ET measurements, because not all crops transpire at the same rate.

Classifying crops on the satellite images begins with the identification of the boundaries or outlines of agricultural fields. A database of Lower Colorado River region field boundaries was initially developed in 1992 from high-resolution SPOT satellite imagery. This database has been maintained and periodically updated as needed on a yearly basis. The information from this database is applied to the Landsat imagery so that each field will be identified as a single block (representing a single crop).

A classification of the image is then carried out to determine which crop species occupies each field. Next, the crops are sorted into groups, according to their typical known rates of ET. Table 2 shows the set of LCRAS crops groups mapped in 2007. Note that melons, for example, can be considered one class of crop for ET estimation purposes, because watermelons, honeydew, squash, cantaloupes, and cucumbers all transpire similarly. Grouping crops this way greatly reduces the number of crop classes to be dealt with in the ET calculations (Congalton, et al., 1998). Finally, the acreage covered by each crop group is calculated from the classified map.

A.3.4 Delineating Riparian Vegetation

Classifying riparian vegetation is more challenging than classifying crops, due to the heterogeneous mixture of plant species observed over small areas in the Lower Colorado River riparian zone. For this reason, classification of riparian vegetation at the species level is not routinely carried out for LCRAS. Rather, classes of common mixtures of species are mapped on the satellite imagery. Table 3 provides a list of the riparian vegetation classes used in LCRAS.

Riparian vegetation maps are updated each year by comparing newly acquired satellite imagery classifications to the previous year's map. Any changes that are detected from the comparison are field checked and corrected in the new map. Finally, the acreage of each riparian vegetation class is calculated for use in ET estimates.

Table A-2: LCRAS Crop Groups Mapped in Calendar Year 2007

Alfalfa (Alfalfa, Alfalfa – Unwatered (dry and senescent)	**Melons** – Spring and Fall (Watermelon, Honeydew, Cantaloupe, Squash, Cucumbers)	**Tomatoes**	**Small Vegetables** (Carrots, Cilantro, Celery, Garlic, Dry Onions, Onions, Parsley, Radishes)
Cotton	**Grapes**	**Sudan** (includes Sunflower and Sesbania)	**Root Vegetables** (Table Beets, Parsnip, Turnip and Rutabaga)
Small Grain (Oats, Rye, Barley, Millet, Wheat)	**Bermuda/Rye Grass** (Bermuda, Bermuda Over seeded with Rye, Klein, Timothy)	**Legume/Solanum Vegetables** (Green, Dry and Garbanzo Beans; Peas, Peanuts, Fresh Peppers, Potatoes)	**Perennial Vegetables** (Artichoke, Asparagus)
Field Grain (Field Corn, Sorghum, Milo)	**Citrus** (Young, mature, Declining)	**Crucifers** (Broccoli, Cauliflower, Cabbage, Bok-Choy, Mustard, Kale, Okra)	**Sugar Beets** (Summer and Winter)
Lettuce - Spring and Fall (Head, Leaf [Red], Leaf [Green], Spinach, Other Lettuce)	**Idle** (Fields currently not in production, includes bare cultivated soil)	**Dates**	**Fallow**
Open-Water (Fish Pond, Duck Pond, Off-Stream Lake or Reservoir)	**Jojoba**	**Safflower**	**Moist Soil Unit**[7]
Seasonal Wetland[8]	**Nursery or Greenhouse** (Citrus Nursery, Native Nursery, Greenhouse, Other Nursery)	**Deciduous Orchards** (Pecans, Peaches, Almonds)	**Other**

Table Courtesy of Bureau of Reclamation (2008)

Table A-3: LCRAS Riparian Vegetation Classes

Group Name	Description
Marsh	40% cattail, bulrush, and phragmites
Barren	Less than 10% vegetation
Sc_low	11% to 60% salt cedar and less than 25% arrowweed
Sc_high	61% to100% salt cedar and less than 25% arrowweed
Sc/ms	11% to 60% salt cedar, 11% to 60% mesquite, and less than 25% arrowweed
Sc/aw	Less than 75% salt cedar and 25% or more arrowweed
Sc/ms/aw	15% to 45% salt cedar, 15% to 45% mesquite, and 20% to 40% arrowweed
Ms-low	11% to 60% screwbean and honey mesquite, and less than 25% arrowweed
Ms-high	61% to 100% screwbean and honey mesquite, and less than 25% arrowweed
Ms/aw	21% to 60% mesquite, 31% to 60% arrowweed, and less than 20% salt cedar
Aw	51% to 100% arrowweed and less than 10% any trees
Cw	61% to 100% cottonwood and willow
Low veg	Greater than 10% and less than 30% any riparian vegetation

Table Courtesy of Bureau of Reclamation (2008)

A.3.5 Delineating Open Water

LCRAS classifies open water sources into three broad categories: The mainstem of the Colorado River, other non-maintained sources (such as marshes or small tributaries), and maintained sources (such as canals, dammed reservoirs, and irrigation ditches.) Similar to the crop field boundary database, an initial open water source database was developed in 2000 for use by LCRAS. It is updated yearly using the Landsat imagery newly acquired each year. The acreage of each category of open water source (natural and maintained) is calculated from the maps. These acreages are used to estimate the amount of water lost from each open water source category via direct evaporation to the atmosphere.

A.4 The LCRAS Water Loss Estimation Procedures due to ET

LCRAS takes five steps to calculate water loss due to ET for each crop and riparian vegetation class in the study area. These steps are:

1. Calculate the **reference ET rate**
2. Calculate **ET coefficients** for every crop and riparian vegetation class
3. Calculate the **effective precipitation** (for crops only, not needed for riparian vegetation)
4. Calculate the **acreage** covered by each crop and riparian vegetation class
5. Use the four parameters above to calculate **final water loss** for each crop and riparian vegetation class

A.4.1 Calculating Reference ET

The reference ET of a region is the amount of water evapo-transpired by a single reference crop per year. The reference ET will later be adjusted for each crop and riparian vegetation group by applying an ET coefficient. Measuring a reference ET for just one or two crops, and then adjusting this value for other crops, allows LCRAS to calculate ET for many classes of vegetation without the need for direct measurement of all of them.

Grass and alfalfa are common crops used for calculating reference ET, because these two crops have been extensively studied. The reference ET of these crops are calculated from in situ data collected by weather monitoring towers placed in the fields where these crops are grown. The towers measure several parameters (sunlight, temperature, wind speed, wind direction, humidity, etc.) which directly affect the rate at which the crops transpire. Those weather parameters are then inserted into an equation which estimates how much water the crops would have transpired under those specific weather conditions.

Because rates of ET vary continuously with the weather, LCRAS must calculate new reference ET values several times a year at several locations in the study area.

A.4.2 Calculating ET Coefficients

ET coefficients relate the ET rates of every crop group to the ET rate of the reference crops. The coefficients used by LCRAS were originally calculated from field measurements in 1998 and refined in 2002. This database of ET coefficients is applied each year by LCRAS in the final ET calculations.

All crops and riparian vegetation groups transpire water to the atmosphere at different rates. Some groups transpire faster than the reference crops (usually grass or

alfalfa), and some groups transpire slower than the reference crops. The ET coefficient for a distinct crop or riparian vegetation group accounts for the difference in ET between the reference crop and the vegetation group in question.

For example, if the ET coefficient of melons is 1.2, this means that (on average) melons transpire 1.2 times the water that the reference crop transpires. If the reference crop was measured to have an ET rate of 79.1 inches of water per year (in_w/yr), then LCRAS would calculate the ET of melons as:

79.1 in_w/yr (reference crop) × **1.2** = **94.92** in_w/yr (melons)

Note this is not the final ET rate of melons, as LCRAS applies another correction factor, the effective precipitation.

A.4.3 Calculating the Effective Precipitation

The effective precipitation is a measure of how rain water subtracts from the total water loss of the Lower Colorado River Basin. LCRAS seeks to quantify the amount of water lost from the Colorado River itself, thus any water transpired by crops which enters the basin via direct rainfall should not be included in the final ET calculation. The effective precipitation correction is applied to crops only, not to riparian vegetation, because the in situ weather data needed for the calculation is only available in crop fields with rain gauges.

Effective precipitation is calculated from in situ weather station measurements of rainfall and a pre-determined precipitation coefficient that relates the rainfall to the ET rates of the crops. The effective precipitation correction is then applied to the ET rate of the crop.

For example, if the effective precipitation for a region growing melons was calculated to be 2.1 in_w/yr, and the reference ET and melons crop coefficient are the same as above, then the new ET rate of melons is:

94.92 in_w/yr (melons) - **2.1** in_w/yr (Eff. Precip.) = **93.82** in_w/yr (corrected ET of melons)

The corrected ET rate for melons is then multiplied by the number of acres of melons grown in the study area to estimate water loss.

A.4.4 Calculating Crop and Riparian Vegetation Acreage

The areas covered by each crop and riparian vegetation group are calculated from the LCRAS maps produced each year from remote sensing and ground truth data. Refer to section "The LCRAS Mapping Procedure". The number of acres of each group is multiplied by its corrected ET rate.

A.4.5 Calculating Final Water Loss via ET of Crop and Riparian Vegetation Groups

The final water loss calculation in LCRAS combines the reference ET, ET coefficient, effective precipitation, and acreage into a final total amount of water transpired by every crop and riparian vegetation group. The total amount is in units of acre-inches of water per year. The amount is divided by 12 to give a final answer in acre-feet per year.

For example, given the following hypothetical parameters for melons in one growing season:

- Reference ET = **79.1** in_w/yr
- Crop Coefficient (melons) = **1.2**

- Effective Precipitation = **2.1** in_w/yr
- Acres of Melons = **1,560** acres

The final amount of water evapo-transpired by melons in the study area, in acre-feet per year is:

{[(**79.1** in_w/yr × **1.2)** - **2.1** in_w/yr] × **1,560** acres} ÷ **12** in/foot =

12,066.6 acrefeet of water per year (melons)

Similar calculations are made for each crop and riparian vegetation group (with no effective precipitation correction applied to the riparian vegetation).

Final ET totals in LCRAS are reported individually by vegetation group by sub-region of the study area and as total ET of all crops and all riparian vegetation groups. Refer to Table 1.

A.5 The LCRAS Evaporation Estimation Procedure of Open Water Sources

LCRAS calculates evaporation from open water sources in a similar fashion as ET from crops. Open water sources are divided into three primary groups:

- Colorado River mainstem
- Non-maintained sources
- Maintained sources

LCRAS calculates evaporation from each type of open water source using the following parameters:

1. **Reference ET** of open water (measured in situ, as for crop reference ET)
2. **Evaporation coefficient** for various open water sources (analogous to a crop ET coefficient, measured empirically)

3. **Precipitation** (analogous to effective precipitation for crops, measured in situ by rain gauges)
4. **Acreage** of critical open water source types

The final calculation is also similar to that of crop water loss via ET, but with the analogous parameters listed above. The total evaporation is calculated separately for each month of the year, and the monthly totals are added to obtain an annual sum. The equation for monthly evaporation, in units of acrefeet per month is:

{[(Reference ET × Evap. Coefficient) - Precipitation] ÷ 12 in/foot} × Acreage of source

Evaporation totals are reported by open water source and sub-region of the study area. See Table 1.

APPENDIX B

REMOTE SENSING AND DIGITAL IMAGERY

B.1 Introduction

Remote sensing is the practice of measuring something indirectly, without being in contact with the subject being measured. Medical images, such as radiographs (X-rays), CAT scans, and MRIs examine the tissues and organs inside the body, without ever being in contact with the target. Marine mammals like dolphins and whales determine distances from, and the sizes of, objects using sonar signals, without directly "seeing" or touching the objects. Weather radar can identify approaching storms and tornadoes long before they reach the instrument. Satellites and cameras mounted on airplanes map objects on the surface of the Earth, and in some cases below the surface of the Earth, despite being many miles away from the surface. It is the last two examples, deriving information about the earth and its atmosphere from satellites or airborne cameras, which serves as the traditional definition of the term "remote sensing."

Primitive remote sensing began in the 1860's, when people first mounted cameras on balloons. Cameras mounted on kites became popular in the 1880's and 1890's. Pictures from airplanes were first taken in 1909, and by WWI it was common to collect photographic information from the ground via aircraft. Aircraft mounted cameras are still commonly used today for a variety of purposes, both civilian and military.

Images of the Earth's surface from space were first taken by cameras mounted on rockets launched during the early years of the Space Race. In 1960, the United States launched its first weather satellite, called TIROS-1. Not only was TIROS the first weather satellite (dedicated at imaging clouds), it was also one of the first remote sensing

platforms with a non-photo sensor (TIROS-1 used a television camera.) The launch of TIROS-1 is considered to be the beginning of space-based remote sensing. Refer to Figure B-1.

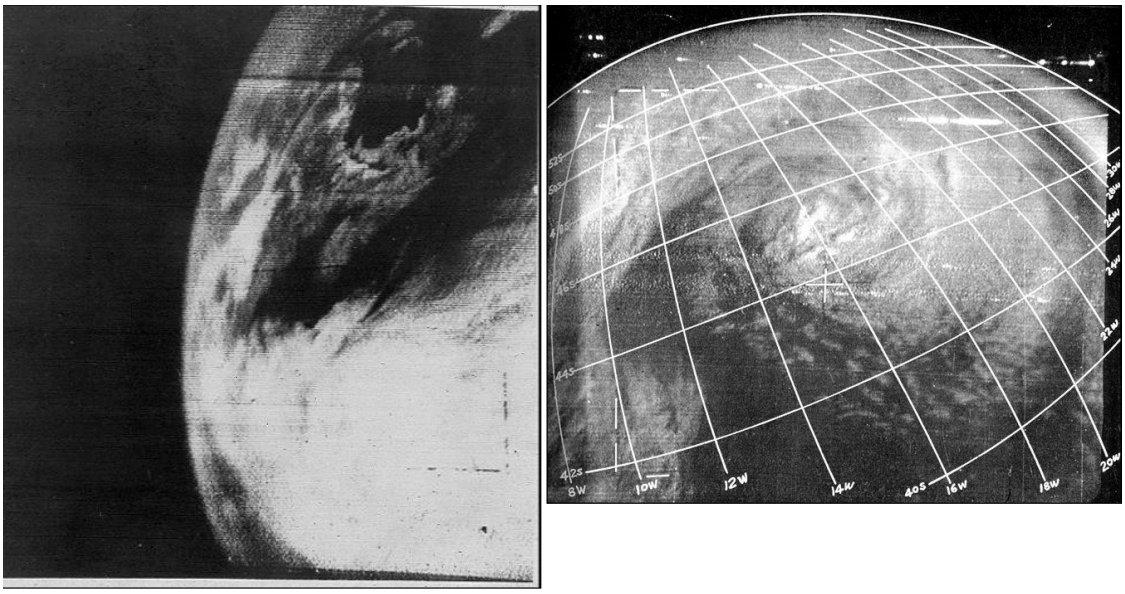

Figure B-1. Images from TIROS-1. The first image transmitted by TIROS-1 was captured on April 1, 1960 (left.) Sometime during its 78 days of operation, TIROS-1 also captured an image of a low pressure system over the South Atlantic (right.)

The invention of the charge-coupled device in the 1969 was quickly followed by the age of digital imagery. Bulky film and other analog recording devices became obsolete for most imaging applications, including airborne and space-based remote sensing. There are now many alternatives to charge-coupled devices to create digital images, by they are by far the most prevalent method. The inventors of the charge-coupled device, Willard Boyle and George Smith, were awarded the Nobel Prize in physics in 2009 for their invention.

Today, there are numerous satellites orbiting the Earth which provide information about the Earth's surface and its atmosphere. Remote sensing has revolutionized weather forecasting, cartography, navigation, surveying, geological exploration, disaster response,

environmental and urban monitoring, and countless other branches of science, government, and defense.

The sections that follow will provide basic descriptions of some of the key concepts in remote sensing and digital imagery.

B.2 The Electro-Magnetic Spectrum

All matter in the universe (from the simplest single atom to massive galaxies, and the things which populate those galaxies) emits some form of energy within the electro-magnetic spectrum (EM spectrum). Remote sensing instruments exploit this property of matter by gathering some of the EM energy emitted by a source. We then interpret these emissions to gather information about the source. EM energy comes in many different types, which we call gamma rays, x-rays, ultraviolet, visible light, infrared, microwaves, and radio waves. Despite the different applications of various types of EM energy (from treating to cancer to transmitting radio shows), they all share some common characteristics.

B.2.1 Wavelength

EM energy travels in waves, without requiring a medium to carry it. (This is unlike sound waves which must be carried by a medium, such as air or water, in order to travel. Sound waves should not be confused with EM energy waves. They are very different entities.) Thus, EM energy can travel through empty space. Waves of EM energy come in different wavelengths, which is the distance from one point on a wave to the corresponding point on the next wave (i.e. peak to peak, or trough to trough.) It is expressed in units of distance (i.e. nanometers, micrometers, meters, etc.) The wavelength determines what kind of EM energy the waves are. Gamma rays have the

shortest wavelengths, and radio waves have the longest. Bear in mind, however, that the EM spectrum is just that: a spectrum. There are no definitive boundaries in nature that separate one type of EM energy from another. We have arbitrarily placed boundaries between certain wavelengths to indicate when one part of the spectrum switches to another. Each part of the spectrum actually represents a range of wavelengths. Thus, not all radio waves (or all gamma rays, or all visible light waves) have the same wavelength. Refer to Figure B-2.

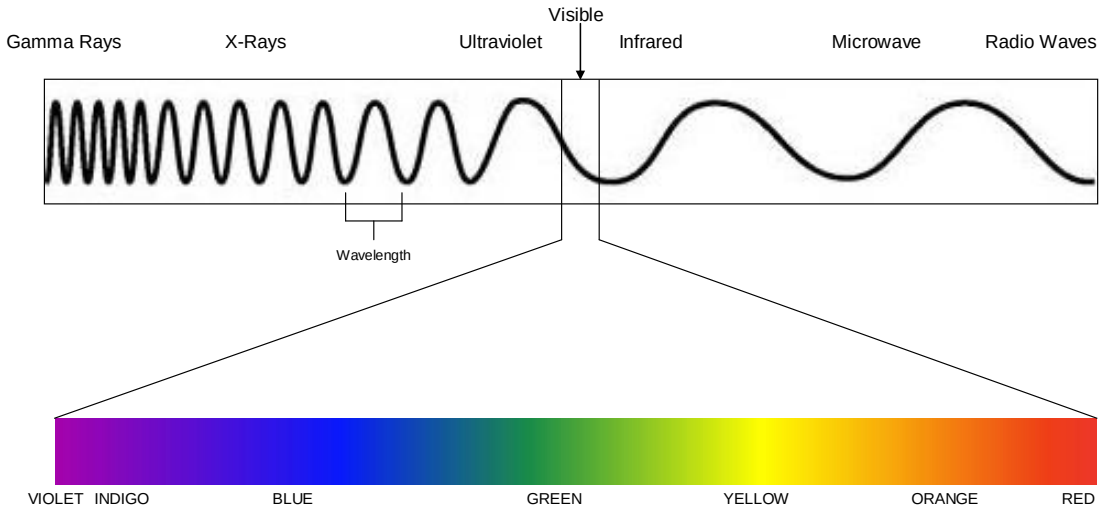

Figure B-2. The Electro-Magnetic Spectrum. The electro-magnetic spectrum places all E-M energy types in order, in this case of increasing wavelength. Shorter wavelengths translate to higher frequency and more energy delivered per photon. The human eye can only detect the wavelengths of E-M energy in the so-called "visible" portion of the spectrum. As the wavelength of visible energy changes, we perceive them different colors. All the other types of E-M energy are of the same nature as visible energy, but they have wavelengths that are harder or impossible for humans to directly detect. We must rely on other instruments to identify this energy.

B.2.2 Frequency

Wavelength is related to frequency, or the number of waves which pass a fixed point in a set amount of time (usually expressed as a number of waves, or cycles, per second. The unit of "one cycle per second" is also called the Hertz.) Since all EM energy travels at the same speed (approximately 300,000 kilometers per second), shorter

wavelengths translate to higher frequencies, and longer wavelengths to lower frequencies. In other words, during one second, a higher number of short waves will be able to pass by you than long waves, because they are shorter (not faster.)

B.2.3 Photons and Intensity

EM waves carry and deliver energy in discrete packets called photons, but not all photons are equal. Photons from shorter wavelengths of EM energy carry more energy per photon than those carried by longer wavelengths. Another way of describing this is to say that shorter-wave photons are more intense than longer-wave photons. Therefore, wavelength is also related to intensity. All other things being equal, shorter wavelengths are more intense, because their photons are more energetic than longer wavelengths.

B.3 Digital Imagery

Digital images and traditional film pictures are both representations of the EM energy emitted by the objects being imaged. Traditionally, the wavelengths of interest are the ones falling within the "visible" part of the EM spectrum, so called because these are the wavelengths that the average human eye can detect. There are also special films and sensors that can detect wavelengths outside of the visible part of the spectrum, and this allows us to "see" the normally invisible EM energy surrounding us.

Traditional camera film operates on the principle that a chemical, or combination of chemicals, will respond differently to different wavelengths of EM energy after exposure to the energy. When the film or exposure is developed, the pattern of different wavelengths is revealed as the image. Digital sensors use electrical devices, instead of chemicals or film, to record EM energy and then convert it to digital information that can be stored and displayed on a computer.

B.3.1 The Charge-Coupled Device

The early days of digital photography date back to the 1970s with the invention of the charge-coupled device. The charge-coupled device (CCD) is a tool which can quickly convert electrical charges into discrete points of data. When paired with an image sensor, like a photoelectric sensor, a CCD can be used to create pictures. In such a set-up, EM energy (radiation) strikes the photoelectric device, creating electric charges proportional to the intensity of the radiation. From there, the CCD converts the electrical charges into digital data. The data is displayed as an array of discrete points, called pixels. Though photoelectric sensors and CCDs are technically separate instruments, when they are paired the whole mechanism is referred to as a CCD.

CCDs are ideally suited for remote sensing. Since there is no film to develop, data is quickly deliverable. Moreover, CCDs, on average, convert 70% of detected energy into useful information. Photographic film is much less efficient. CCDs can also be tuned to detect very specific wavelengths of energy from the ultraviolet to the near infrared regions of the EM spectrum. Thus, several CCDs can be used in concert to gather information about a subject in multiple wavelengths.

CCDs are limited in their application to the ultraviolet, visible, and near infrared regions of the EM spectrum. Other wavelengths require very different technology to capture them. However, the practicality of CCDs helped bring about the modern satellite era and sophisticated Earth observing systems.

B.3.2 Image Resolution

The quality and/or usefulness of a digital image is closely tied to its resolution. Resolution is defined as the degree to which adjacent pieces of information can be

distinguished from each other. In remote sensing digital imagery, resolution comes in two forms: spatial resolution and spectral resolution.

B.3.2.1 Spatial Resolution

Spatial resolution refers to the effective size of the pixels in a digital image. In all cases, a single pixel is the smallest unit that can be discerned in an image. But, how much area of the Earth's surface that the pixel represents varies tremendously among remote sensing platforms (both space-borne and aerial.) For example, the Landsat 5 TM satellite sensors have a spatial resolution of 30 m. This means that each pixel in an image captured by the satellite represents an area of 30 m by 30 m, or 900 m^2 on the Earth's surface. Objects that are smaller than this may not be displayed in detail. On the other hand, the Quickbird satellite is capable of achieving 60 cm by 60 cm (0.36 m^2) spatial resolution. Any objects which are at least 60 cm long or wide will be displayed with some detail. Many weather satellites have a spatial resolution of 1 kilometer.

B.3.2.2 Spectral Resolution

Spectral resolution refers to the platform's ability to differentiate one wavelength (type) of EM energy from another. For example, separate sensors may be tuned to detect either blue, green, or red wavelengths of light. Each sensor in this case, is said to be monitoring a different "spectral band." Information from each band can be displayed and manipulated independently. Conversely, a sensor can be configured to detect all energy across the visible spectrum in one spectral band, meaning that the blue, green, and red wavelengths cannot be separated. In this manner, the set of three sensors would have the better spectral resolution.

Any remote sensing platform which gathers information in more than one spectral band is referred to as "multi-spectral". For example, the sensors aboard Landsat 5 are collectively called the "Multi-Spectral Scanner", because it collects data in seven different spectral bands (spread among the visible and near, middle, and far infrared spectrum.) The Moderate Resolution Imaging Spectroradiometer (MODIS), an instrument aboard two different satellites can detect 37 individual wavelengths of energy, spread among the visible and near, middle, and far infrared spectrum. There are other instruments referred to as "hyperspectral", because they are sensitive to a high number of specific wavelengths over a short portion of the E-M spectrum. The Airborne Visible/Infrared Imaging Spectrometer, or AVIRIS (an airplane mounted instrument) is considered hyperspectral. It can detect 224 individual wavelengths, all confined to the visible and near infrared portion of the spectrum

There can be a trade-off between spatial and spectral resolution. The better the spatial resolution of a sensor (meaning smaller pixels), the fewer the number of photons it can receive for each pixel. Likewise, better spectral resolution (meaning more bands per range of the spectrum) means that each band will receive its share of the photons, and more bands mean fewer photons per band. At some point the photons are too spread out among pixels and/or bands that there are not enough to be detectable by the sensor. One solution to this issue is to use aerial photography instead of satellite imagery. Aerial photographs are taken closer to the Earth's surface, where there is less atmosphere to attenuate the energy before reaching the sensor. For satellites, there is often a decision to be made as to which aspect of the imagery is more important: better spatial or better spectral resolution? By making the size of the pixels bigger, a sensor has the opportunity

to capture more photons over that larger area, but spatial detail will be lost. By reducing the number of spectral bands, and widening the sensitivity of the remaining band/s to cover the holes in the spectrum, one also increases the number of photons that the sensor can detect. Doing so, however, means having less spectral information in the final data. The Landsat ETM 7 satellite does a bit of both. It has different sensors for blue, red, and green energy (in addition to several other bands) which can achieve a spatial resolution of 30 m. It also contains another sensor which detects energy across the visible spectrum with a resolution of 15 m. Thus, this last band has sacrificed spectral resolution in favor of spatial resolution.

B.4 Practical Applications of Remote Sensing

The applications of remote sensing imagery are virtually limitless, but the primary uses are for weather monitoring, environmental monitoring, intelligence gathering, and mapping. There are numerous applications within each of these fields.

Many applications involve "spectroscopy," or the study of how objects of different composition reflect/emit EM energy differently. In one well-studied example, healthy vegetation (whether dark forest or bright cornfield) reflects quite a bit of near-infrared energy, but paved surfaces do not. Therefore, vegetation, which from the height of a satellite may resemble paved surfaces in the visible spectrum, is easily distinguishable from paved surfaces by the amount of near infrared radiation reflected/emitted by each. The unique spectral profiles of similar-looking objects are extremely useful in identifying them.

Other image processing techniques combine spectroscopy with statistics, mathematical transformations, and/or spatial attributes (such as shape) to study objects.

Remote sensing is often incorporated into Geographic Information Systems (GIS.) New applications for remote sensing imagery emerge every year.

For further reading:

Remote Sensing of the Environment: An Earth Resource perspective, John R. Jensen, Prentice Hall Series in Geographic Information Science, 2nd edition, 2007.

The Landsat Program, NASA http://landsat.gsfc.nasa.gov/

Scientific Charge-coupled Devices, James R. Janesick, SPIE – The International Society for Optical Engineering, 2001.